AD NUMBER
AD086189
CLASSIFICATION CHANGES
TO: **UNCLASSIFIED**
FROM: **CONFIDENTIAL**
LIMITATION CHANGES
TO: **Approved for public release; distribution is unlimited.**
FROM: **Distribution authorized to U.S. Gov't. agencies and their contractors; Administrative/Operational Use; 30 NOV 1955. Other requests shall be referred to Office of Naval Research, 875 Randolph Street, Arlington, VA 22203-1995.**
AUTHORITY
20 Dec 1956, per document marking; ONR ltr, 28 Jul 1977

TRANSPORT HELICOPTER DESIGN ANALYSIS METHODS

FC

FOR THE
UNITED STATES ARMY
THROUGH THE
OFFICE OF NAVAL RESEARCH - AIR BRANCH

Report No. 473.6
30 November 1955

ENGINEERING DIVISION HILLER HELICOPTERS

DISCLAIMER NOTICE

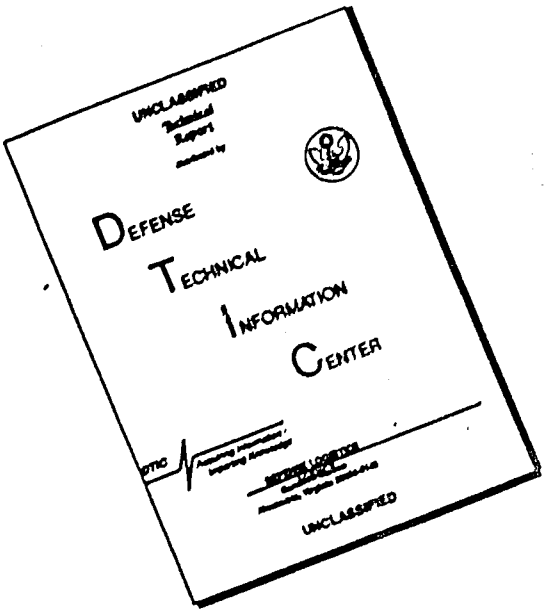

THIS DOCUMENT IS BEST QUALITY AVAILABLE. THE COPY FURNISHED TO DTIC CONTAINED A SIGNIFICANT NUMBER OF PAGES WHICH DO NOT REPRODUCE LEGIBLY.

TRANSPORT HELICOPTER DESIGN ANALYSIS METHODS

REPORT NO. 473.6
30 November 1955

Contract No. Nonr-1340(00)

PREPARED BY
TRANSPORT HELICOPTER STUDY GROUP

Dean P. Joy. . . . Aerodynamics and Power Plants Analyses
Robert M. Simonds. Weight Analyses

APPROVED BY

Robert A. Wagner . Chief Engineer

ENGINEERING DIVISION - HILLER HELICOPTERS

TABLE OF CONTENTS

INTRODUCTION
AND
GENERAL PHILOSOPHY

SECTION 1 - INTRODUCTION AND GENERAL PHILOSOPHY

This report forms a part of the requirement of Contract Nonr 1340(00), the basic objective of which was to develop coherent technical, economic, and operational criteria for future Army helicopter transport systems. This concept evolved from an earlier interpretation of the contract, which specified a design study of a three ton payload transport helicopter. After due consideration, it was decided that the development of parametric analysis methods for helicopter design optimization from the standpoint of performance, weight, cost, and operation, should precede specific design studies.

Such methods have been developed and applied to a parametric analysis of a large range of transport helicopter design possibilities, and the resulting trends and recommendations have been published in a summary report[1] entitled "Military Helicopter Transport Systems".

A second report[2], entitled "Transport Helicopter Operating Cost Analysis Methods", provides supplementary data and methods for estimating the pertinent direct and indirect cost of helicopter transport systems.

This third report provides the necessary supplementary data and methods for performance and weight analysis of helicopters, and is intended primarily for use by military procurement personnel in helicopter design evaluation.

The contemporary methods of rotary wing design analysis have of necessity evolved by a rapid build-up of practical rules-of-thumb and approximations gained from experience. It is therefore understandable that there has been to date very little standardization in helicopter performance and weight analysis techniques used within the industry. There are perhaps as many variations of performance and weight estimation methods as there are organizations in the rotary wing industry. The final answers obtained by each variation, however, are quite probably within a few percent of agreement, for their differences lie primarily in the form of the equations and the notation used.

In addition to the generalized design analysis methods presented, this report includes example analyses illustrating their application to each of the design possibilities covered in the summary report[1] of this contract. These example analyses were carried out with certain arbitrarily specified dimensions and performance criteria, in order to limit the charts to a reasonable number. Such assumptions as have been made are believed in all cases to lie within the spectrum of present and foreseeable state of the art.

The data and methods in this report cover the following configurations and power plant types:

1. Geared Power Plants

   Reciprocating Engines
   Geared Gas Turbine Engines } Both Single and Tandem Rotor Configurations

---

1. Hiller Report 350.1, "Military Helicopter Transport Systems"
2. Hiller Report 360.1, "Transport Helicopter Operating Cost Analysis Methods"

TRANSPORT HELICOPTER DESIGN ANALYSIS METHODS

2. Rotor Tip Drive Power Plants

- Tip-mounted Ramjets
- Tip-mounted Turbojets
- Pressure Jets

} Single Rotor Configuration Only

No analyses of compound or "unloaded rotor" type helicopters such as those with stub wings and/or propellers are included in this report, since these types were outside of the scope of the contract. Also, no consideration is given to the details of helicopter stability and control, since this is a special field in which it is difficult to generalize, and its inclusion could not, generally speaking, have a major effect on weight and performance.

It should be mentioned that there are certain detailed refinements to the theories and methods for helicopter performance analysis which have not been incorporated in the methods presented herein, one example of which is the extended rotor theory applicable to high rotor inflow angles, developed by the NACA. Refinements of this nature can be superimposed upon or integrated into the methods presented herein if required for detailed analysis, but they involve considerably more labor in calculation, and for this reason have been omitted. The approximate methods are adequate for the purpose of design evaluation and comparison of one helicopter type to another.

The data and methods which follow are presented in three sections (sections 2, 3, and 4). Section 2, entitled "Aerodynamics and Performance Analysis Techniques", covers the methods used in calculating power required (based on modifications to references 3 and 4), power plant characteristics, and helicopter performance.

Section 3, entitled "Weight Analysis Techniques", covers the methods used in estimating the weights of the various components comprising the empty weight, based on modifications to and extrapolations of the statistical weight analysis data compiled in reference 13.

Section 4, entitled "Configuration Selection Technique", contains an explanation and illustration of the graphical method which was developed for the selection of helicopter design parameters for minimum gross weight.

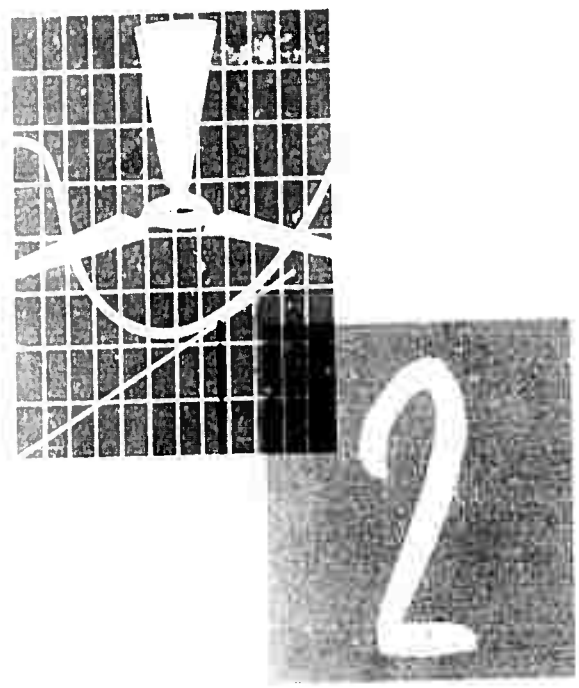

AERODYNAMICS AND PERFORMANCE ANALYSIS

SECTION 2 - AERODYNAMICS AND PERFORMANCE ANALYSIS TECHNIQUES

CONTENTS

SECTION 2 - AERODYNAMICS AND PERFORMANCE ANALYSIS TECHNIQUES

A. FUNDAMENTAL HELICOPTER AERODYNAMIC PARAMETERS

The symbols used in the aerodynamics and performance analysis are listed at the end of this section, on a pull-out sheet for the reader's convenience.

The total installed power required by a helicopter, the efficiency with which this power is used in hovering and in forward flight, and the performance capabilities of the helicopter, are dependent upon certain fundamental aerodynamic and design parameters, which are discussed below:

Rotor disk loading, w, defined as the gross weight W divided by the swept area of the main lifting rotor(s), with units of lbs/ft^2, is of primary importance in establishing the power required to produce lift, commonly referred to as induced power.

Rotor tip speed, V_T, defined as the tangential speed of the rotor blade tips, with units of ft/sec, is of primary importance in establishing the rotor power loss due to profile drag of the blades, commonly referred to as rotor profile power.

Rotor solidity, σ , defined as the ratio of rotor blade area to swept disk area, is also a factor affecting rotor profile power.

Rotor blade loading, w/σ , defined either as the ratio of disk loading to solidity, or as the ratio gross weight W divided by the lifting rotor(s) blade area, with units of lbs/ft^2, is a useful parameter having a direct interrelationship with the tip speed in determining rotor lift coefficient and rotor profile power, as will be shown.

Rotor blade section profile drag coefficient, c_{d_o}, has a direct effect on rotor profile power.

Rotor tip speed ratio, μ , defined as the ratio of forward speed V (in ft/sec) to rotor tip speed V_T (in ft/sec), is a useful parameter entering into calculation of the increase in rotor profile power with forward speed due to the dissymetry of airflow over the rotor disk, as blades advance into and retreat from the direction of flight.

Rotor tip loss factor, B, is a nondimensional factor which takes into account the reduction in thrust near the blade tips due to air "spillage" from the high pressure under surface of the blades to the lower pressure upper surface.

Helicopter equivalent flat plate parasite drag area, A_π , defined as total parasite drag of the fuselage, landing gear, empennage, cooling air inlets, etc., divided by the free stream dynamic pressure q, is the factor which determines the power required to overcome the parasite drag, referred to as parasite power.

Design power loading, l_p, defined as the ratio of gross weight W to installed "normal rated" horsepower at sea level, with units of lbs/hp, is a design parameter which has a direct affect on helicopter performance in hover, climb, and cruise.

Mass density of air, ρ , in units of slugs/ft^3, is of course directly involved in all aerodynamic calculations.

The ten parameters listed above are the more important of the many factors involved in helicopter aerodynamic and performance analysis. Additional factors and dimensional relationships which are involved in the analysis will be defined as needed, in the following sections.

B. HELICOPTER POWER REQUIRED

The method used herein for calculating helicopter power required has been developed from work originally done by Wiesner (Ref. 3) and later modifications (Ref. 4).

The power required by a lift-producing rotor in hovering or in level, unaccelerated flight, is commonly divided into three parts:

Total Power Required at Rotor(s) = Induced Power + Profile Power + Parasite Power

$$rhp = ihp + Rhp + php \qquad 2\text{-}1$$

1. Induced Power, ihp, for Single, Isolated Rotors

The induced horsepower or that required to produce lift, may be calculated for a single, isolated lifting rotor with radius R, from expressions derived from momentum theory:

Thrust T = (air mass flow per second)×(increase in velocity)

$$\text{or } T = \rho \pi R^2 V(dV) \qquad 2\text{-}2$$

where V is the total velocity at the rotor disk, and dV is the total increase in velocity. In the hovering case, the total velocity is the induced velocity, u_H, and it can be shown (Refs. 3, 4, or 5, for example) that the incremental increase in velocity dV is equal to twice the induced velocity, or $dV = 2u_H$.

$$\text{Hence, } T = \rho \pi R^2 u_H (2u_H) = 2\rho \pi R^2 u_H^2 \qquad 2\text{-}3$$

Equation 2-3 may be solved for u_H and written in terms of the disk loading, $w = T/\pi R^2$, as follows:

$$u_H = \sqrt{\frac{T}{2\rho \pi R^2}} = \sqrt{\frac{w}{2\rho}} \qquad 2\text{-}4$$

Equations 2-2 through 2-4 are based on the assumption of an ideal actuator disk in which there are no losses at the periphery of the disk. In the actual case, however, where the number of blades are finite, the loss in thrust at the blade tips is accounted for by the introduction of a factor B, which is defined as the ratio of the effective, lift-producing radius, divided by the actual geometric radius. This tip loss factor, discussed in detail in a following paragraph, must therefore be incorporated in the above equations by substituting

SECTION 2 - AERODYNAMICS AND PERFORMANCE ANALYSIS TECHNIQUES

BR for R. Equation 2-4 then becomes

$$u_H = \sqrt{\frac{T}{2\rho\pi B^2 R^2}} = \sqrt{\frac{w}{2\rho B^2}} \qquad 2\text{-}5$$

The induced horsepower required to produce the thrust T is, from the energy concept,

$$ihp = \frac{Tu}{550} \qquad 2\text{-}6$$

or in the hover,

$$ihp_H = \frac{Tu_H}{550} = \frac{T}{550}\sqrt{\frac{w}{2\rho B^2}} \qquad 2\text{-}7$$

In forward flight, the momentum analysis of NACA ARR L5E10 (Ref. 6) is used for the calculation of induced velocity. Derivations are presented therein of the ratio of induced velocity in forward flight to induced velocity in hover, u/u_H, which varies as a function of the ratio of forward flight speed (in ft/sec) to the induced velocity in hover, or symbolically, V/u_H. A plot of this relationship derived by the NACA, for a single, isolated rotor, is reproduced in Figure 2-1 below. The ratio u/u_H is denoted herein by K_u. The curve shown is for a tilt angle α' of the rotor tip path plane with respect to the horizontal, of zero degrees, which is a conservative assumption (i.e. tilt angles other than zero, which occur in forward flight, would give slightly lower values of K_u in forward flight, and hence slightly lower induced horsepower).

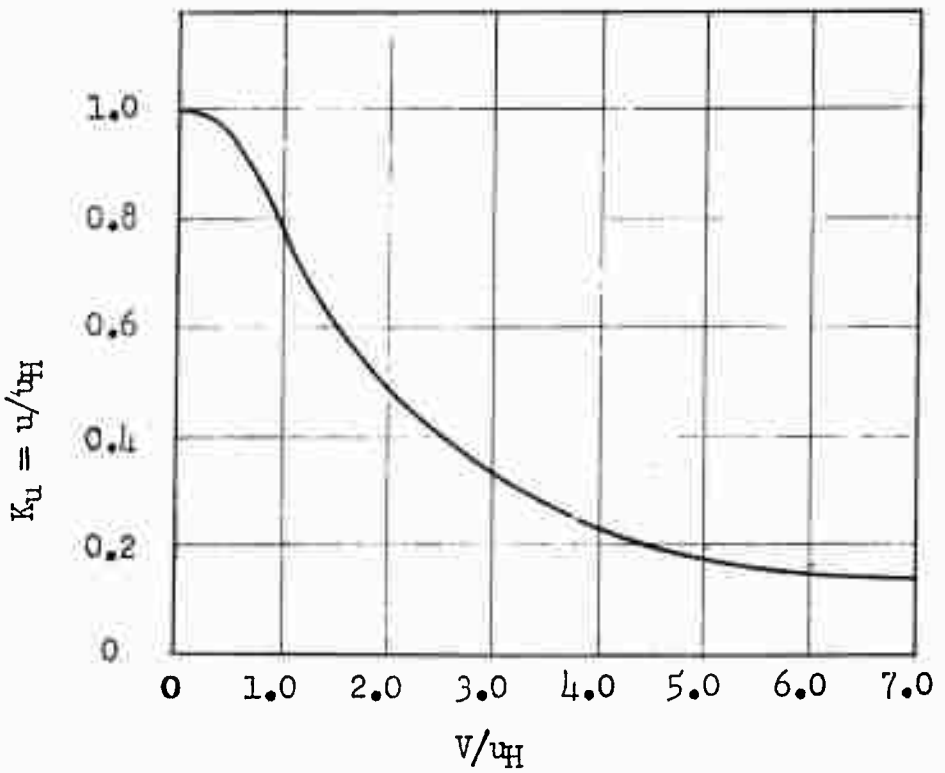

Figure 2-1 Induced Velocity Variation with Airspeed For Single, Isolated Rotors

Using this plot, the induced horsepower in forward flight may be simply calculated by including the factor in K_u in equation 2-7, giving

$$ihp = ihp_H K_u = \frac{T}{550}\sqrt{\frac{w}{2\rho B^2}}\,K_u \qquad 2\text{-}8$$

since $ihp = \frac{Tu}{550}$ and $u = u_H K_u$

It should be noted that all of the above equations are based upon the assumption of a uniform distribution of the induced inflow, u (or u_H in hovering) over the rotor disk. The actual distribution is generally not uniform, although the use of highly tapered and twisted blades theoretically tends to approach this ideal flow condition. In most cases, the actual distribution is probably more nearly parabolic or triangular, over the blade span. It is assumed, conservatively, in the analyses herein, that the distribution is triangular. As shown in Ref. 4, this triangular distribution would theoretically increase the induced horsepower by a factor 1.13 above the ideal, uniform distribution value represented by equation 2-8. Throughout the remainder of this report, then, the induced horsepower is calculated from the corrected expression

$$ihp = \frac{1.13}{550}\,T\sqrt{\frac{w}{2\rho B^2}}\,K_u \qquad 2\text{-}9$$

2. Induced Power for Tandem Rotors

When two rotors are arranged in tandem, an induced power correction factor is required in forward flight as a result of the fact that the rear rotor is influenced by the downwash generated by the front rotor. To analyze this effect, an analogy with fixed wing momentum theory is used. Assume that the two rotors operate at any instant on an air mass represented by two spheres (truncated in the case of overlapping rotors), as shown in Figure 2-2 below.

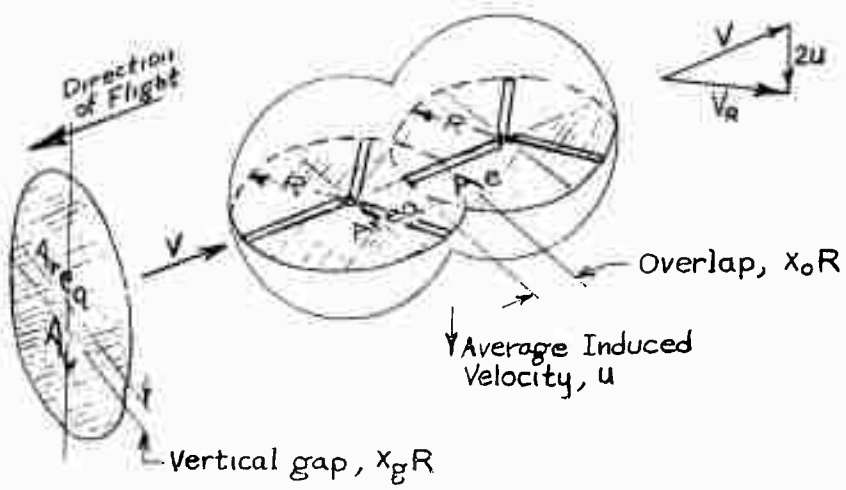

Figure 2-2 Schematic Diagram for Tandem Rotor Momentum Theory Analysis

SECTION 2 - AERODYNAMICS AND PERFORMANCE ANALYSIS TECHNIQUES

The frontal projected cross sectional area of these truncated spheres, A_V, is equal to

(a) the disk area of one isolated rotor if there is no vertical gap between front and rear rotors,

or (b) an area slightly larger than that of one disk, if a vertical gap exists, in which case the area is formed by the superimposition of the two circles whose centers are eccentric by the amount of the gap, as shown in Figure 2-2.

The effective disk area, A_e, of the overlapped rotors, is as shown equal to the plan view projected area of the two rotor disks, whose centers are eccentric by one diameter less the overlap distance x_oR, where x_o is the overlap expressed as a fraction of one rotor radius. In this report, the disk loading of tandem rotor helicopters is defined as the thrust divided by the effective disk area A_e.

The free stream velocity V is perpendicular to the cross sectional area A_V, ahead of the rotors, and the induced velocity u is perpendicular to the effective disk area A_e.

From momentum theory, an equation for total thrust can be written similar to equation 2-2:

$$T = \rho(A_V^2V^2 + A_e^2u^2)^{\frac{1}{2}}dV \qquad 2\text{-}10$$

where the quantity $\rho(A_V^2V^2 + A_e^2u^2)^{\frac{1}{2}}dV$ is the vector mass flow of air per second. Again it can be shown that dV, the total change in velocity downstream of the rotors, is equal to 2u, or twice the induced inflow velocity at the rotor disk. Thus, equation 2-10 can be written

$$T = 2\rho A_e\left[\left(\frac{A_V}{A_e}\right)^2 + u^2\right]^{\frac{1}{2}}u \qquad 2\text{-}11$$

Now in the hovering state, V = 0, $u = u_H$, and $dV = 2u_H$, hence from equation 2-10

$$T = \rho A_e u_H dV = 2\rho A_e u_H^2$$

or
$$u_H^2 = \frac{T}{2\rho A_e} = \frac{w}{2\rho} \qquad 2\text{-}12$$

where w is the disk loading T/A_e.

Hence, equation 2-11 can be rewritten as

$$u_H^2 = \left[\left(\frac{A_V}{A_e}\right)^2 + u^2\right]^{\frac{1}{2}}u \qquad 2\text{-}13$$

which may be arranged as a quartic in u/u_H:

$$\left(\frac{u}{u_H}\right)^4 + \left(\frac{A_v}{A_e}\right)^2\left(\frac{V}{u_H}\right)^2\left(\frac{u}{u_H}\right)^2 - 1 = 0$$

or substituting $K_u = u/u_H$

$$K_u^4 + \left(\frac{A_v}{A_e}\right)^2\left(\frac{V}{u_H}\right)^2 K_u^2 - 1 = 0 \qquad 2\text{-}14$$

The area A_e may be calculated, if the fractional overlap x_o is known, from the following equation:

$$A_e = 2R^2\left[\pi - \sin^{-1}\sqrt{x_o - \frac{x_o^2}{4}} + \left(1 - \frac{x_o}{2}\right)\sqrt{x_o - \frac{x_o^2}{4}}\right] \qquad 2\text{-}15$$

and the area A_v may be calculated, if the vertical gap x_g, expressed as a fraction of one rotor radius, is known, from the following approximate equation:

$$A_v = R^2(\pi + 2x_g) \qquad 2\text{-}16$$

Equation 2-14 is plotted in Figure 2-3 on the following page, for various values of the area ratio A_v/A_e. Note that for an area ratio of 1.0, the curve is identical to that for single, isolated rotors given in Figure 2-1. At airspeeds greater than zero, the curves for area ratios less than 1.0 show higher values of K_u than does the single, isolated rotor curve. This difference represents the increase in tandem rotor induced power in forward flight, over that for single rotors. Equation 2-14 and the curves in Figure 2-3 are of course approximations, but they have been found to provide good agreement with results of more rigorous tandem rotor analyses and with experimental data.

3. Blade Tip Loss Factor, B

As shown in Reference 5, an approximate solution for the tip loss factor B for lightly loaded rotors yields the following expression, plotted in Figure 2-4.

$$B = 1 - \frac{\sqrt{2C_T}}{b} \qquad 2\text{-}17$$

where b = number of blades per rotor, and C_T = thrust coefficient = $T/\rho\pi R^2 V_T^2$

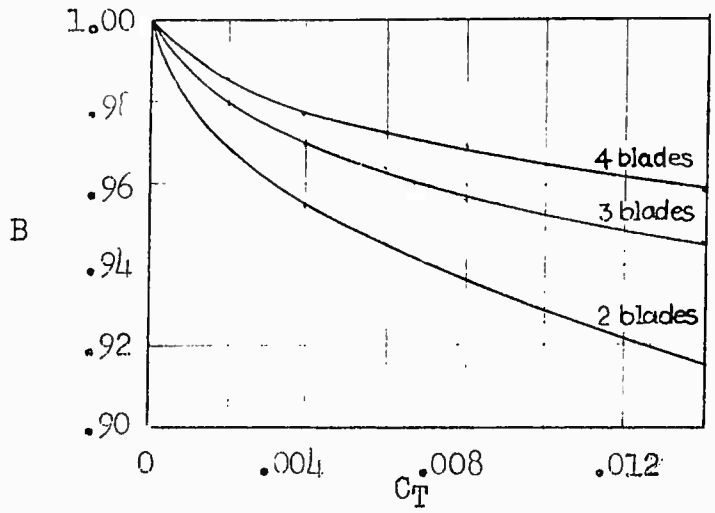

Figure 2-4 Blade Tip Loss Factor

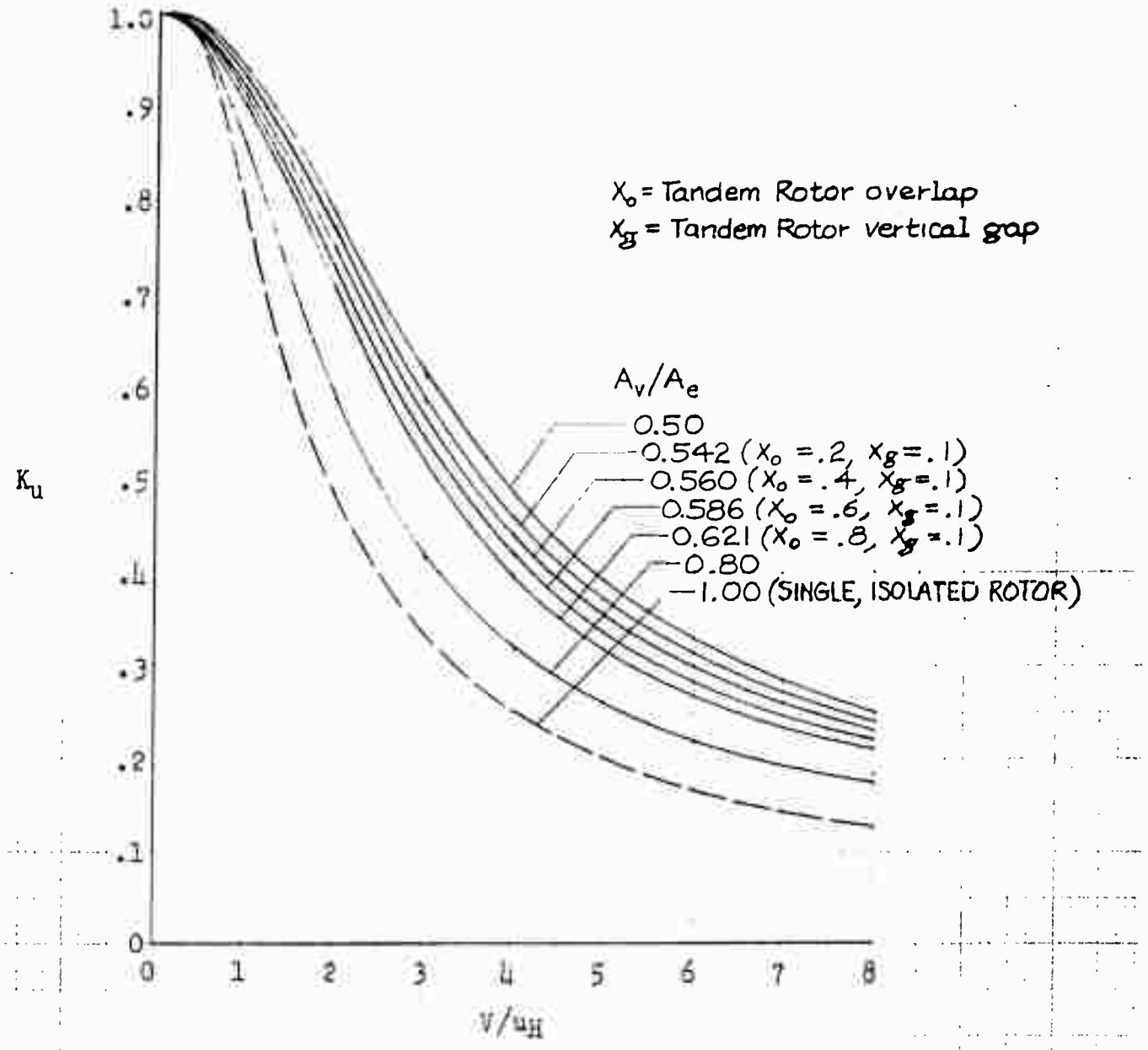

Figure 2-3: Induced Velocity Factor K_u, for Tandem Rotors

For preliminary analyses, in order to avoid determining a different value of B for each of a series of thrust coefficients at different disk loadings and altitudes, it is sufficient to assume B a constant. A value of B = 0.96 has been assumed for main rotors in the example analyses in this report. Statistics indicate that most present operational helicopters are designed for thrust coefficients not less than .0015 and not greater than .012, and it can be seen from Figure 2-4 that these extremes in C_T yield values of B which differ from 0.96 by only 3 or 4%.

For tail rotors, past practice at Hiller has been to assume a constant B = 0.90, to account for the higher tail rotor thrust coefficients, which may run as high as 0.C2 in hovering.

4. Rotor Profile Power, Rhp

The rotor profile horsepower, or that required to balance the profile drag of the rotating blades, is calculated herein using expressions derived from those in Reference 3. As shown therein, a blade element theory approach coupled with the assumption of a constant blade section drag coefficient c_{d_o} along the blade span and around the azimuth, leads to an expression for Rhp as follows:

$$Rhp = \frac{c_{d_o} \rho A_b V_T^3}{4400} K_\mu \qquad 2\text{-}18$$

where K_μ is a factor which accounts for the power rise due to the dissymetry of forward flight, A_b is the total blade area, and V_T is the tip speed of the rotor.

(a) Mean blade profile drag coefficient, c_{d_o}:

In Wiesner's method (Ref. 3) as modified by Ref. 4, the two-dimensional c_{d_o} is assumed to be equivalent to a mean value, dependent on the mean blade lift coefficient C_{L_r}, or its corresponding mean blade angle of attack α_r. The mean blade lift coefficient is defined as

$$C_{L_r} = \frac{6C_T}{\sigma} \qquad 2\text{-}19$$

and since the thrust coefficient $C_T = \frac{T}{\rho \pi R^2 V_T^2} = \frac{w}{\rho V_T^2}$ 2-20

equation 2-19 may be rewritten

$$C_{L_r} = \frac{6(w/\sigma)}{\rho V_T^2} \qquad 2\text{-}21$$

The mean section angle of attack α_r is related to C_{L_r} by the lift curve slope, $a = dC_l/d\alpha$. Thus,

$$\alpha_r = \frac{C_{L_r}}{a} = \frac{6(w/\sigma)}{a \rho V_T^2} \qquad 2\text{-}22$$

The relationship between c_{d_o} and α_r is commonly expressed in the parabolic form

$$c_{d_o} = \delta_o + \delta_1 \alpha_r + \delta_2 \alpha_r^2 \qquad 2\text{-}23$$

Quantitatively, a mean profile drag coefficient for "good" practical construc-

tion blades of conventional airfoil section has in the past been assumed by the NACA to be represented by

$$c_{d_o} = .0087 - .0216\alpha_r + .4\alpha_r^2 \qquad 2\text{-}24$$

However, it is noted that equation 2-24 gives minimum drag at a positive angle of attack, which is not true for the symmetrical airfoil sections most commonly used for helicopter rotor blades. For this reason, and to simplify calculations, the expression for c_{d_o} used herein assumes $\delta_1 = 0$, thereby giving minimum drag at zero angle of attack.

$$c_{d_o} = \delta_o + \delta_2\alpha_r^2 \qquad 2\text{-}25$$

By substituting for α_r^2 from equation 2-22, equation 2-25 is converted to

$$c_{d_o} = \delta_o + \frac{36\,\delta_2(w/\sigma)^2}{a^2\rho^2 V_T^4} \qquad 2\text{-}26$$

For the example analyses in this report, the following values for δ_o and δ_2 were assumed:

$$\delta_o = .009$$

$$\delta_2 = .3$$

These assumptions represent a drag polar which is slightly higher than the NACA variation, equation 2-24, as shown by the comparison in Figure 2-5 on the following page. The higher curve is selected as a reasonably conservative mean approximation to the section drag characteristics of NACA airfoils of the 0012 to 0018 series.

(b) Dissymetry profile power correction factor, K_μ :

This factor, defined by Wiesner (Ref. 3) is a function only of tip speed ratio, μ, and the drag losses associated with stall of the retreating blade, and the slightly higher drag of the reversed flow regions. Ideally, if these latter effects were not present, the blade element integration results in the follow- expression for K_μ :

$$K_\mu = 1 + 3\mu^2 + \frac{3}{8}\mu^4 \qquad 2\text{-}27$$

The effects of retreating blade stall and increased drag of the reversed flow regions are accounted for in Wiesner's method by use of a more general expression

$$K_\mu = 1 + 3\mu^2 + c_4\mu^4 \qquad 2\text{-}28$$

where the coefficient c_4 replaces the value 3/8, and is intended to account for these additional stall and reversed flow effects. Wiesner recommends a value of $c_4 = 30$ for C_{L_r} values of 0.6 or less. Figure 2-6 on the following page shows plots of K_μ versus the tip speed ratio μ, for values of c_4 from 3/8 up to 30.

By substituting for blade area from its definition

$$A_b = \frac{T}{w/\sigma} \qquad 2\text{-}29$$

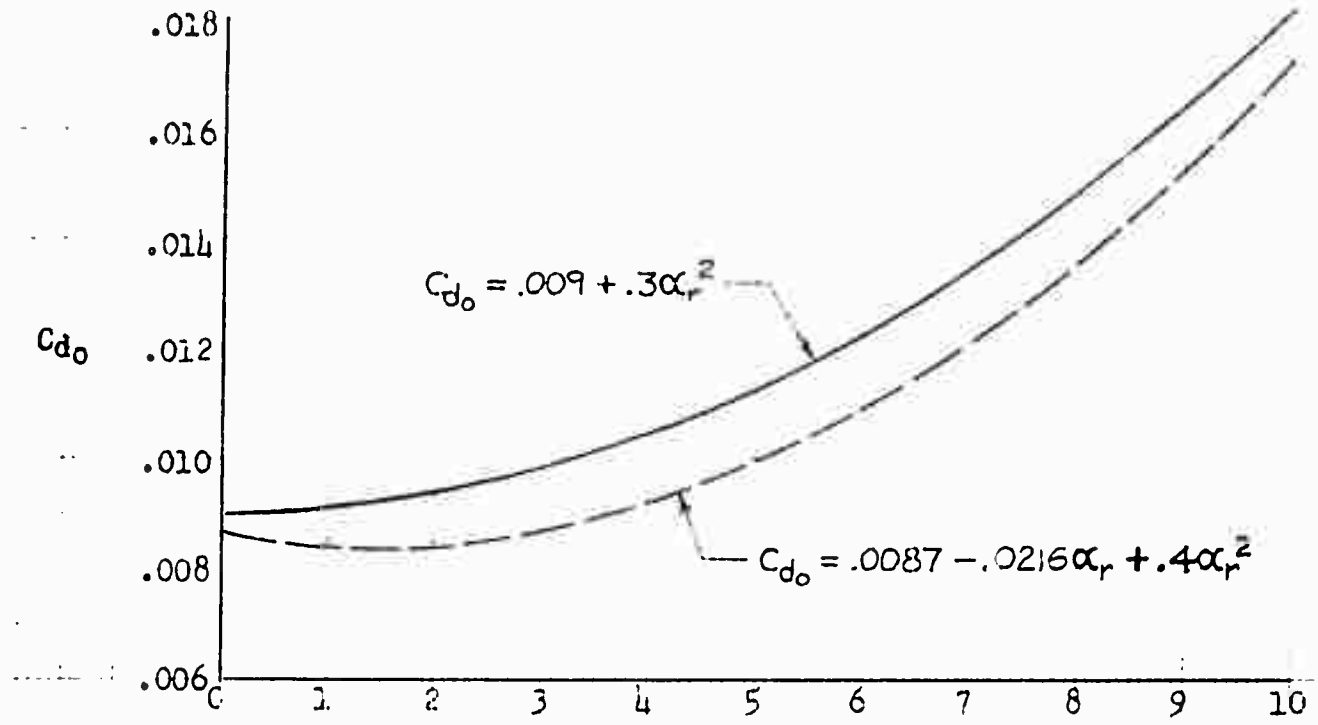

Figure 2-5

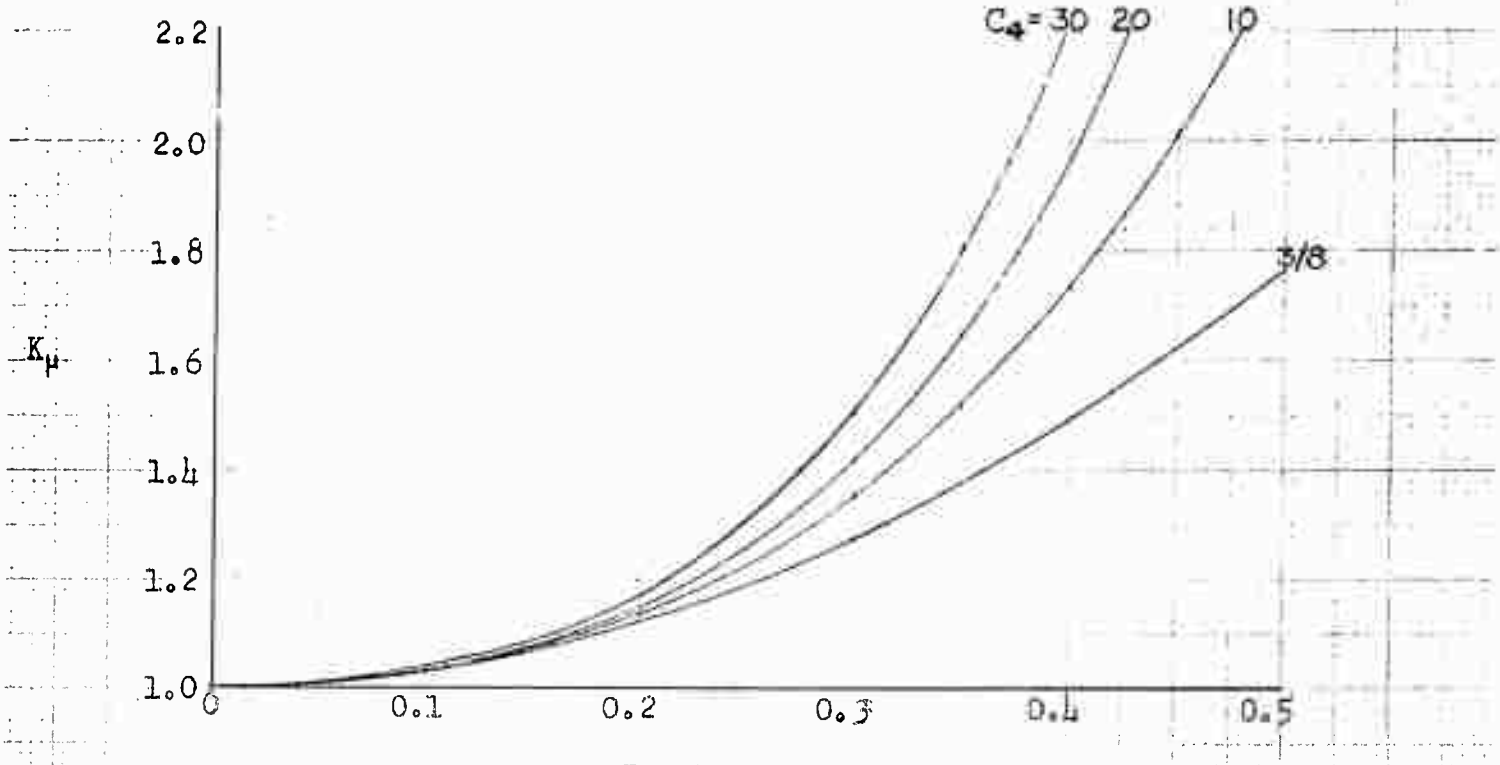

Figure 2-6

and substituting for c_{d_o} from equation 2-26, equation 2-18 can be rewritten in a form more convenient for parametric analysis calculations:

$$Rhp = \frac{T}{4400}\left[\frac{\delta_o \rho V_T'}{w/\sigma} + \frac{36\,\delta_2\, w/\sigma}{a^2 \rho V_T}\right] K_\mu \qquad 2\text{-}30$$

5. Helicopter Parasite Power, php

The parasite drag and parasite horsepower of helicopters are generally estimated by the same procedure used for fixed wing aircraft, namely, by making a "drag breakdown" of the various contributing components (fuselage, tail boom, empennage, rotor hubs, landing gear, and so forth). The concept of an equivalent flat plate drag area, A_π, is used. This drag area is simply the sum of all the contributing component drag areas, ΔA_{π_n}, or

$$A_\pi = \sum_1^n \Delta A_{\pi_n} \qquad 2\text{-}31$$

where the components number from 1 to n.

The individual component ΔA_π's are defined as

$$\Delta A_\pi = C_D \Delta S \qquad 2\text{-}32$$

where C_D is the drag coefficient of the component, and ΔS is its projected frontal area.

The total parasite drag is then

$$D_p = A_\pi q \qquad 2\text{-}33$$

where q is the free-stream dynamic pressure, $(\rho/2)V^2$, (V in ft/sec).

The parasite power required to overcome this drag is

$$php = \frac{D_p V}{550} = \frac{A_\pi q V}{550} = \frac{\rho}{1100} A_\pi V^3, \text{ (V in ft/sec)} \qquad 2\text{-}34$$

It is well to note that past experience has shown helicopter manufacturers' preliminary parasite drag estimates to be generally over-optimistic. This may have been due in part to the lack of reliable wind-tunnel test data in flow conditions which actually exist over the helicopter components in flight. When this is the case, the only recourse for a preliminary design estimate of A_π is the experience and judgement of the aerodynamics engineer in making adequate allowances for interference effects.

For broad parametric analyses over a large range of gross weight, such as that covered in the Summary Report of this contract (Ref. 1), drag analyses of typical configurations of varying sizes, augmented by statistics where available, will generally permit the establishment of a mathematical variation of A_π with gross weight. Figure 2-7 shows the three typical variations which were used in Reference 1 for transport type helicopters with

(a) fixed landing gear and payload carried internally

TRANSPORT HELICOPTER DESIGN ANALYSIS METHOD

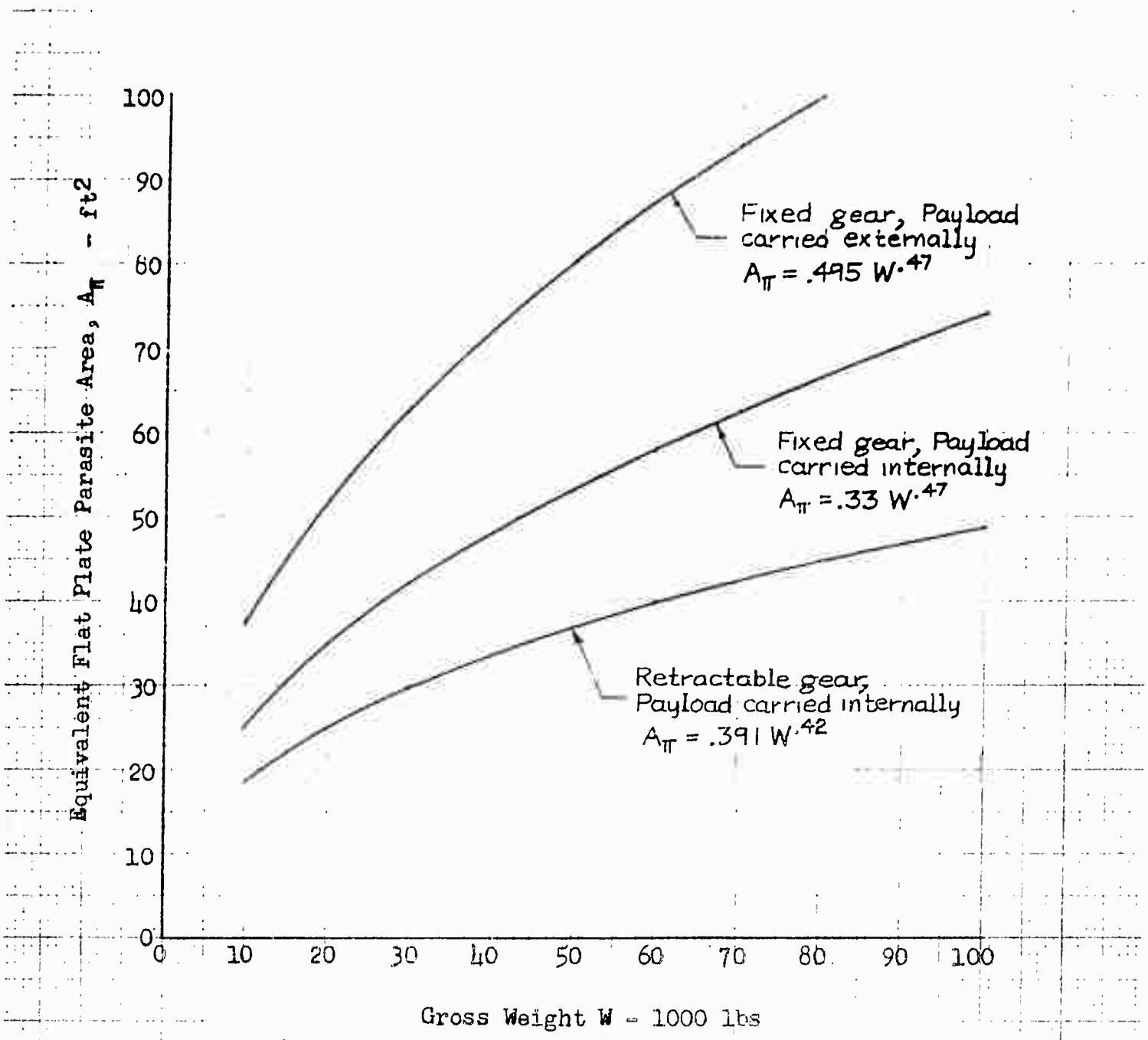

Figure 2-7: Variation of Flat Plate Area with Gross Weight

(b) retractable landing gear and payload carried internally

(c) fixed landing gear and payload carried externally

6. Total Power Required at Rotor, rhp

As was shown by equation 2-1, the total power required at the main rotor(s), rhp, is the sum of

ihp (equation 2-9)
Rhp (equation 2-30)
php (equation 2-34)

For generalized parametric analyses, it has been found expedient to calculate power required per pound gross weight, rph/W. Making the following substitutions in the above equations,

(a) $\rho = .002378(\rho/\rho_o)$ 2-35

where ρ/ρ_o is the ratio of air mass density ρ at any altitude and temperature, to the standard NACA value at sea level, $\rho_o = .002378$;

(b) $T = W$, since for steady, unaccelerated level flight the thrust T of a lifting helicopter rotor is for all practical purposes equal to the gross weight W;

(c) Forward velocity V is converted to units of knots by the relationship, knots = .592 x ft/sec, where it occurs in equation 2-35 for php;

and dividing all equations through by the gross weight W, then the final, generalized expression for rhp/W is

$$\frac{rhp}{W} = \frac{.0297\sqrt{w}}{\sqrt{\rho/\rho_o}\,B} K_u + \left[.54(\rho/\rho_o)\frac{\delta_o V_T^3 \times 10^{-6}}{w/\sigma} + \frac{3.44\,\delta_2(w/\sigma)}{(\rho/\rho_o)a^2 V_T}\right] K_\mu + 10.45(\rho/\rho_o)\left(\frac{V}{100}\right)^3 \frac{A_\pi}{W} \qquad 2\text{-}36$$

where V, in the last term, is in knots.

For given values of w, B, ρ/ρ_o, δ_o, δ_2, w/σ, V_T, a, and A_π (or A_π/W), this power required equation will have the general appearance shown in Figure 2-8 below, when plotted versus airspeed V.

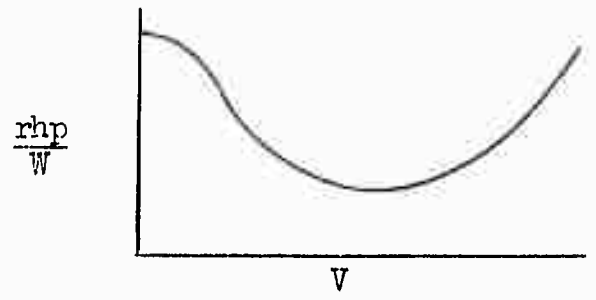

Figure 2-8

7. Tail Rotor Power, hp_t

a) Anti-Torque Tail Rotors:
For geared-drive single main rotor helicopters, the main rotor torque Q which must be balanced by tail rotor thrust T_t is

$$Q = \frac{550R(rhp)}{V_T} \qquad 2\text{-}37$$

where R = main rotor radius in feet, V_T = main rotor tip speed in ft/sec, and rhp = main rotor power (equation 2-36).

Thus, if the tail rotor moment arm is l_t in feet, then

$$T_t = \frac{Q}{l_t} = \frac{550R(rhp)}{V_T\, l_t} \qquad 2\text{-}38$$

and the tail rotor disk loading is

$$w_t = \frac{T_t}{\pi R_t^2} = \frac{550R(rhp)}{V_T l_t \pi R_t^2} \qquad 2\text{-}39$$

Tail rotor induced power can be calculated from the same equation used for main rotor induced power, equation 2-9, except that T_t replaces T, w_t replaces w, and K_u as read from Figure 2-1 is based on the ratio V/u_{Ht} instead of V/u_H. The tail rotor induced velocity in static thrust is

$$u_{Ht} = \sqrt{\frac{w_t}{2\rho B^2}} \qquad 2\text{-}40$$

As was discussed in paragraph 3., it is sufficient for normal accuracy to assume a constant value for tail rotor tip loss factor B, and a value of 0.90 is recommended.

Either equation 2-18 or 2-30 may be used to calculate tail rotor power, provided tail rotor blade area A_{bt} and tail rotor tip speed V_{Tt} are substituted, and K_μ is based on the tail rotor tip speed ratio, $\mu_t = V/V_{Tt}$. Although the tail rotor profile drag coefficient $c_{d_{ot}}$ will actually change with forward speed, as the tail rotor pitch angles and corresponding angles of attack change with changing tail rotor thrust requirements, it is generally sufficient to assume a constant value for $c_{d_{ot}}$, since the tail rotor profile power is a very minor fraction of the total helicopter power required. A value of $c_{d_{ot}} = 0.02$ is recommended as a conservative mean approximation.

Total tail rotor power required, hp_t, for anti-torque tail rotors, is the sum of the induced power (equation 2-9, modified) and the profile power (equation 2-18 or 2-30, modified).

b) Tail Rotors for Tip-Powered Helicopters:
Since the tail rotor on tip-powered helicopters is required only for directional control, as there is no main rotor torque reaction, the tail rotor thrust for this type is essentially zero throughout the range of flight speeds from hover to maximum speed, when the flight path is straight and level. The diameter, blade area, solidity, and moment arm (distance from main rotor to tail rotor hub) are therefore selected as the minimum to give adequate directional control capabilities. In this report, the tail rotor dimensions used in the example analyses of tip-powered helicopters were based

on the directional control requirements specified in Military Specification MIL-H-8501, (Ref. 17). The power required by the tail rotor for tip powered helicopters, in straight and level flight, consists only of profile power, and may be calculated as for the anti-torque tail rotors discussed in (a) above, from either equation 2-18 or 2-30. Again, the assumption of a constant $c_{d_{ot}} = 0.02$ is recommended as a conservative approximation.

8. Propulsive Efficiency and Total Brake Horsepower Required:

The total b ake horsepower required by a helicopter may be written as the sum of

Total brake horsepower required	=	Horsepower required at main rotor(s)	+	Tail rotor Horsepower required	+	Gear losses

$$Bhp = rhp + hp_t + hp_g \qquad 2\text{-}41$$

For generalized analyses, it has been found expedient to express both hp_t and hp_g in terms of ratios with the total horsepower required, Bhp. These ratios are defined as

$$K_t = \frac{hp_t}{Bhp} \qquad 2\text{-}42$$

and

$$K_g = \frac{hp_g}{Bhp} \qquad 2\text{-}43$$

Equation 2-41 can then be written as

$$\frac{Bhp}{W} = \frac{rhp}{W} + \frac{Bhp}{W}(K_t + K_g)$$

or

$$\frac{Bhp}{W} = \frac{rhp/W}{1-K_t-K_g} = \frac{1}{\eta}\frac{rhp}{W} \qquad 2\text{-}44$$

where η is the propulsive efficiency, equal to $1 - K_t - K_g$.

For geared-drive single rotor helicopters, a 3% gear loss ($K_g = 0.03$) is recommended, and for geared-drive tandem rotor helicopters, a 4% gear loss ($K_g = 0.04$) is recommended. The higher gear loss for tandem rotors accounts for the additional main transmission and intermediate or right-angle gear boxes.

For tip-powered helicopters, 3% of tail rotor power is recommended as a reasonable assumption for gear losses. In this case, the procedure is to include this loss in the calculation of the tail rotor power, factor K_t, and assume $K_g = 0$.

In general, it has been found from calculations of tail rotor power for representative sets of design parameters and conventional tail rotor dimensions, that the variation of K_t with forward speed may be represented by a single curve which holds approximately for all disk loadings and altitudes. Curves of K_t

and η versus forward flight speed, used for the example analyses herein, are included in Part E of this section.

C. ROTOR TIP STALL AND COMPRESSIBILITY LIMITS

The power required equations developed in the preceding part of this report are valid only at forward speeds below the limits at which either the retreating blade tip stalls, or the advancing blade tip encounters compressibility drag divergence due to its high Mach number. At speeds beyond the retreating tip stall limit, it is a well documented fact that not only extreme increases in power, but also control and vibration problems must be reckoned with. The high Mach number compressibility effects, though not so well documented, are known to give rise also to a rapid power rise, but there is no absolute indication that control and vibration problems are as severe in this case as for the case of tip stall. Both of these limits depend primarily on rotor tip speed, forward speed, and blade angle of attack variation around the azimuth and along the blade span. Approximate methods for establishing these limits are given below.

1. Retreating Blade Tip Stall

Denoting the angle of attack of any blade element at a spanwise position $r = xR$ and at azimuth Ψ as $\alpha_{x,\Psi}$, then from Figure 2-9 it may be seen that

$$\alpha_{x,\Psi} = \theta_{x,\Psi} - \phi_{x,\Psi} \qquad 2\text{-}45$$

where $\theta_{x,\Psi}$ is the pitch of the blade section, defined as

$$\theta_{x,\Psi} = \theta_0 + x\theta_\epsilon + \theta_1 \sin\Psi + \theta_2 \cos\Psi \qquad 2\text{-}46$$

θ_0 is the collective pitch at the blade root.
θ_ϵ is the blade twist from root to tip (negative when tip angle is less than root angle).
θ_1 is the cyclic pitch amplitude when the blades are at $\Psi = 90^\circ$ or 270°.
θ_2 is the cyclic pitch amplitude when the blades are at $\Psi = 0^\circ$ or 180°.

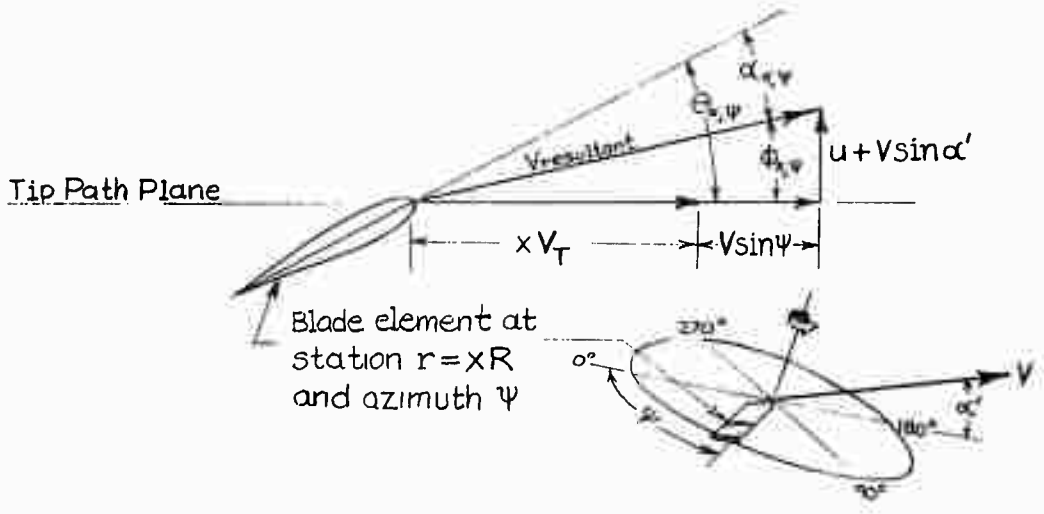

Figure 2-9 Blade Element Geometry

SECTION 2 - AERODYNAMICS AND PERFORMANCE ANALYSIS TECHNIQUES

The inflow angle

$$\Phi_{x,\psi} = \tan^{-1}\frac{\lambda - V\sin\alpha'}{(V_T - V\sin\Psi)} \cong \frac{\lambda - V\alpha'}{(V_T - V\sin\Psi} \qquad 2\text{-}47$$

where α' is the angle of incidence of the tip path plane to the free stream velocity.

Defining the inflow ratio, referred to the tip path plane, as

$$\lambda' = \frac{\lambda - V\alpha'}{V_T} \qquad 2\text{-}48$$

and making the substitution

$$\lambda - V\sin\Psi = V_T(\lambda' + \mu\sin\Psi) \qquad 2\text{-}49$$

then $$\Phi_{x,\psi} = \frac{\lambda'}{x + \mu\sin\Psi} \qquad 2\text{-}50$$

and $$\alpha_{x,\Psi} = \theta_o + x\theta_\epsilon + \theta_1\sin\Psi + \theta_2\cos\Psi - \frac{\lambda'}{x + \mu\sin\Psi} \qquad 2\text{-}51$$

In Reference 4, modifications to Lichten's original work show that the collective pitch θ_o is related to $2C_T/\sigma a$, λ', and θ_ϵ, in the following manner:

$$\frac{2C_T}{\sigma a} = -K_1\lambda' + K_2\theta_o + K_3\theta_\epsilon \qquad 2\text{-}52$$

or $$\theta_o = \frac{1}{K_2}\left(\frac{2C_T}{\sigma a}\right) + \frac{K_1}{K_2}\lambda' - \frac{K_3}{K_2}\theta_\epsilon \qquad 2\text{-}53$$

where the coefficients K_1, K_2, and K_3 are functions only of tip speed ratio μ, and tip loss factor B.

Figure 2-10 on the following page presents plots of these coefficients versus μ, for an assumed value of B = 0.96.

It is also shown in Reference 4 that, in straight and level unaccelerated flight, the cyclic pitch amplitude θ_2 is approximately zero, and the cyclic pitch amplitude θ_1 is related to λ', θ_o, and θ as follows:

$$\theta_1 = C_2\lambda' - C_3\theta_o - C_4\theta_\epsilon \qquad 2\text{-}54$$

where the coefficients C_2, C_3, and C_4 are also functions only of tip speed ratio μ, and tip loss factor B. Figure 2-11 on the following page presents plots of these coefficients versus μ, for an assumed value of B = 0.96.

Note that the algebraic sign on λ' in equations 2-48, 2-50, 2-52, 2-53, and 2-54 is reversed from the sign convention used in Reference 4, since in this report λ' is defined as positive when the inflow is downward through the rotor, whereas in Reference 4, λ' was defined as positive when the inflow is upward through the rotor (autogyro sign convention).

Since rotor stall usually occurs first on the retreating blade tip (x = 1), at or very close to the azimuth $\Psi = 270°$, an expression for the angle of attack of

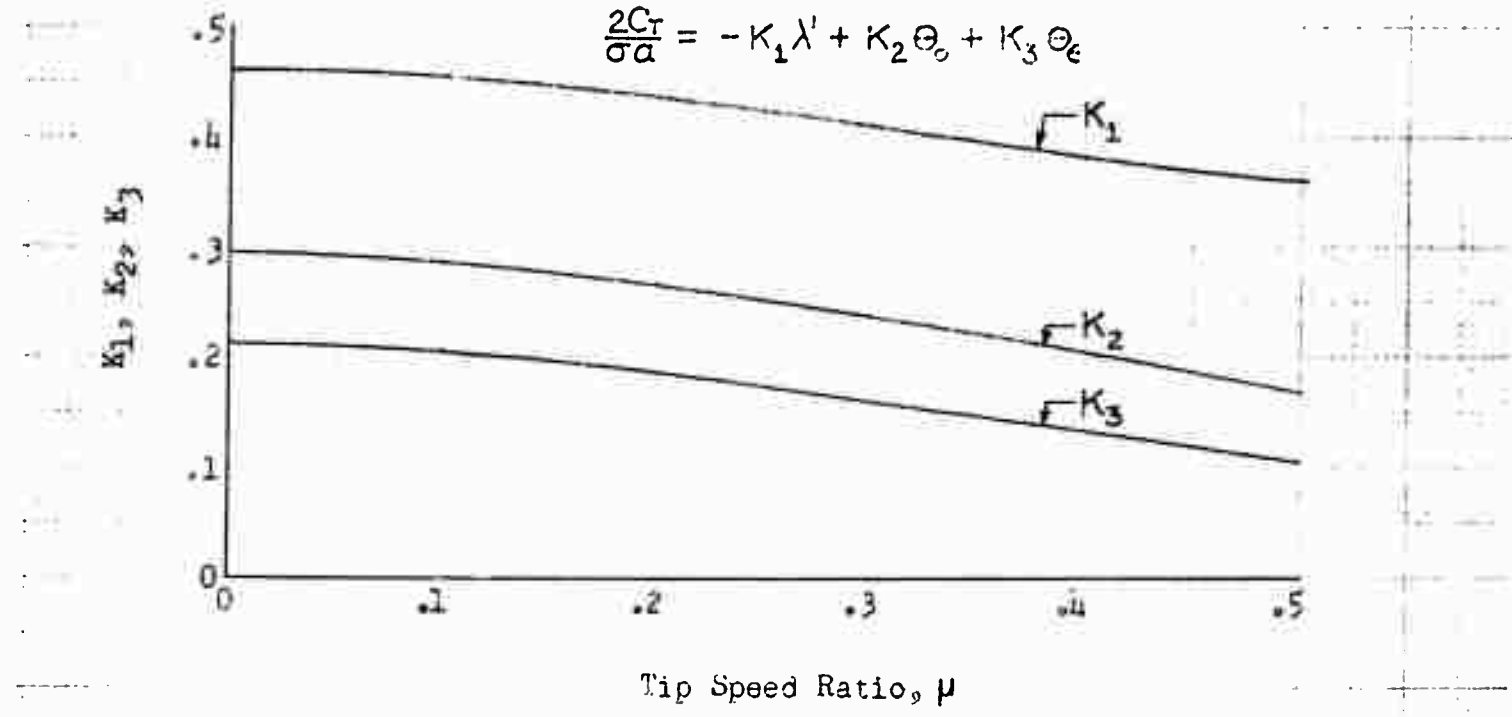

Figure 2-10

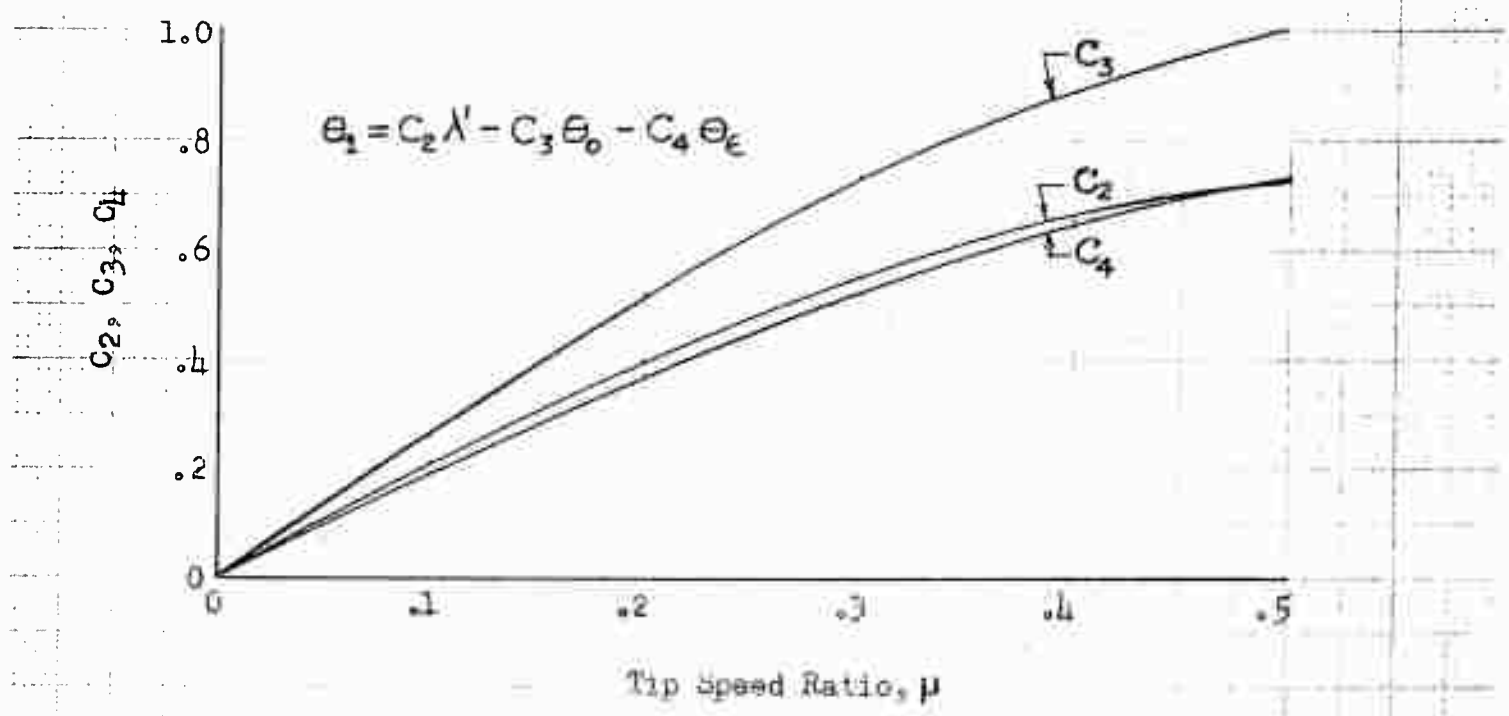

Figure 2-11

the tip at $\Psi = 270^\circ$ is needed to determine tip stall limits. Substituting $x = 1$, $\Psi = 270^\circ$, and $\theta_2 = 0$ in equation 2-51, substituting for θ_0 and θ_1 from equations 2-53 and 2-54, and substituting $2C_T/\sigma a = C_{L_r}/3a$ (equation 2-19), an expression for the retreating tip angle of attack may be written

$$\alpha_{(1)(270)} = A_1 C_{L_r} + A_2 \lambda' + A_3 \theta_\epsilon \qquad 2\text{-}55$$

A similar expression for the tip angle of attack on the advancing side at $\Psi = 90^\circ$, useful in determining the advancing blade compressibility limits as discussed in paragraph 2 which follows, is

$$\alpha_{(1)(90)} = A_1' C_{L_r} + A_2' \lambda' + A_3' \theta_\epsilon \qquad 2\text{-}56$$

The coefficients A_1, A_2, A_3, A_1', A_2', and A_3' involve only the coefficients K_1, K_2, K_3, C_2, C_3, and C_4, from equations 2-52 and 2-54, and are therefore also functions only of tip speed ratio μ and tip loss factor B.

Figure 2-12 on the following page is a plot of these A coefficients versus μ, for the assumed value of B = 0.96.

The incidence angle of the tip path plane α' can be calculated as the angle whose tangent is the overall helicopter drag-lift ratio, as follows:

$$\alpha' = \tan^{-1}\left(\frac{D_p + H}{W}\right) \qquad 2\text{-}57$$

In this equation, D_p is the parasite drag (equation 2-33), and H is the residual downstream drag force of the rotor, which may be shown (Reference 4) to be equal to

$$H = \frac{550}{V}(Rhp_H)2\mu^2 \qquad 2\text{-}58$$

where Rhp_H is the hovering profile horsepower, calculated from either equation 2-18 or 2-30, with $K_\mu = 1.0$, and V is in ft/sec.

As may be seen from equation 2-55, a given set of values of λ', θ_ϵ, and μ (which fixes the values of A_1, A_2, and A_3), establishes a direct relationship between the mean blade lift coefficient C_{L_r} and the retreating tip angle of attack. Thus $\alpha_{(1)(270)}$ increases as C_{L_r} increases. From inspection of equation 2-21 which shows the relationship between C_{L_r}, blade loading w/σ, density ρ, and tip speed V_T, it can be seen that $\alpha_{(1)(270)}$ will increase as blade loading increases, or as tip speed decreases.

Figure 2-13 on the following page is a typical plot of $\alpha_{(1)(270)}$ and $\alpha_{(1)(90)}$ versus tip speed ratio μ, for a series of mean blade lift coefficients and tip speeds. This chart was prepared for a single rotor helicopter with a blade twist of -8° and an assumed flat plate area ratio $A_\pi/W = 0.0025$, which from Figure 2-7 may be shown to correspond to a 10,000 lb. gross weight helicopter with fixed landing gear, carrying payload internally. The disk loading assumed for this chart was 4 lb/ft^2, however, it has been found that other disk loadings up to 12 lb/ft^2 changes the tip angles of attack shown in Figure 2-13 by a negligible amount. Thus, for preliminary analyses it is sufficient to assume that $\alpha_{(1)(270)}$ and $\alpha_{(1)(90)}$ are independent of disk loading. Note also that changing the tip speed from 600 to 700 ft/sec causes essentially no change in $\alpha_{(1)(90)}$ and causes only a slight increase in $\alpha_{(1)(270)}$ at the higher values of μ.

TRANSPORT HELICOPTER DESIGN ANALYSIS METHODS

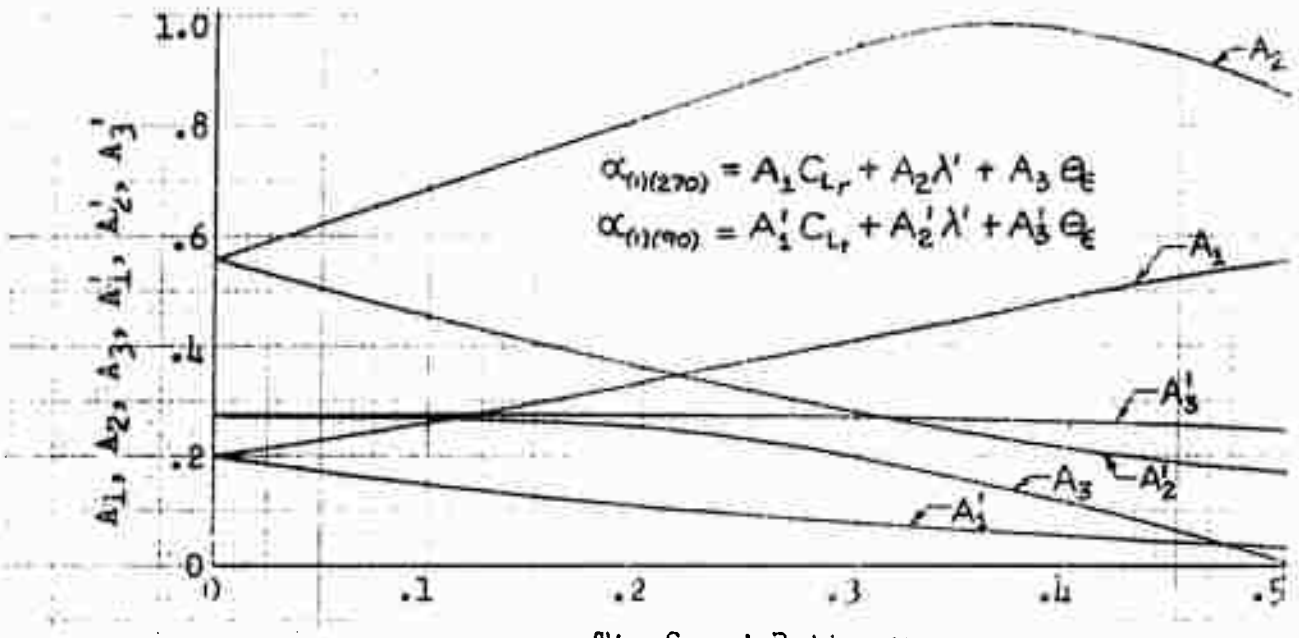

Figure 2-12

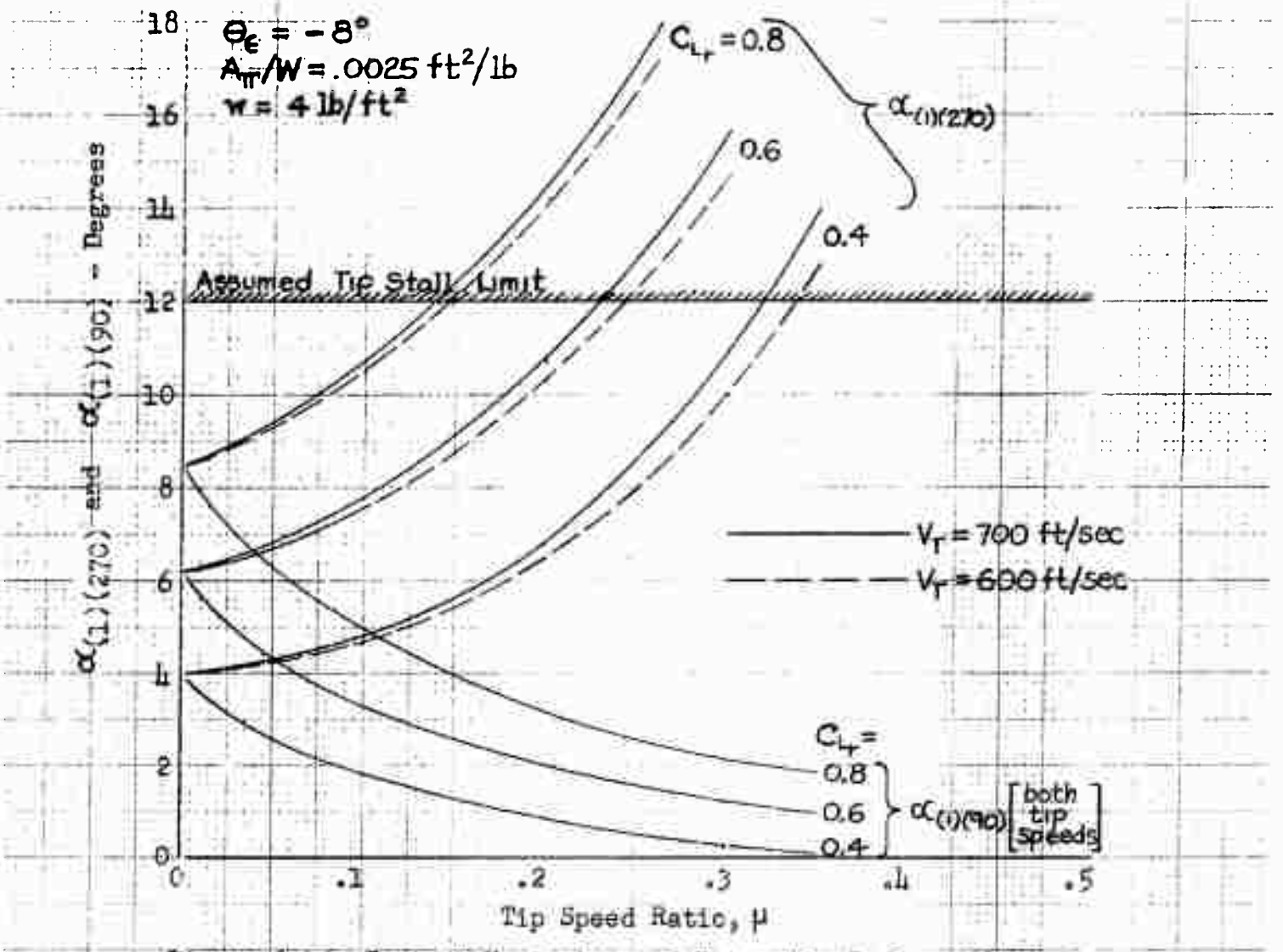

Figure 2-13: Typical Variations of Rotor Tip Angles of Attack

SECTION 2 - AERODYNAMICS AND PERFORMANCE ANALYSIS TECHNIQUES

Assuming a tip stall limit of $\alpha_{(1)(270)} = 12^\circ$, which is commonly used by the NACA for most airfoils now used on helicopter blades, the stall-limited values of μ for each C_{L_r} may, from Figure 2-13, be converted to limits on forward speed in knots at a given tip speed. Figure 2-14 below presents an example of these limits in the form of a chart of minimum (stall-limited) tip speed versus C_{L_r} at sea level, for selected forward speeds of 100 knots and 120 knots.

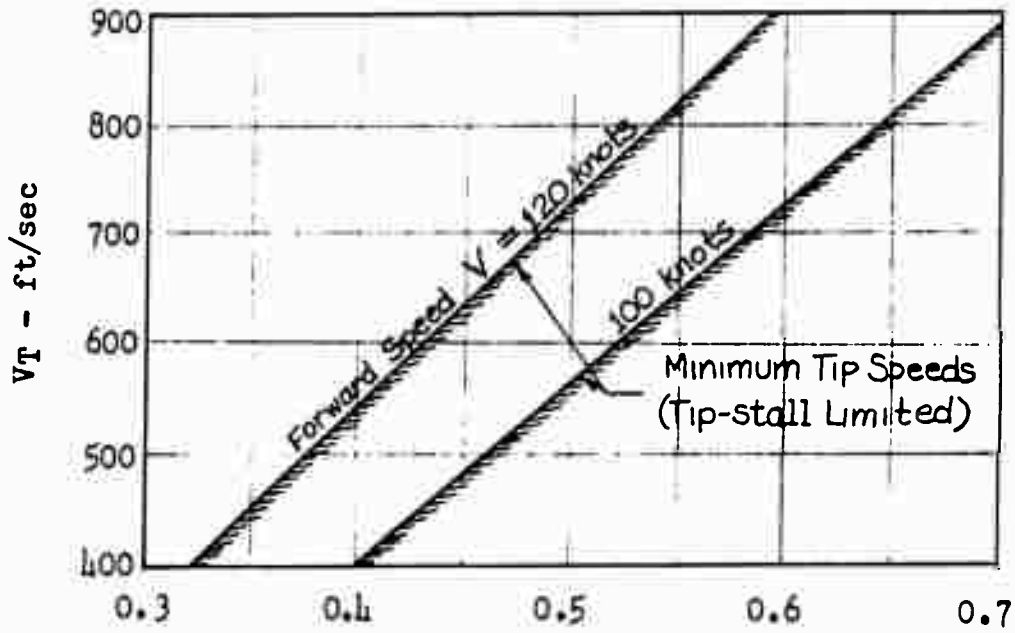

Figure 2-14

2. Advancing Blade Tip Compressibility Drag Rise

The NACA (Reference 7) has established from tests of a helicopter rotor at zero forward speed at a series of tip speeds, a variation of "drag divergence" Mach number of the blade tip, beyond which a marked increase in torque and power was measured. A mean fairing of this NACA data is plotted as the lower dashed line in Figure 2-15. Since the NACA data were taken in the zero forward speed condition, in which the blade angles of attack and attendant drag are the same for any azimuth position, this curve may be somewhat conservative as a limit for the advancing blade tip in forward flight, since in the latter condition only the blade tips at or near $\Psi = 90^\circ$ contribute to the compressibility rise in power (except in cases of extremely high C_{L_r} at intermediate forward speeds, in which case drag divergence may occur first on the retreating blade tip). The probability that actual limiting advancing tip Mach numbers are not as severe as the NACA data would indicate is apparently borne out by actual flight tests of Sikorsky, Piasecki, and Bell machines, publicized reports of which indicate advancing tip Mach numbers as high as 0.8 or 0.9 have been demonstrated with no noticeable adverse effects. In the absence of more definite quantitative data, the upper curve included in Figure 2-15, taken from Reference 8, is suggested as a practical limit, for currently used helicopter blade sections.

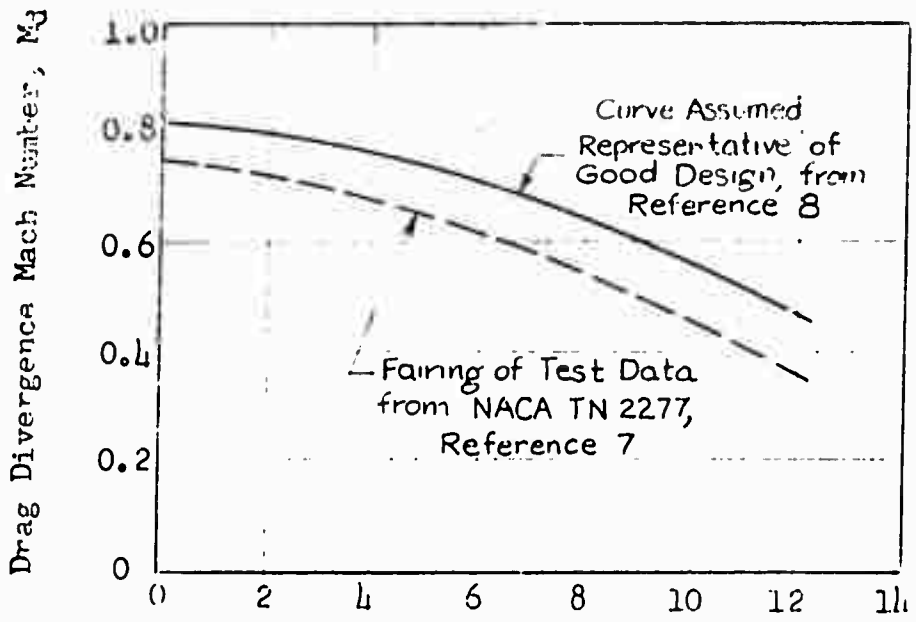

Figure 2-15

Using advancing tip angle of attack data, from plots of $\alpha_{(1)(90)}$ versus μ similar to Figure 2-13, compressibility limits on tip speed and forward speed can be determined from Figure 2-15. At a given μ and forward speed, the compressibility-limited tip speed, in ft/sec, is

$$V_{T_{max}} = \frac{a_s M_d}{1 + 1.69\mu_{min}} \qquad 2\text{-}59$$

where $\mu_{min} = V/V_{Tmax}$
V = forward speed in knots
M_d = assumed drag divergence Mach number, from Figure 2-15, corresponding to $\alpha_{(1)(90)}$ from Figure 2-13 for given C_{L_r} and μ_{min}
a_s = speed of sound in ft/sec
1116 ft/sec at sea level
1097 ft/sec at 5000 ft
1076 ft/sec at 10000 ft

The resulting limits may again be presented, as was done for the tip stall limits, in a chart of V_T versus C_{L_r} for given values of forward speed. Figure 2-16 on the following page combines the compressibility limits calculated for the example used previously ($A_T/W = 0.0025$, blade twist $\theta_\epsilon = -8^o$) for forward speeds of 100 and 120 knots, at sea level, with the tip stall limits from Figure 2-15. Also included on this chart are lines of constant blade loading, w/σ. Charts of this type are quite useful in delineating the areas of tip speed, mean blade lift coefficient, and blade loading in which it is permissable to operate, at given forward speeds, with no tip stall or compressibility effects.

$\Theta_c = -8°$
$A_\pi/W = .0025\ ft^2/lb$

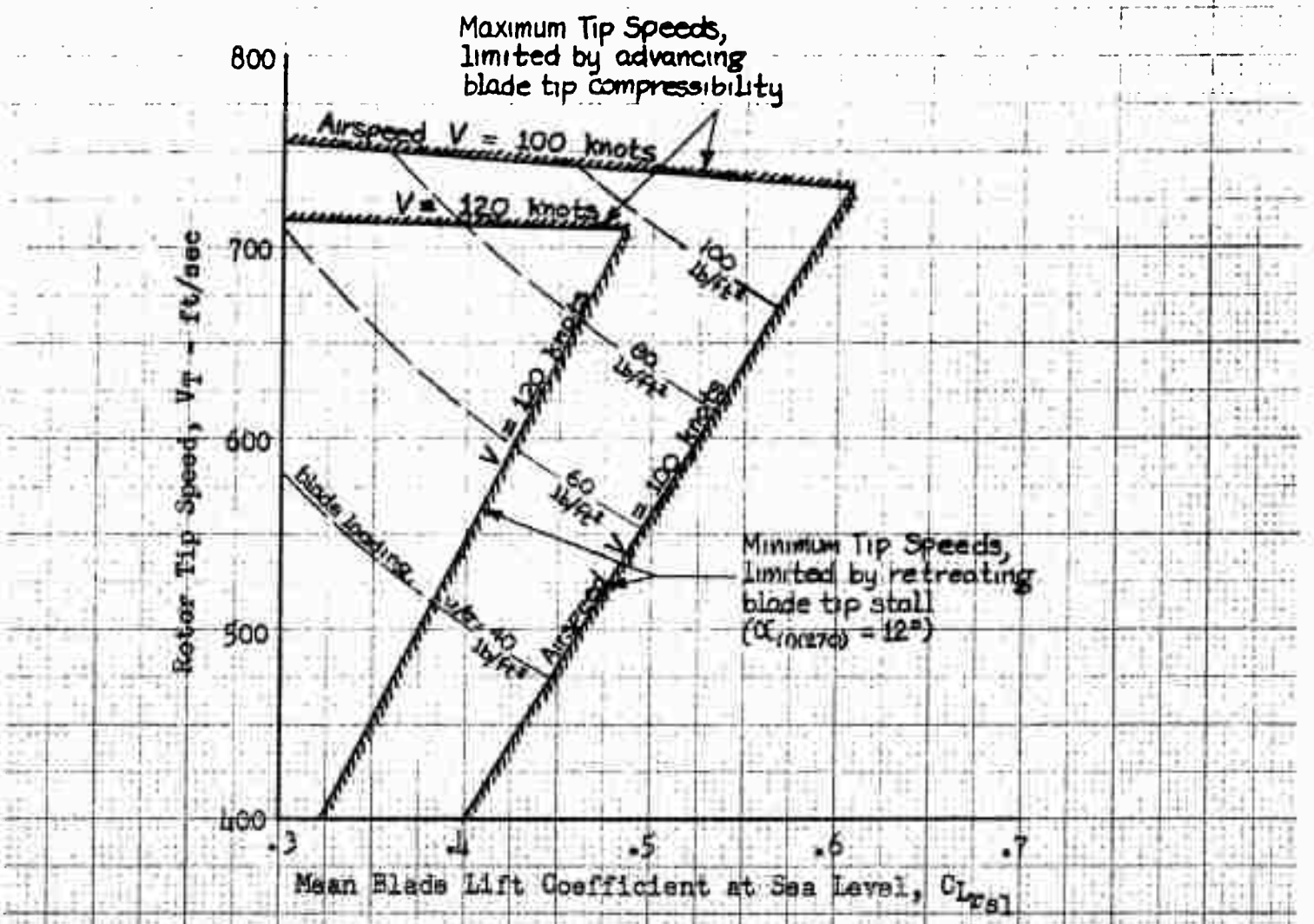

Figure 2-16: Typical Rotor Tip Stall and Compressibility Limits

TRANSPORT HELICOPTER DESIGN ANALYSIS METHODS

For an optimization study such as that of Reference 1, the advancing blade tip angles of attack may be held at an ideal zero degrees at any specified forward speed and tip speed, by proper selection of the blade twist. As seen from Figure 2-15, setting $\alpha_{(1)(90)} = 0^{\circ}$ gives the maximum possible Mach number for drag divergence. Analytically, this is accomplished by setting equation 2-56 for $\alpha_{(1)(90)}$ equal to zero, and solving for θ_{ϵ}, which then represents the optimum blade twist for any specified cruise condition. Thus

$$\alpha_{(1)(90)} = 0 = A_1' C_{L_r} + A_2' \lambda' + A_3' \theta_{\epsilon_{opt.}}$$

or

$$\theta_{\epsilon_{opt.}} = -\frac{A_1'}{A_3'} C_{L_r} - \frac{A_2'}{A_3'} \lambda' \qquad 2\text{-}60$$

The retreating blade tip angle of attack, equation 2-55, can then be rewritten for this ideal condition, substituting for θ_{ϵ} from equation 2-60, as follows:

$$\alpha_{(1)(270)} = A_1 C_{L_r} + A_2 \lambda' - \frac{A_3}{A_3'} A_1' C_{L_r} - \frac{A_3}{A_3'} A_2' \lambda'$$

or

$$\alpha_{(1)(270)} = \left(A_1 - \frac{A_3}{A_3'} A_1'\right) C_{L_r} + \left(A_2 - \frac{A_3}{A_3'} A_2'\right) \lambda' \qquad 2\text{-}61$$

The retreating tip stall limits for this ideal case are determined by the procedure outlined in paragraph (1), and the advancing tip compressibility limits are simply determined by the drag divergence Mach number at zero angle of attack ($M_d = 0.82$ from the assumed upper curve of Figure 2-15).

The maximum tip speed will then no longer decrease as C_{L_r} increases, and the rotor limits chart will have the appearance similar to that shown in Reference 1, Figure B-2, Appendix B.

For an analysis of the incremental power rise when and if it is determined feasible to exceed the tip stall and tip compressibility limits discussed above, the approximate method of Reference 9 is suggested.

SECTION 2 - AERODYNAMICS AND PERFORMANCE ANALYSIS TECHNIQUES

D. PERFORMANCE ANALYSIS

1. Power Available and Design Power Loading

In order to calculate hover ceiling, rate of climb, and cruise performance of the helicopter, the installed power available at sea level, and the manner in which this installed power drops off with altitude, must be known. It is convenient to express the available power in terms of a ratio with gross weight. The design power loading provides a commonly used design parameter for this purpose.

Specifically, design power loading is defined in this report as

$$l_p = \frac{W}{HP} \qquad 2\text{-}62$$

where HP is defined as the engine "Normal Rated Horsepower" at sea level, sometimes referred to as "maximum continuous" power.

For all air-breathing engines, the power available drops off in some fashion as altitude increases, and also as temperature increases. A qualitative and comparative illustration of the general trends in power drop-off at altitude for reciprocating, geared-turbine, turbojet, and ramjet engines is shown in Figure 2-17 below. The power drop of the so-called "pressure jet" helicopter power plant would correspond to the drop-off of whichever type of power plant (reciprocating or geared-turbine) is used to drive the air-source compressor.

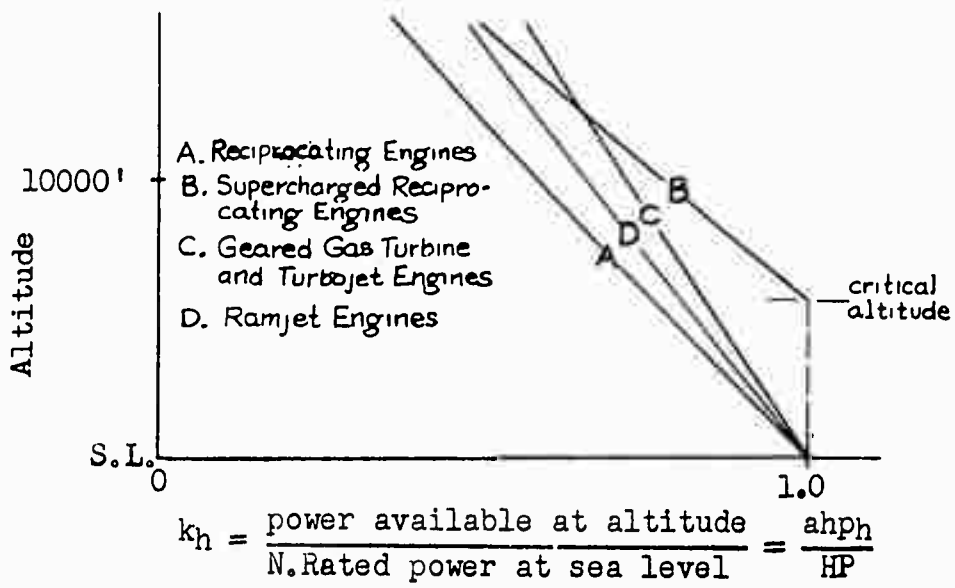

Figure 2-17

Curve B, for reciprocating engines with a single-speed supercharger having one critical altitude, shows constant power below the critical altitude (limited by maximum design internal engine pressures), and a power drop above this altitude at the same rate as for the unsupercharged reciprocating engines.

The reciprocating engines manifest a more rapid drop in power with altitude than do the jet types, because the latter are much more sensitive to inlet air temperature changes, thus as temperature decreases with increases in altitude, the jet engines regain more of the losses due to air pressure and density decreases than do the reciprocating engines. Conversely, if temperature increases at a constant pressure altitude, the reciprocating engines suffer only a slight power

drop, whereas the jet types suffer a very large power drop.

Ramjet engines (Curve D) operate at higher combustion temperatures than the turbine types, hence a decrease in temperature has less effect in changing the temperature ratio of the ramjet, upon which the power output depends, than it does for the turbine types. This explains the more rapid power drop of the ramjet compared with the turbines, as altitude increases.

Generalized quantitative power plant characteristics for the types discussed above, as well as for helicopter pressure jet power plant systems, are included in the example analyses in Part E which follows.

2. Hover Ceiling Analysis

a) Out of Ground Effect:
Hover ceiling is most generally determined graphically, by plotting hover power required (equation 2-36, with $V = 0$, $K_u = 1.0$, and $K_\mu = 1.0$) versus altitude, and superimposing on this a plot of power available versus altitude. The altitude at which these two curves cross is the hover ceiling, as illustrated in Figure 2-18.

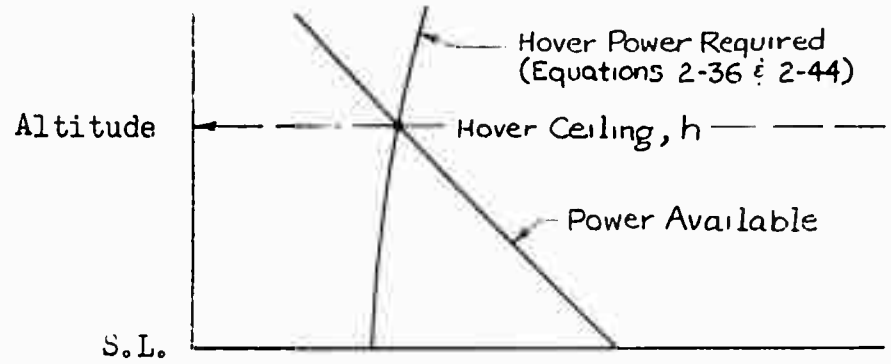

Figure 2-18

If the hover ceiling is specified, and it is desired to determine the sea level design power loading required to achieve this hover ceiling, the following mathematical procedure may be used:

Let h = specified hover ceiling altitude (where, by definition, hover power required equals power available)

$\left(\frac{Bhp_H}{W}\right)_h$ = hover power required per pound gross weight, at altitude h

$\left(\frac{ahp}{W}\right)_h$ = power available per pound gross weight, at altitude h

$k_h = \frac{ahp_h}{HP} = \frac{\left(\frac{ahp}{W}\right)_h}{\left(\frac{HP}{W}\right)}$ = ratio of available power at altitude h, to sea level normal rated power, (obtained from chart such as Figure 2-17)

Then by definition

$$\left(\frac{Bhp_H}{W}\right)_h = \left(\frac{ahp}{W}\right)_h = k_h\left(\frac{HP}{W}\right) = \frac{k_h}{l_p} \qquad 2\text{-}63$$

or

$$l_p = \frac{k_h}{\left(\frac{Bhp_H}{W}\right)_h} \qquad 2\text{-}64$$

Thus, for a given hover ceiling h, and a given engine power drop-off factor k_h, the power loading l_p decreases as $(Bhp_H/W)_h$ increases.

Disk loading is the major influential design parameter affecting hover power required. As may be seen from equation 2-36, if all other design parameters are fixed, then the hover power required per pound gross weight (at V = 0) increases with disk loading. Figure 2-19 below is a general chart illustrating this increase. Included on this chart are dashed curves of available power per pound gross weight necessary for a hover ceiling at altitude h. By definition, (see equation 2-62) the sea level values of these power available curves are the inverse of the design power loading, or $HP/W = 1/l_p$. By this graphical procedure, the variation of l_p with w for a given hover ceiling h can be determined, and plotted in a chart such as Figure 2-20.

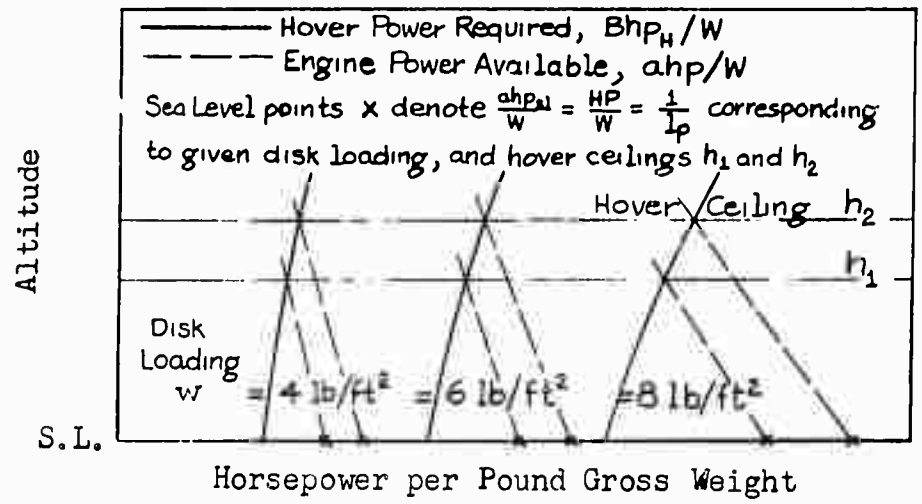

Figure 2-19

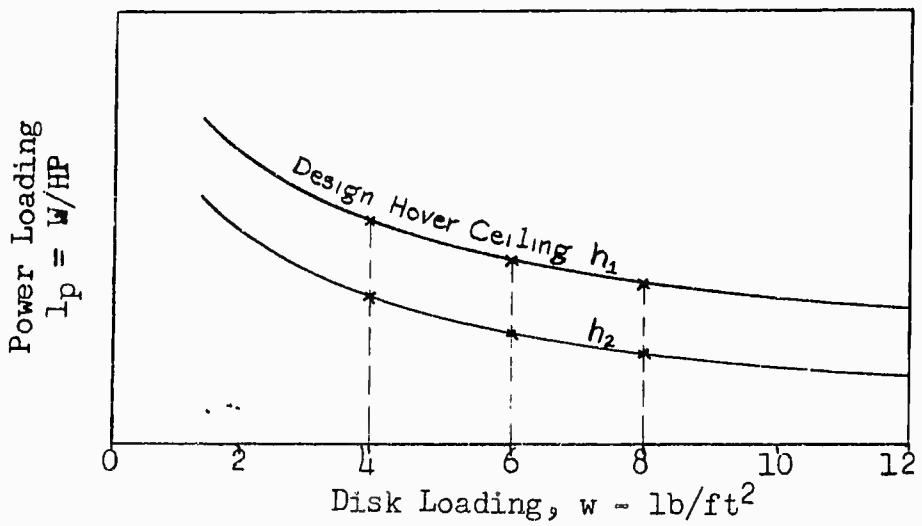

Figure 2-20

b) In Ground Effect:

The effect of the proximity of a lifting rotor to the ground plane is the creation of an air "cushion" of higher pressure, which manifests itself in a reduction of the induced power required to produce given thrust. There are several theoretical treatments of this phenomenon in the technical literature, however, the results of these analyses have not in general given consistent good agreement with test data. For this reason, and in the interest of simplicity, it is considered sufficient for most purposes to rely on fairings from test data, such as shown in Figure 2-21 below.

Figure 2-21 shows a variation of the ratio (ihp_H'/ihp_H) versus the ratio Z/D, where

ihp_H is the hovering induced horsepower out of ground effect
ihp_H' is the hovering induced horsepower in ground effect
Z is the height of the rotor above the ground plane
and D is the rotor diameter.

This chart is based primarily on test data of the Hiller H-23 series helicopters, however, analyses have shown it to predict the hover performance of other manufacturers' helicopters within a few percent of published figures. The curve shows that the ground effect is non-existent ($ihp_H'/ihp_H = 1.0$) at a rotor height of two diameters from the ground plane ($Z/D = 2.0$).

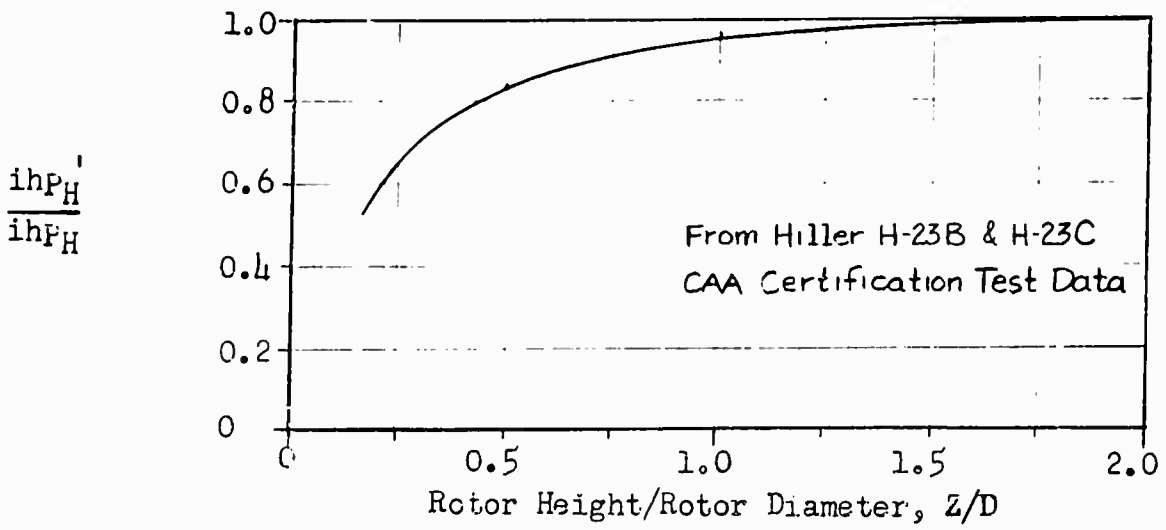

Figure 2-21: Ground Effect

Using Figure 2-21, the hover induced power required at a given Z/D may be calculated by multiplying the hover induced power from equation 2-9 by the ratio ihp_H'/ihp_H. The total power required is then calculated by the procedure previously discussed, and the hover ceiling in ground effect determined in the same manner as illustrated in paragraph 2(a) above.

3. Vertical Rate of Climb

Vertical rate of climb, R/C_V, is calculated herein by the method developed by Wiesner (Ref. 3). In this method, the total flow through the rotor in vertical climb is

$$U_c = R/C_v + u_c \qquad 2\text{-}65$$

where u_c is the induced velocity in climb, which may be shown by momentum theory to be related to vertical rate of climb, and to induced velocity in hover, u_H, by the following relationship:

$$u_c = -\frac{R/C_v}{2} + \left[\frac{(R/C_v)^2}{4} + u_H^2\right] \qquad 2\text{-}66$$

From considerations of kinetic energy, the total flow through the rotor, U_c, is

$$U_c = \frac{550}{1.13}\frac{chp}{W} \qquad 2\text{-}67$$

where the 1.13 factor, as discussed in Part B, paragraph 1 of this section, accounts for the assumption of triangular inflow distribution, and chp is the power available to produce this flow. Hence, chp is the difference between the available power at the rotor, ahp, and the profile power required to overcome the profile drag of the blades. Since the profile power is the same in vertical climb ($\mu = 0$) as in hovering, chp can be written as

$$chp = \eta\, ahp - Rhp_H \qquad 2\text{-}68$$

Dividing equation 2-68 through by gross weight W, then

$$\frac{chp}{W} = \eta\frac{ahp}{W} - \frac{Rhp_H}{W} \qquad 2\text{-}69$$

or, substituting for l_p from equation 2-64, the chp/W available at altitude h is

$$\left(\frac{chp}{W}\right)_h = \eta\frac{k_h}{l_p} - \left(\frac{Rhp_H}{W}\right)_h \qquad 2\text{-}70$$

where $(Rhp_H/W)_h$ is the hover profile power per pound, at altitude h, calculated from equation 2-30 with $\mu = 0$, and ρ/ρ_o corresponding to altitude h.

Equation 2-67 for U_c can be re-written, substituting from chp/W from equation 2-70, as follows:

$$U_c = \frac{550}{1.13}\left[\eta\frac{k_h}{l_p} - \left(\frac{Rhp_H}{W}\right)_h\right] \qquad 2\text{-}71$$

Combining equations 2-65 and 2-66, and re-arranging terms, the vertical rate of climb in ft/sec is

$$R/C_v = U_c - \frac{u_H^2}{U_c} \qquad 2\text{-}72$$

Equation 2-72 is plotted in the form of curves of R/C_v in ft/min. versus U_c Figure 2-22, for various values of hovering induced velocity u_H in ft/sec, which may be calculated as a function of disk loading w from the relationship given in equation 2-5.

4. Maximum Rate of Climb

Maximum rate of climb R/C_{max} of a helicopter is determined in the same manner as for fixed-wing aircraft. The rate of climb at a given forward speed depends on the excess power available for climb (or the difference between power available and power required for level flight), and the maximum occurs at that forward speed at which this excess power is a maximum. Figure 2-23 illustrates

$$R/C_V = 60(U_c - u_H^2/U_c) \text{, in ft/min}$$

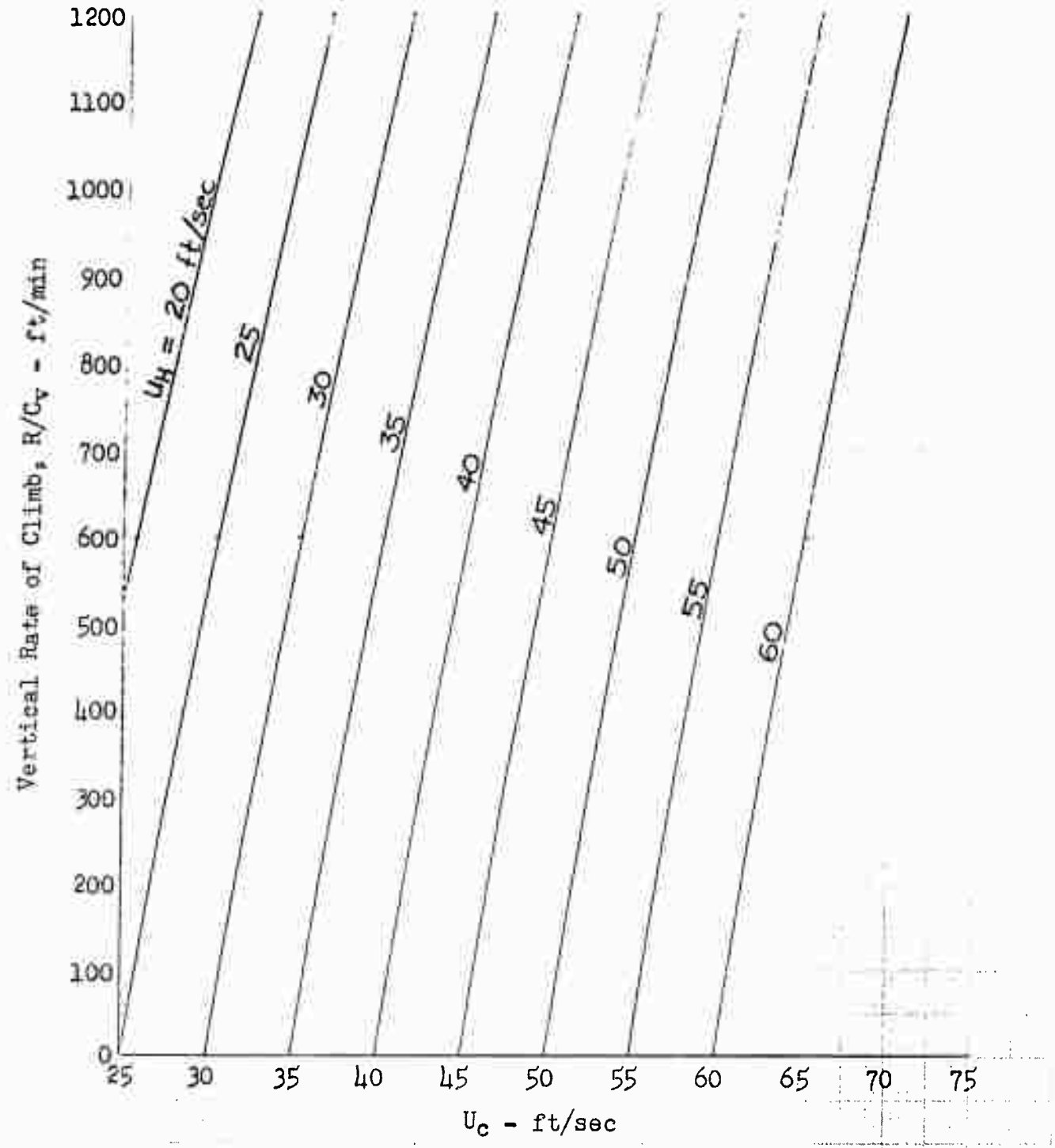

Figure 2-22: Vertical Rate of Climb

the graphical determination of this maximum excess power and corresponding best climb speed, V_c.

The equation for maximum rate of climb is simply derived from the fact that the excess power is converted into climb energy, ft-lbs/min, or the product of the weight being raised times the rate at which it is being raised. Thus

$$\frac{W(R/C)_{max}}{33000} = \eta(ahp - Bhp_{min})$$

or
$$R/C_{max} = 33000\,\eta\left(\frac{ahp}{W} - \frac{Bhp_{min}}{W}\right) \qquad 2\text{-}73$$

The propulsive efficiency, η, is included since the actual excess power available for climb is that available at the main rotor(s).

A general expression for R/C_{max} at any altitude h can be written from equation 2-73, converting the term ahp/W into terms of power loading l_p and engine power drop-off factor k_h (equation 2-64) as follows:

$$(R/C_{max})_h = 33000\,\eta\left[\frac{k_h}{l_p} - \left(\frac{Bhp_{min}}{W}\right)_h\right] \qquad 2\text{-}74$$

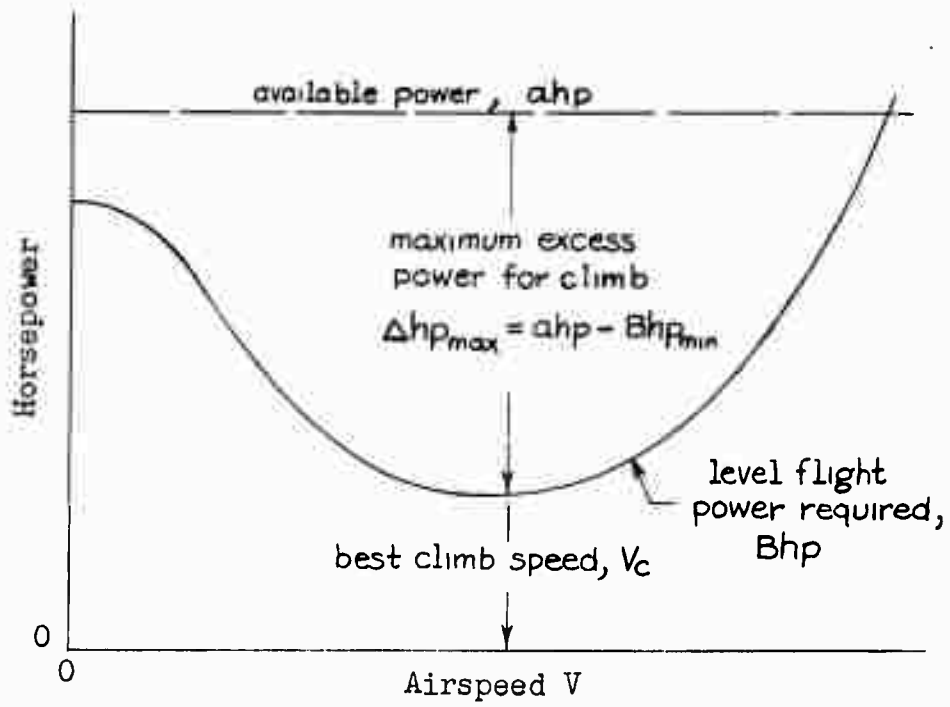

Figure 2-23

5. Cruise Fuel Rate

The cruise fuel rate depends on the level flight power required, at cruise speed, and on the engine fuel consumption characteristics, generally given in terms of the specific fuel consumption, SFC, in lbs. fuel per horsepower-hour. Engine specifications generally present charts of SFC versus the power setting in percent of normal rated power, defined herein as ahp. The percent of ahp in cruise is then

$$\%\text{Power} = 100\ \frac{Bhp_{cruise}}{ahp}$$

or in terms of power loading 1_p and Bhp/W,

$$\%\text{Power} = 100\ (1_p)\left(\frac{Bhp}{W}\right)_{cruise} \qquad 2\text{-}75$$

Defining W_F = fuel weight in pounds
$R_F = W_f/W$ = fuel weight to gross weight ratio

then, the cruise fuel rate in pounds per hour is the derivative

$$\frac{dW_F}{dt} = SFC\,(Bhp)_{cruise} \qquad 2\text{-}76$$

and the cruise fuel rate in pounds of fuel per pound gross weight per hour is the derivative

$$\frac{dR_F}{dt} = SFC\left(\frac{Bhp}{W}\right)_{cruise} \qquad 2\text{-}77$$

For range and radius of action mission analyses, it is convenient to express the fuel rate in terms of pounds fuel per pound gross weight per mile (or per nautical mile, since speed and range are now generally specified by the military in knots and nautical miles, respectively).

Defining R = range or distance traveled, in nautical miles, then the pounds of fuel per nautical mile may be expressed as the derivative

$$\frac{dW_F}{dR} = \frac{1}{V}\frac{dW_F}{dt} = \frac{SFC}{V}\,Bhp_{cruise} \qquad 2\text{-}78$$

and the corresponding derivative of R_F, in pounds per pound per nautical mile is

$$\frac{dR_F}{dR} = \frac{1}{V}\frac{dR_F}{dt} = \frac{SFC}{V}\left(\frac{Bhp}{W}\right)_{cruise} \qquad 2\text{-}79$$

For endurance missions wherein the endurance time T_e is of primary importance, equation 2-77 is useful, since for a given fuel weight/gross weight ratio R_F,

$$\text{Endurance } T_e = \frac{R_F}{(dR_F/dt)}, \quad \text{in hours} \qquad 2\text{-}80$$

and for range missions wherein the distance R is of primary importance, Equation 2-79 is useful, since

$$\text{Distance } R = \frac{R_F}{(dR_F/dR)}, \quad \text{in nautical miles} \qquad 2\text{-}81$$

SECTION 2 - AERODYNAMICS AND PERFORMANCE ANALYSIS TECHNIQUES

It is apparent that maximum endurance is attained at the speed at which dR_F/dt is a minimum, and maximum distance is attained at the speed at which dR_F/dR is a minimum, for a given fuel weight/gross weight ratio, R_F.

The method and steps suggested for determining minimum dR_F/dt and minimum dR_F/dR, and corresponding best endurance and best cruise speeds, $V_{end.}$ and V_{cr}, are illustrated below in Figure 2-24.

① Given engine SFC curve vs. %power ⇒ SFC

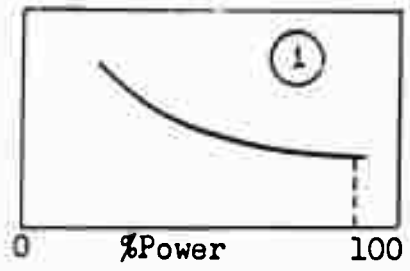

② For a given set of design parameters (w, l_p, A_π/W, V_T, η, cd_o), calculate Bhp/W vs. V from equations 2-36 and 2-44. ⇒ $\frac{Bhp}{W}$

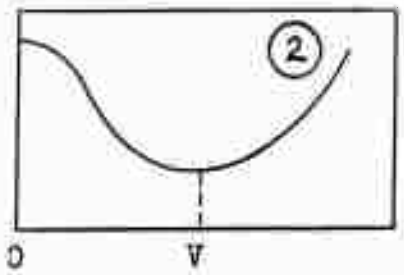

③ Using data in ② and specified power loading l_p, calculated % power vs. V from equation 2-75. Read SFC for this variation in %power from ① , and calculate dR_F/dt from equation 2-77. Determine minimum dR_F/dt and corresponding V_{end}, graphically, from plot as shown. ⇒ $\frac{dR_F}{dt}$

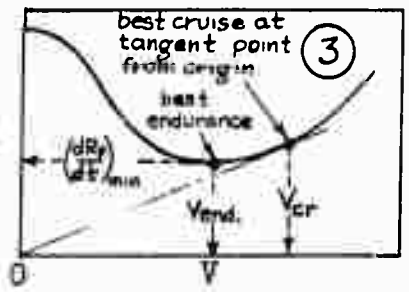

④ Using data in ① , ② , and/or ③ , calculate dR_F/dR from equation 2-79. Determine minimum dR_F/dR and corresponding best cruise speed V_{cr} graphically, from plot as shown. ⇒ $\frac{dR_F}{dR}$

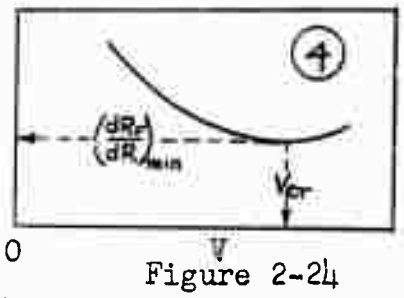

Figure 2-24

NOTE: Best cruise speed V_{cr} and minimum dR_F/dR may also be determined from chart in step ③ . Tangent to dR_F/dt curve, drawn from origin, establishes V_{cr}, and from equation 2-79 the minimum $dR_F dR$ is equal to $(dR_F/dt) @ V_{cr} \div V_{cr}$.

TRANSPORT HELICOPTER DESIGN ANALYSIS METHODS

6. Fuel Weight Ratio, R_F, for Specified Missions:

Usually the mission is spelled out in detail, including for example a specified time for start and warm-up at normal rated power, climb on course to a specified cruise altitude, cruise at altitude to a remote base, descend to landing at remote base (with no fuel used and no distance credit - a simplifying approximation), followed by a return to home base in same manner as above, and a specified percentage of total fuel remaining as reserve at the end of the mission. Military Specification MIL-C-5011A (Ref. 16) is an example publication in which standard missions for helicopters are specified.

a) Radius of action mission:
The fuel weight ratio R_F required to meet the given mission requirements is calculated as the sum of the incremental R_F for climb, cruise, and start, plus the percent held in reserve.

Total Fuel	=	Climb Fuel	+	Cruise Fuel	+	Start & Warm-up Fuel	+	Reserve Fuel

$$R_F = \Delta R_{F_1} + \Delta R_{F_2} + \Delta R_{F_3} + k_r R_F \qquad 2\text{-}81$$

where climb fuel

$$\Delta R_{F_1} = 2\left(\frac{h_1 - h_o}{R/C}\right)\left(\frac{V_c}{60}\right)\left(\frac{dR_F}{dR}\right)_o \qquad 2\text{-}82$$

cruise fuel

$$\Delta R_{F_2} = 2\left(R - \frac{h_1 - h_o}{R/C}\,\frac{V_c}{60}\right)\left(\frac{dR_F}{dR}\right)_{min} \qquad 2\text{-}83$$

start and warm-up fuel

$$\Delta R_{F_3} = 2\left(\frac{t_s}{60}\right)\left(\frac{dR_F}{dt}\right)_o \qquad 2\text{-}84$$

reserve fuel fraction k_r.

and h_1 = cruise altitude in feet

h_o = base altitude in feet

R/C = average maximum rate of climb in ft/min, from h_o to h_1

V_c = airspeed for maximum rate of climb in knots

$\left(\frac{dR_F}{dR}\right)_o$ = full throttle fuel rate per pound gross weight per n. mile

$\left(\frac{dR_F}{dt}\right)_o$ = full throttle fuel rate per pound gross weight per hour

$\left(\frac{dR_F}{dR}\right)_{min}$ = cruise fuel rate per pound gross weight per n. mile

t_s = time for one start and warm-up in minutes

R = mission radius of action in n. miles

SECTION 2 - AERODYNAMICS AND PERFORMANCE ANALYSIS TECHNIQUES

b) Endurance mission:
The R_F for an endurance mission is calculated in the same manner as for the radius of action mission, with the exception that the cruise fuel at altitude h_1 is

$$\Delta R_{F_2} = \left(T_e - \frac{h_1 - h_2}{60 R/C}\right)\left(\frac{dR_E}{dt}\right)_{min} \qquad 2\text{-}85$$

and the 2 is removed from the expressions for climb and start fuel if only one start and one climb are specified.

c) Range mission:
The R_F for a range mission, which is the same as the radius of action mission with the exception that there is only one start, climb, cruise and landing, is calculated in the same manner as indicated by equations 2-81 through 2-84, except that the 2 is removed from the equations 2-82, 2-83 and 2-84, and R is defined as the range rather than the radius.

TRANSPORT HELICOPTER DESIGN ANALYSIS METHODS

E. EXAMPLE ANALYSES

As discussed in the Introduction to this report, the data and methods herein are applicable to both single and tandem rotor helicopters, and to geared power plants (reciprocating, and gas turbine) and rotor tip-drive power plants (ram-jets, turbojets, and pressure jets).

The Summary Report of this contract (Ref. 1), presented the results of a parametric analysis of an entire matrix of helicopters of each type, with design hover ceilings varying from 5000 ft. to 10000 ft. out of ground effect, in standard NACA atmosphere, using normal rated power, design payloads varying from one to five tons, and design radii-of-action varying from 25 to 150 nautical miles. The rotor tip-propulsion type of power plants were assumed applicable only to the single rotor helicopters, in these examples. In the following paragraphs, certain of the important aerodynamic data, fixed design parameters and standardized curves, generalized power plant characteristics, design power loadings, and cruise fuel rates are presented for these example helicopters.

1. Fixed Design Parameters and Standardized Curves

For the helicopters in Reference 1, the following design parameters were fixed:

Rotor tip speed V_T.....700 ft/sec
Tip loss factors, B
main rotor.....0.96
tail rotor.....0.90
Main rotor mean blade lift
coefficient at sea level, C_{L_r}.....0.45

Main rotor blade loading, w/σ.....87.3 lbs/ft
Mean blade drag coefficients,
(main rotor) δ_o 0.009
δ_2 .....0.3 (see Figure 2-5)

(tail rotor) $c_{d_{o_t}}$ .....0.02 (constant)

Variation of equivalent parasite
flat plate area with gross weight..... A_e/W $.33W^{.47}$ (see Figure 2-7)

Tail rotor/main rotor diameter
ratios, geared drive helicopters.....0.18
tip-drive helicopters.....0.12

Tail rotor arm/main rotor radius
ratios, geared drive helicopters.....1.23
tip-drive helicopters.....0.75

Tandem rotor overlap, x_o.....0.60
Tandem rotor vertical gap, x_g.....0.10

Gear losses, single rotor, geared.....3%, (K_g = .03)
tandem rotor, geared.....4%, (K_g = .04)

SECTION 2 - AERODYNAMICS AND PERFORMANCE ANALYSIS TECHNIQUES

Using the procedure outlined in Part B, paragraph 7, the variation of K_t (ratio of tail rotor power to total power) versus forward flight speed for geared-drive and tip-drive single main rotor helicopters was calculated. This was done for several representative main rotor disk loadings and flat plate area ratios A/W, and it was found that mean fairings of K_t versus V, adequately represented the calculated values of K_t over the entire range of disk loadings (2 to 12 lbs/ft^2) and flat plate area ratios (.0008 to .0030 ft^2/lb) considered, with an accuracy of ±10%. Since the maximum value of K_t was in the order of 0.1, ±10% accuracy yields an overall maximum error in total power required of ±1%. These mean fairings of K_t for the two single main rotor types are presented in Figure 2-25.

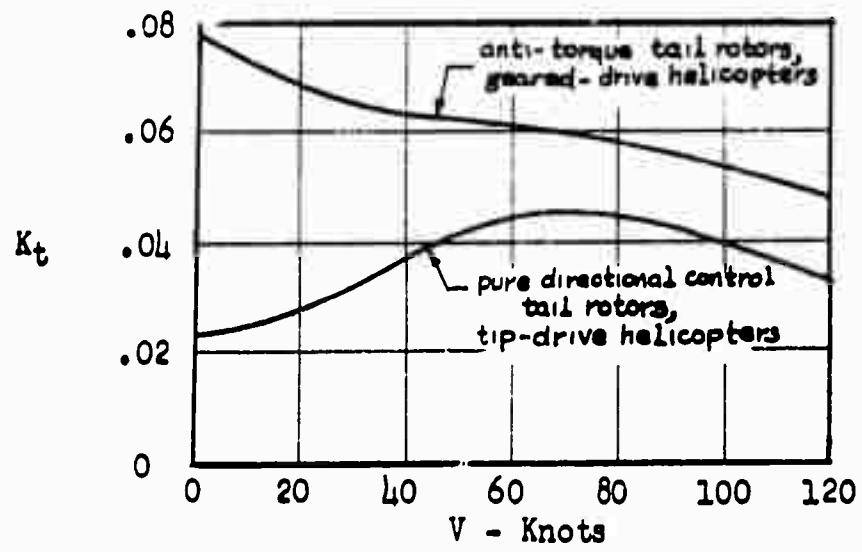

Figure 2-25: Tail Rotor Power Ratio vs. V

The propulsive efficiency $\eta = 1 - K_t - K_g$ corresponding to the K_t variations above, and the assumed constant values of K_g, are plotted in Figure 2-26. Since $K_t = 0$ for the tandem rotor type, its propulsive efficiency is a constant at all airspeeds, equal to 0.96.

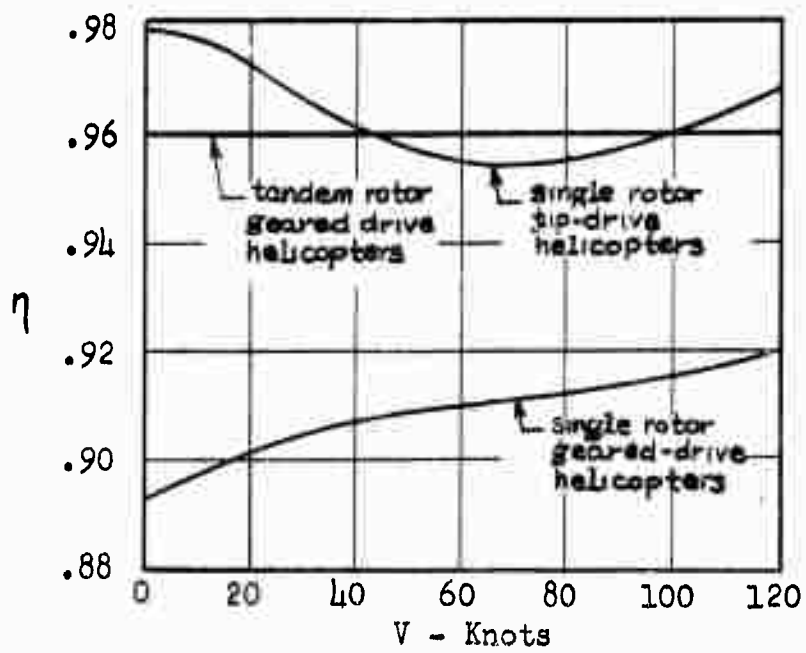

Figure 2-26: Propulsive Efficiency vs. V

2. Assumed Power Plant Characteristics:

Figures 2-27, 2-28, and 2-29 show the assumed power plant characteristics for the example analyses of transport helicopters.

The reciprocating engines were assumed to be radial, aircooled types supercharged to 5000 ft. critical altitude by single-speed, gear-driven superchargers. The performance characteristics for this type of power plant were based on statistics given in a power plant survey, Reference 10. Cooling power loss for the reciprocating engines was assumed to be 5% of normal rated power at sea level, with this percentage decreasing directly as the density ratio at altitude. Hence, the net power available per pound gross weight for reciprocating engines was calculated as

$$\left(\frac{ahp}{W}\right)_{net} = (1 - .05\rho/\rho_o)\left(\frac{ahp}{W}\right)_{chart} \qquad 2\text{-}86$$

The performance characteristics for the geared gas turbine types are based on mean fairings of statistical data taken from published specifications for engines ranging in size from the Continental Artouste to the Allison T-56.

The performance characteristics for the tip turbojet types are based on Packard Motor Car Company estimates presented in Reference 12. These estimates were made in 1954, and have recently been superceded with more optimistic data, particularly with regard to fuel consumption rates.

The tip ramjet engine performance characteristics are based on justifiable estimates, in Reference 11, of expected improvements over present operational types.

The pressure jet performance characteristics are based on the discussion and analysis in the Appendix to this report. Only the "cold cycle" pressure jet was considered, since the "hot cycle" pressure jet is a complex system requiring an entire study by itself. Compressed air at 2.5 atmospheres was assumed to be supplied from separate compressors, driven by geared turbine engines having characteristics identical to those for direct geared power applications. For the example analysis, pressure jet power was set to permit cruising without tip burning, and full power with tip burning up to 3000°F tip burner temperature.

Figure 2-28 is included to show the comparative effects of high temperature on engine power output of the several power plant types. This chart is drawn for an atmospheric air temperature 57°F higher than standard NACA temperature, and thus corresponds to a temperature of 95° at 6000 ft. pressure altitude, or 116°F at sea level pressure altitude.

Figure 2-29 shows the assumed standard variations of SFC with percent of normal rated power at altitude. The percent of normal rated power at altitude is calculated from equation 2-75, repeated below:

$$\%\text{Power} = 100\left(\frac{l_p}{k_h}\right)\left(\frac{Bhp}{W}\right) \qquad 2\text{-}75$$

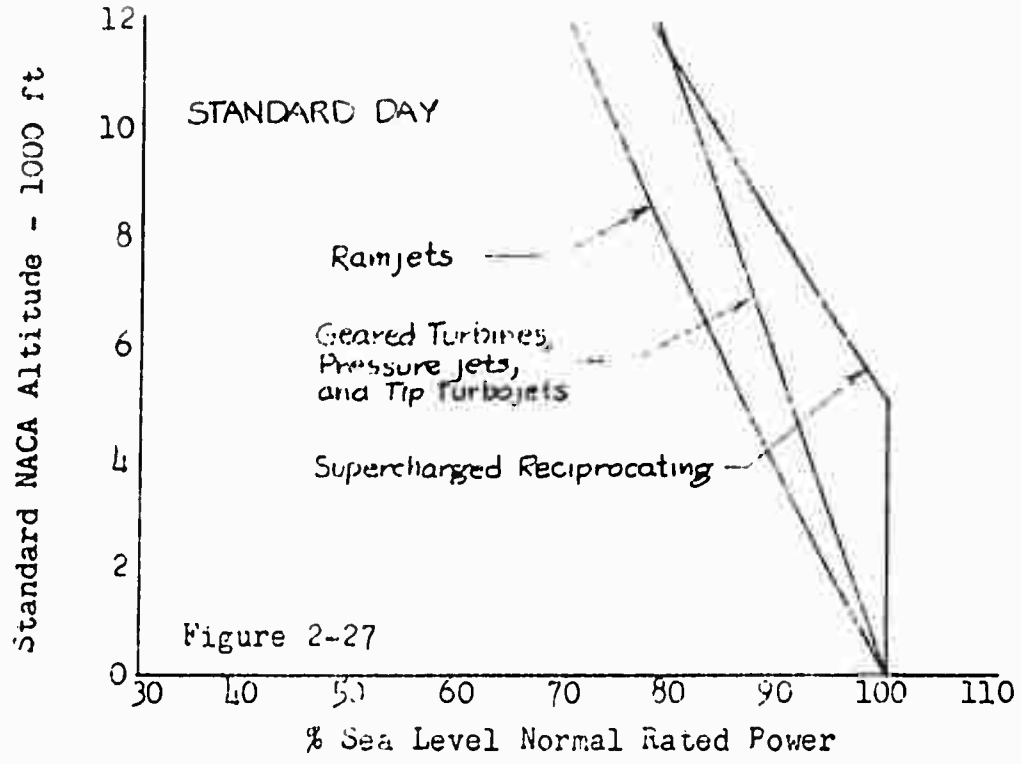

Figure 2-27

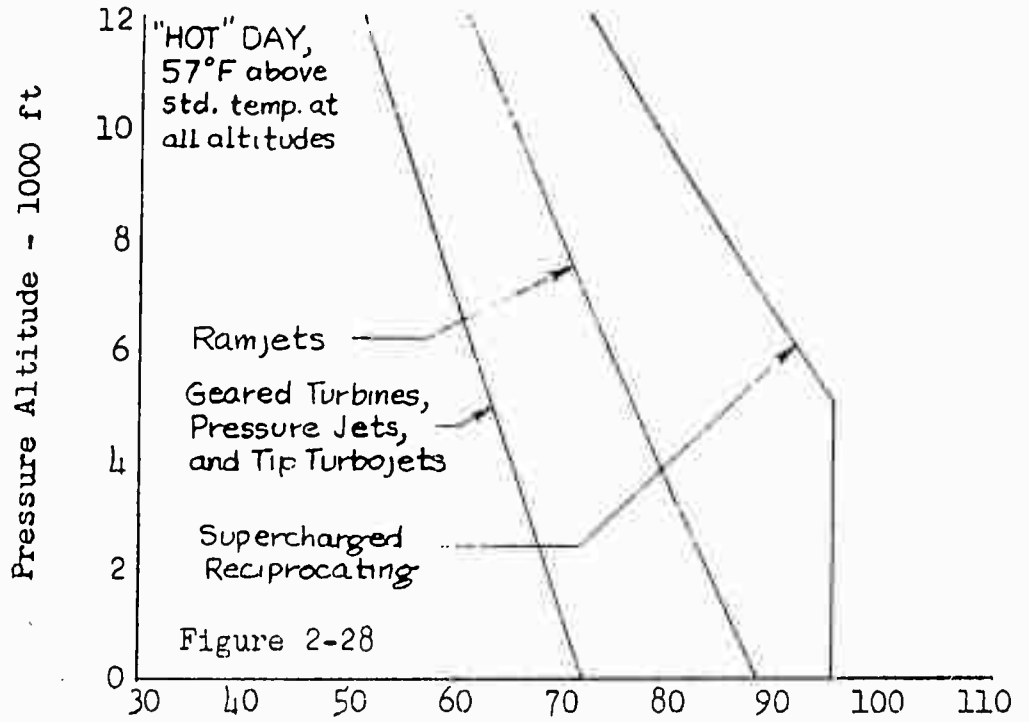

Figure 2-28

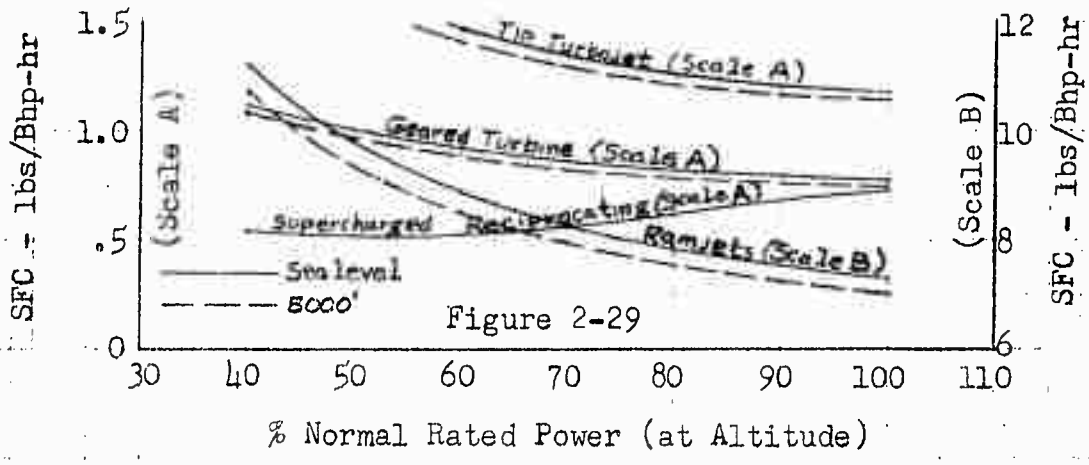

Figure 2-29

3. Design Power Loading for Selected Hover Ceilings

Using the procedures, equations, and assumptions outlined in the preceding paragraphs of Parts B, D, and E, design power loadings were calculated for standard day, out of ground effect hover ceilings of 5000 ft., 7500 ft., and 10000 ft., over a range of disk loadings varying from 2 to 12 lbs/ft^2. This was done for each of the example combinations of rotor configuration and power plant type, and the results are plotted in the form of l_p vs. w in the charts at the end of this Section, listed as follows:

Figure 2-30: Reciprocating Engines
Single Rotor and Tandem Rotor Configurations

Figure 2-31: Geared Gas Turbine Engines
Single Rotor and Tandem Rotor Configurations

Figure 2-32: Tip-Mounted Turbojet Engines
Single Rotor Configurations only

Figure 2-33: Tip-Mounted Ramjet Engines
Single Rotor Configurations only

Figure 2-34: Tip-Mounted Pressure Jets
Single Rotor Configurations only

For the purposes of a parametric analysis to determine the optimum disk loading (yielding minimum gross weight) for a given set of performance specifications (payload, range or radius of action, design hover ceiling) charts such as these are useful for the determination of %Power in cruise, SFC in cruise, and engine weight per pound gross weight. In addition they may be used to determine vertical rate of climb and maximum rate of climb as functions of hover ceiling and disk loading, through the dependence of these performance parameters on power loading l_p, as manifested in equations 2-71 and 2-74. Vertical rate of climb at sea level for all of the examples considered was in excess of 800 ft/min, and maximum rate of climb at sea level was in all cases in excess of 1500 ft/min, for the lowest hover ceiling (5000 ft.) considered. The higher hover ceilings, 7500 and 10000 ft, requiring higher installed power (lower power loading) resulted of course in progressively higher vertical and maximum climb performance.

TRANSPORT HELICOPTER DESIGN ANALYSIS METHODS

3. Design Power Loading for Selected Hover Ceilings

Using the procedures, equations, and assumptions outlined in the preceding paragraphs of Parts B, D, and E, design power loadings were calculated for standard day, out of ground effect hover ceilings of 5000 ft., 7500 ft., and 10000 ft., over a range of disk loadings varying from 2 to 12 lbs/ft^2. This was done for each of the example combinations of rotor configuration and power plant type, and the results are plotted in the form of l_p vs. w in the charts at the end of this Section, listed as follows:

Figure 2-30: Reciprocating Engines
Single Rotor and Tandem Rotor Configurations

Figure 2-31: Geared Gas Turbine Engines
Single Rotor and Tandem Rotor Configurations

Figure 2-32: Tip-Mounted Turbojet Engines
Single Rotor Configurations only

Figure 2-33: Tip-Mounted Ramjet Engines
Single Rotor Configurations only

Figure 2-34: Tip-Mounted Pressure Jets
Single Rotor Configurations only

For the purposes of a parametric analysis to determine the optimum disk loading (yielding minimum gross weight) for a given set of performance specifications (payload, range or radius of action, design hover ceiling) charts such as these are useful for the determination of %Power in cruise, SFC in cruise, and engine weight per pound gross weight. In addition they may be used to determine vertical rate of climb and maximum rate of climb as functions of hover ceiling and disk loading, through the dependence of these performance parameters on power loading l_p, as manifested in equations 2-71 and 2-74. Vertical rate of climb at sea level for all of the examples considered was in excess of 800 ft/min, and maximum rate of climb at sea level was in all cases in excess of 1500 ft/min, for the lowest hover ceiling (5000 ft.) considered. The higher hover ceilings, 7500 and 10000 ft, requiring higher installed power (lower power loading) resulted of course in progressively higher vertical and maximum climb performance.

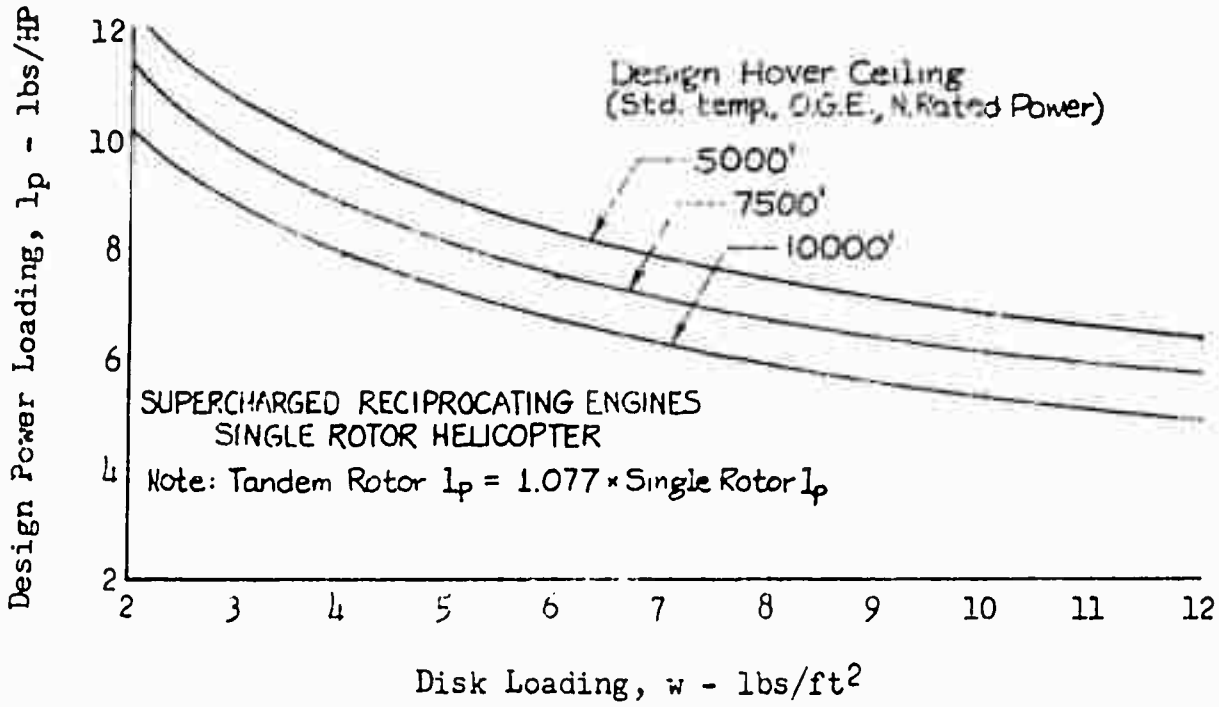

Figure 2-30

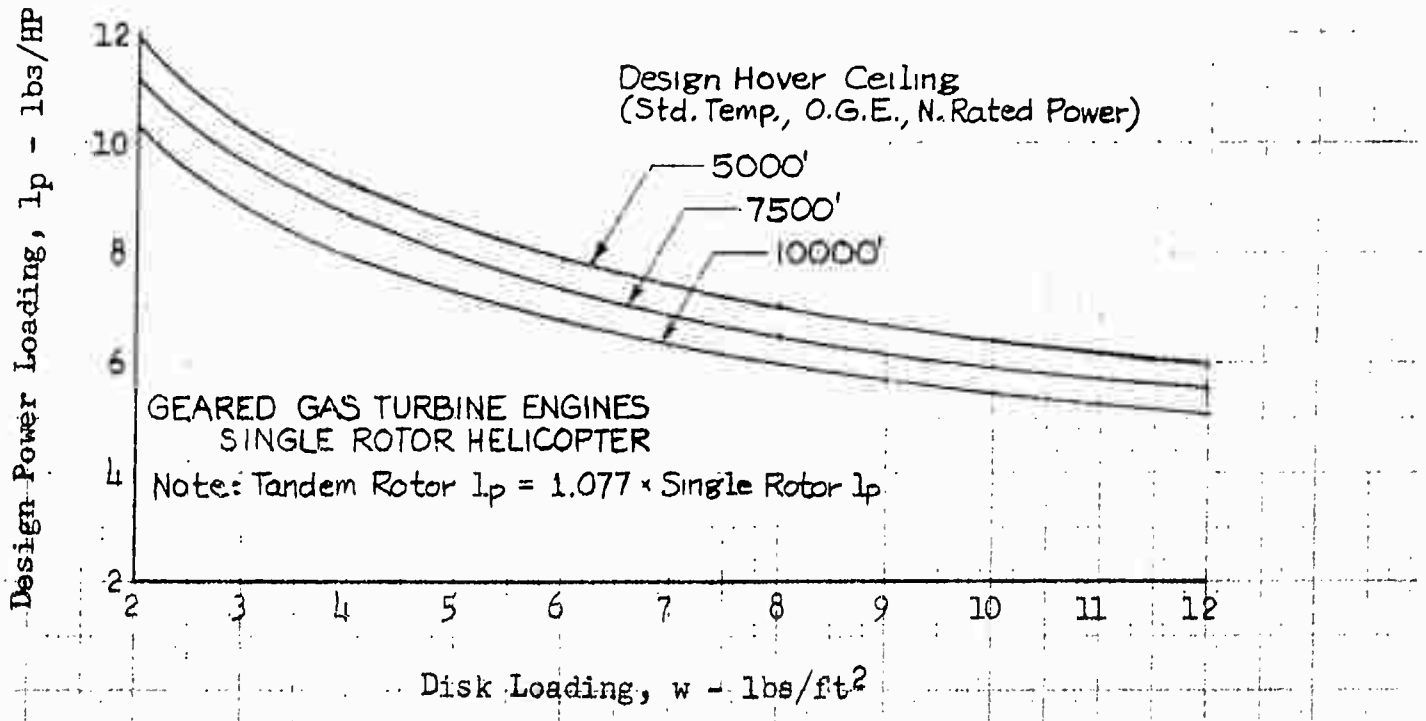

Figure 2-31

TRANSPORT HELICOPTER DESIGN ANALYSIS OF [illegible]

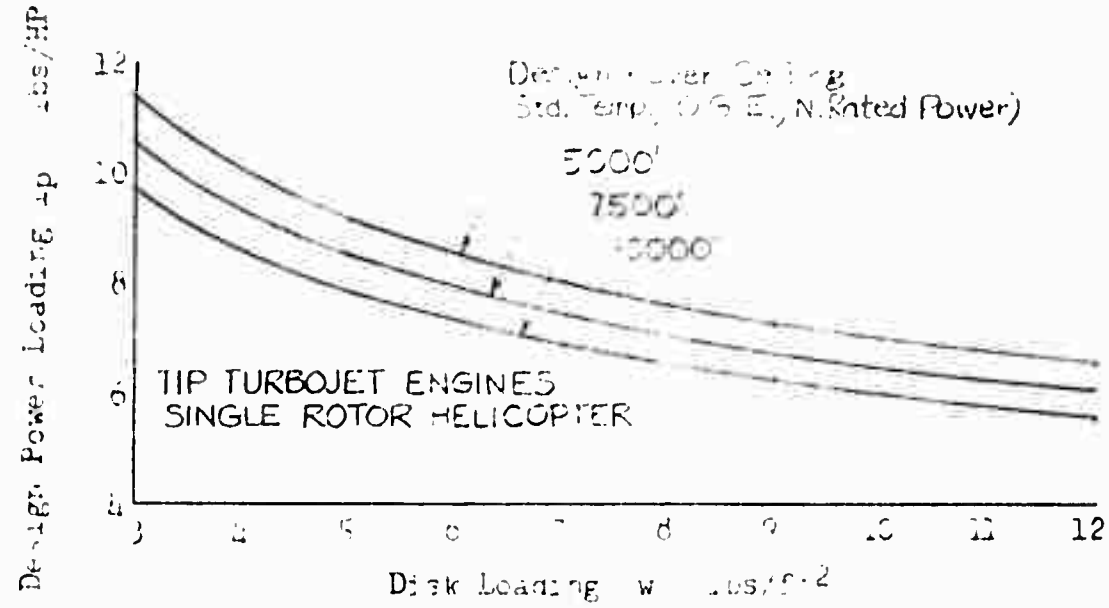

Figure 2-32

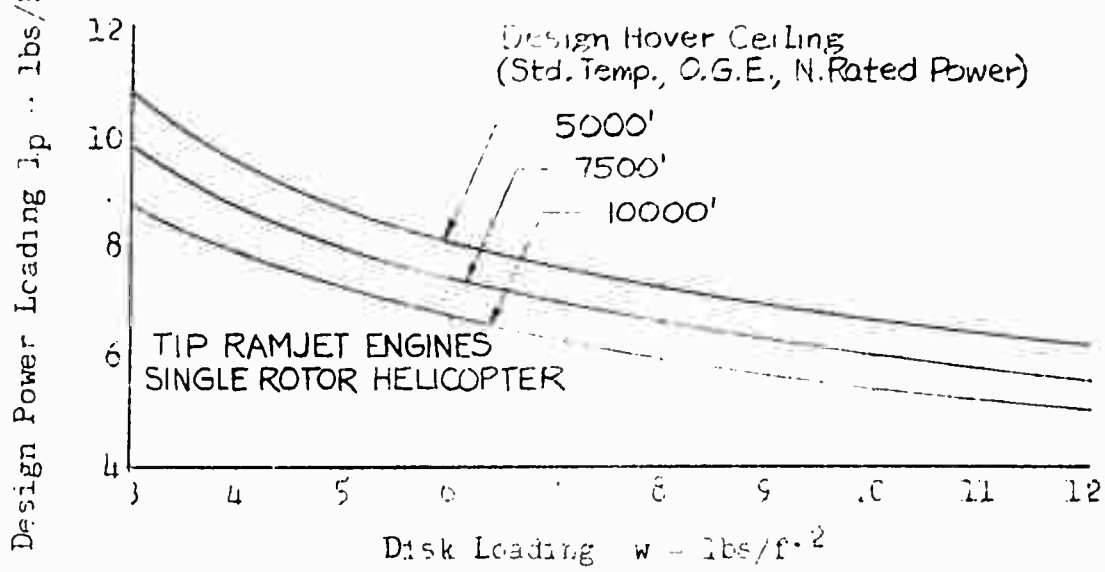

Figure 2-33

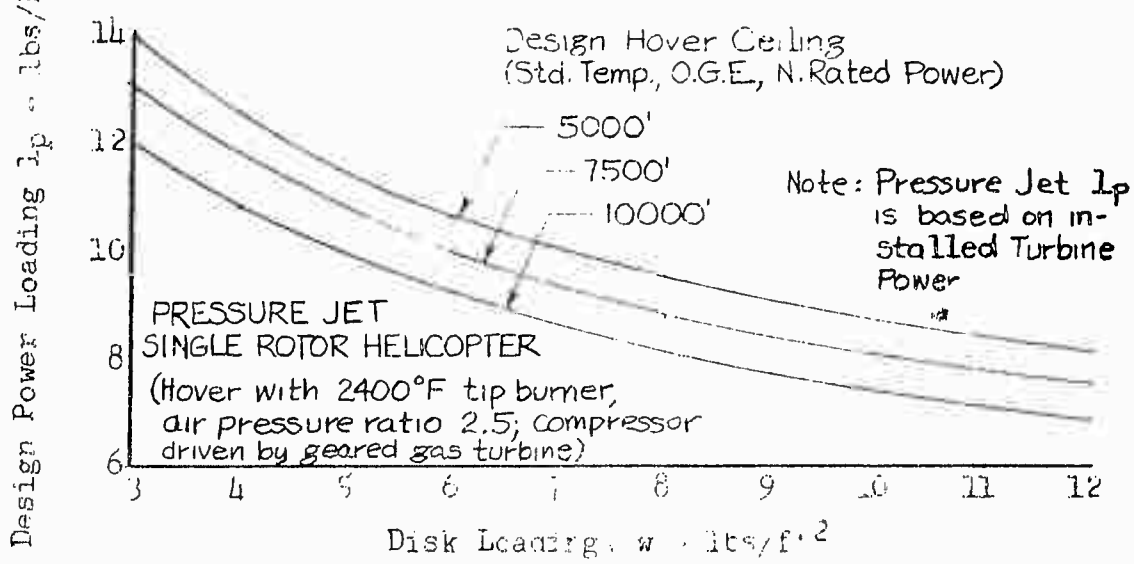

Figure 2-34

4. Charts of Fuel Rate per Mile, dR_F/dR and R_F

In Section 4 of this report, a graphical procedure is presented for determination of minimum gross weight helicopters and corresponding design characteristics from intersections of the curves of fuel weight ratio R_F required for a given mission range or radius of action and fuel weight ratio R_F available for a given mission payload. The required R_F is dependent upon the dR_F/dR derivative, which as has been shown (Part D, paragraph 5) is dependent upon the power required, the design power loading, and engine SFC. The determination of the available R_F is based upon the weight breakdown of the helicopter, the analysis of which is presented in the following Section 3 of this report.

As an illustration, then, of the pertinent charts which evolve from the aerodynamic and power plant performance characteristics of the helicopters, and which are required in the graphical solution procedure discussed in Section 4, plots of dR_F/dR versus cruise speed V, and plots of required R_F versus gross weight for various mission radii of action and various design disk loadings are presented on the following pages. The dR_F/dR curves were calculated from equation 2-79, and the R_F curves from equations 2-81 through 2-84.

These charts are based on the example assumptions listed in paragraphs 1 and 2 above, and on the design power loading charts in paragraph 3, Figures 2-30 through 2-34. In addition, the "required" R_F calculations were based on an assumed standard mission, outlined below in Figure 2-35. The only variables in this general mission sequence are the mission radius of action R, and the allotted time for start and warm-up, which varies as indicated depending on the type of power plant. The lower start times were assumed for the jet type power plants due to their inherent lower times required for warm-up, and their higher SFC, when compared with the reciprocating engines.

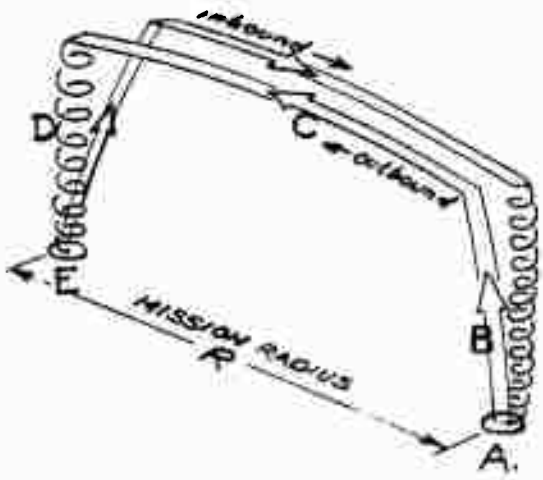

Both home base and remote base ground elevation 4000 ft.
Standard NACA atmosphere, 45°F at ground elevation, 41°F at cruise altitude

A. Start, warmup,* minutes at normal rated (maximum continuous) power.
B. Climb 1000 ft., on course, at best rate of climb, to cruise altitude of 5000 ft.
C. Cruise at 5000 ft. and best cruise power setting, to position directly above remote base.
D. Descend to remote base. No distance credit, no fuel used.
E. Land, stop engines, unload outbound cargo, load inbound cargo, start, warmup, and return to home base in accordance with above.

*Assumed time for start and warmup:

1. Reciprocating engines	5 minutes
2. Gas turbine engines	2 minutes
3. Pressure jets	2 minutes
4. Tip turbo jets	2 minutes
5. Ramjets	½ minute

Figure 2-35 Mission Flight Plan

TRANSPORT HELICOPTER DESIGN ANALYSIS

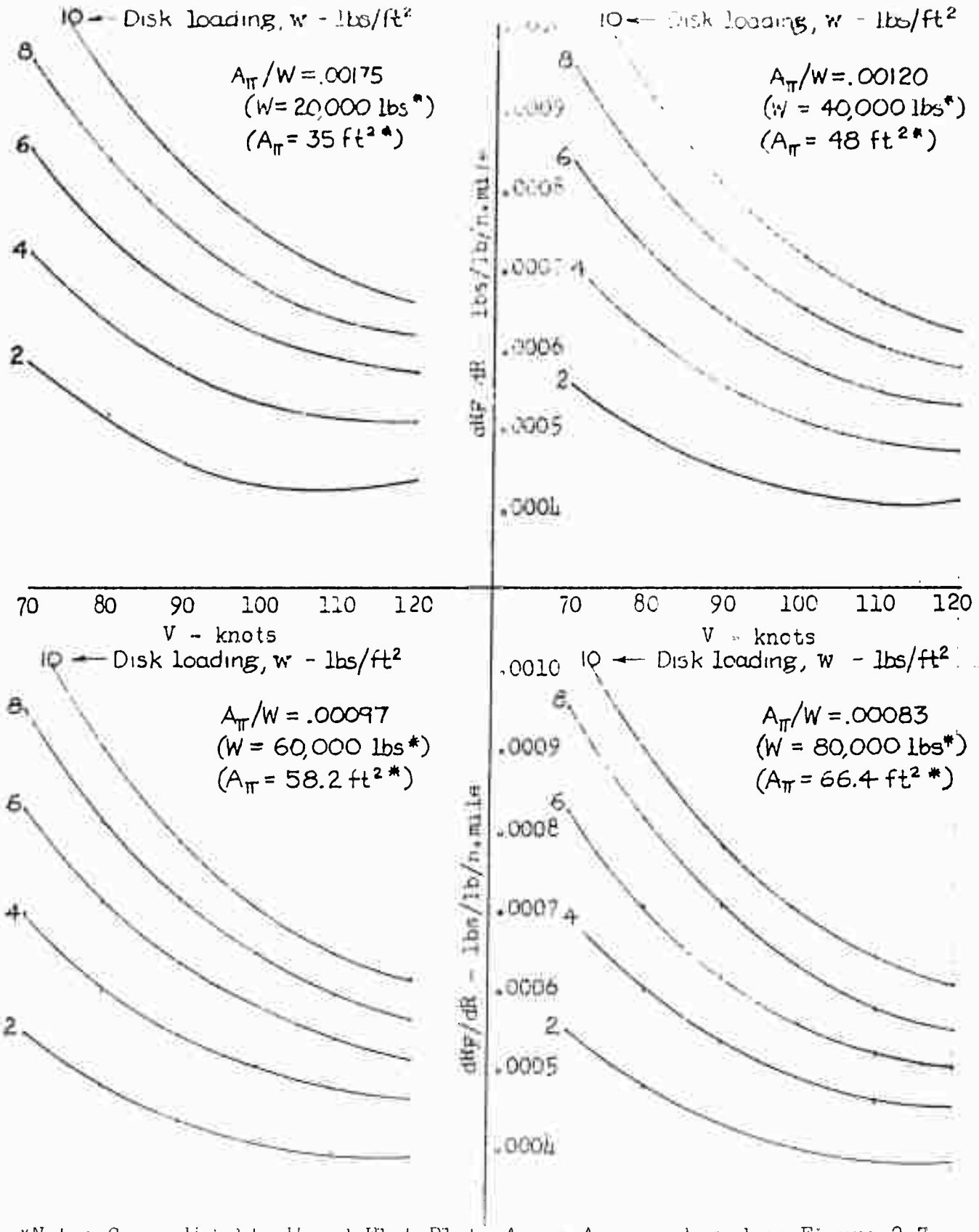

*Note: Gross Weights W and Flat Plate Areas A_{π} are based on Figure 2-7, fixed landing gear, internal payload, $A_{\pi} = .33W^{.47}$

Figure 2-36: Typical Variations of Cruise Fuel Rate dR_F/dR vs. V, at 5000 ft. Cruise Altitude
- Single Rotor Helicopters
- Geared Gas Turbine Engines
- Design Hover Ceiling 5000 ft.

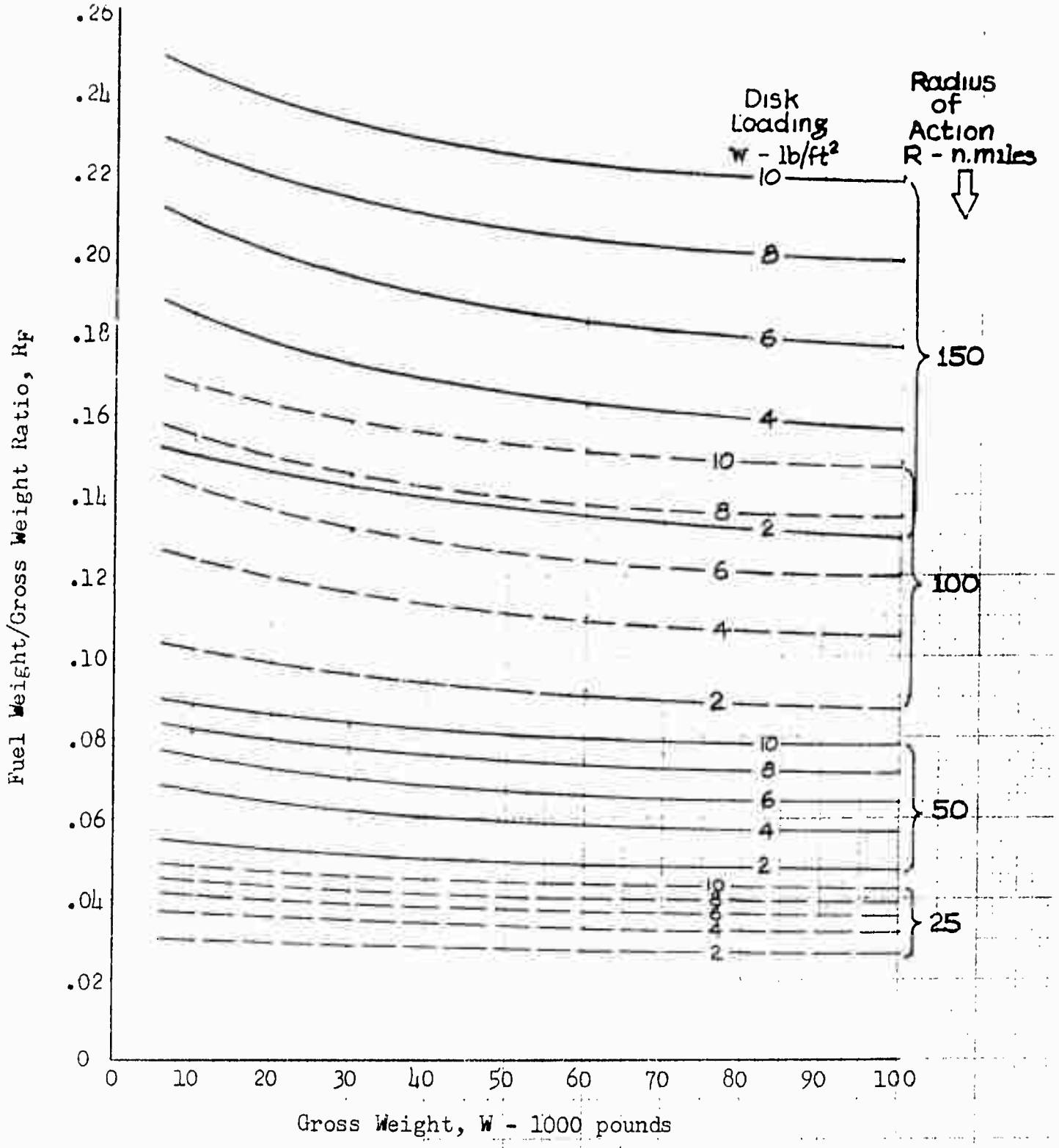

Figure 2-37: Typical Variations of Fuel Weight Ratio R_F vs. Gross Weight for Various Radii-of-Action
- Single Rotor Helicopters
- Geared Gas Turbine Engines
- Design Hover Ceiling 5000 ft.

SECTION 2 - AERODYNAMIC AND PERFORMANCE ANALYSIS TECHNIQUES

SYMBOLS

A_b...Rotor blade area, ft^2
A_e...Projected disk area, tandem rotors, ft^2
A_v...Area used in tandem rotor momentum analysis (see Figure 2-2), ft^2
A_π ..Equivalent parasite flat plate area, ft^2
A_1, A_2, A_3..Coefficients in eq. for $\alpha_{(1)(270)}$
A_1, A_2, A_3..Coefficients in eq. for $\alpha_{(1)(90)}$
a....Slope of airfoil section lift curve, $dC_L/d\alpha$
a_s...Speed of sound, ft/sec
ahp_h.Power available at any altitude h
B....Rotor tip loss factor
Bhp..Total power required in level flight
b....No. of blades per rotor
C_D...Drag coefficient of parasite components
C_{L_r}..Rotor mean blade lift coefficient $6C_T/\sigma$
C_T...Rotor thrust coefficient $T/\rho\pi R^2 V_T^2$
C_2, C_3, C_4..Coefficients in eq. for θ_1
c_{do}.Rotor mean blade drag coefficient
c_4..Coefficient in eq. for K_μ
chp..Induced power + excess for vert. climb
D....Rotor diameter = 2R, ft
D_p...Helicopter parasite drag, lbs
H....Residual downstream drag of rotor, lbs
HP...Installed "Normal Rated" power at S.L.
h....Altitude, ft
hp_g..Gearing power loss
hp_t..Tail rotor power required
ihp..Rotor induced power
K_g... = hp_g/Bhp
K_t... = hp_t/Bhp
K_u... = u/u_H
K_μ .. $1 + 3\mu^2 + c_4\mu^4$
K_1, K_2, K_3..Coefficients in eg. for θ_o
K_h... ahp_h/HP
l_p...Design power loading = W/HP, lbs/hp
l_t...Tail rotor moment arm, ft
M_d...Airfoil section drag divergence Mach No.
php..Helicopter parasite power required
Q....Main rotor torque, lb-ft
q....Free stream dynamic pressure, lbs/ft^2
R....Rotor radius, ft; or mission range or radius of action, naut. miles
R_F...Fuel weight ratio = W_F/W
R/C_v.Vertical rate of climb
R/C..Rate of climb in forward flight
Rhp..Rotor profile power
r....Radius to a blade element, ft
rhp..Total power required at main rotor(s)
ΔS..Frontal area of parasitic component, ft^2
SFC..Specific fuel consumption, lb/hp-hr
T....Rotor thrust, lbs
T_e...Endurance time, hours
t_s...Time allotted for start & warmup, min.
U_c...Total flow thru rotor in vert.climb, ft/sec
u....Rotor induced velocity, ft/sec
u_c...Induced velocity in vert. climb, ft/sec
u_H...Induced velocity in hover, ft/sec
V....Forward flight speed, ft/sec or knots
V_c...Speed for best climb, knots
V_{cr}..Speed for best range, knots
V_{end}.Speed for best endurance, knots
V_T...Rotor tip speed, ft/sec
W....Gross weight, lbs
W_F...Fuel weight, lbs
w....Disk loading, lbs/ft^2
= $W/\pi R^2$(sgl. rotor), = W/A_e(tandem rotor)
x....Fractional blade element radius, = r/R
x_o...Tandem rotor overlap/Rotor radius
x_g...Tandem rotor vertical gap/Rotor radius
z....Height of rotor above ground, ft
α' ..Rotor tip path plane incidence, rad.
α_r..Blade element angle of attack, rad.
$\delta_o, \delta_1, \delta_2$.. Blade element drag coefficients
η ...Propulsive efficiency = $1 - K_t - K_g$
θ....Blade pitch at any station, rad.
θ_o...Coll. pitch @ root (extended to C.L.)rad.
θ_1...Cyclic pitch @ $\Psi = 90^o$, rad.
θ_2...Cyclic pitch @ $\Psi = 270^o$, rad.
θ_ϵ ..Blade twist = $\theta_{x=1} - \theta_{x=o}$, rad.
λ' ..Rotor inflow ratio = $(u + V\alpha')/V_T$
μ ...Rotor tip speed ratio = V/V_T
ρ ...Mass density of air, $slugs/ft^3$
σ ...Rotor solidity = A_b/Ww
ϕ....Blade element inflow angle
$\tan^{-1}\left[\lambda'/(x+\mu\sin\Psi)\right]$, rad.
Ψ....Blade azimuth (positive aft, measured counter clockwise from above), deg.

3

WEIGHT ANALYSIS

SECTION 3 - WEIGHT ANALYSIS TECHNIQUES

CONTENTS

SECTION 3 - WEIGHT ANALYSIS TECHNIQUES

A. SCOPE AND METHODS OF ANALYSIS

1. Introduction

The purpose of the weight analysis presented in this report is first, to present a survey of the available statistical data of helicopter component weights and secondly to show the development of methods of preparation and evaluation of preliminary design weight data for various helicopter configurations.

The weight data survey is general in nature and applicable to any components typical of a "pure helicopter", i.e., one relying on conventional rotors for lift and propulsion in all flight regimes. The greater part of this data is a statistical compilation of existing helicopter component weights (Reference 13) and is limited since it represents "state of the art" development of helicopters to approximately the year 1952. It is therefore questionable to what extent this data may be extrapolated to predict weights of future machines. Corresponding trends of component weight for fixed wing aircraft (Reference 14) show that the earlier aircraft, in terms of the development period, show the largest deviation from the correlated trends, indicating that the advancing "state of the art" may be the largest factor in altering the component weight trends. Coincident with this however, the effect of increased size of more recent fixed wing aircraft has afforded design advantages inherent in larger sizes, increased complexity notwithstanding. Since the available helicopter statistical weight data reflects a relatively early stage of development of the type, the extrapolation required by the scope of the study may result in conservative weight predictions, however, this would not invalidate the comparative results of the primary part of the study presented in the report: "Military Helicopter Transport Systems, 1956 to 1961", (Reference 1).

To determine the reliability of the extrapolation of the data and of the methods developed in the study, the actual weights of several recently developed helicopters were compared with the predicted gross weights based on the published payload, range and hover ceiling for the actual machines. It was found that the actual and predicted gross weights were within five percent for both single and tandem rotor helicopters. The data was therefore considered to provide reasonably reliable trends of helicopter component weights for the more conventional shaft driven rotor types and to provide conservative extrapolations of weight trends for the relatively advanced tip powered configurations.

The prediction of gross weight for a given configuration and performance specification is the ultimate objective of the weight and aerodynamic analyses presented in this report. Accordingly, the analysis of each of the two parts is directed toward obtaining a "common denominator" which satisfies the requirements of both analyses. This link has been found to be the fuel weight ratio, and is derived from the aerodynamic analysis as the fuel weight per pound of gross weight required for a given range or radius of action and from the weight analysis as the fuel weight ratio available for a given payload and gross weight. Methods of analysis have been formulated such that both the available and the required fuel weight can be written as analytical functions of design parameters including gross weight and in addition as functions of payload and radius of action, respectively. The simultaneous solution of the two expressions results in a singular design gross weight which satisfies both payload and radius of action criteria and indicates the best combination of design parameters to obtain minimum gross weight. Section 4 discusses in more detail the procedure

involved in obtaining the simultaneous solutions for gross weight. The derivation of the generalized weight equation for determining the available fuel weight ratio is shown in the following paragraphs, and the detail derivations of component weight expressions are shown in Part B. Part C shows the integration of the individual components weights of Part B into empty weight equations for specific transport helicopter configurations.

2. Derivation of Generalized Weight Equation

As discussed in the preceding paragraphs, the final objective of the weight analysis is to express the available fuel weight in terms of design parameters. From the statistical weight data, the empty weight of the helicopter can be written as a function of four primary variables: gross weight, disk loading, power loading and tip speed. Based on this empty weight relationship, the fuel and fuel tank weight is:

$$W_F + W_{FT} = W - W_P - W_C - W_E$$

where: W_F = allowable fuel weight

W_{FT} = fuel tank weight

W = design gross weight

W_P = design payload

W_C = crew weight

W_E = empty weight less fuel tank weight

In ratio form, dividing by gross weight:

$$R_F + R_{FT} = 1 - R_P - R_C - \phi$$

Where ϕ has been designated as the ratio of empty weight less fuel tank weight to gross weight. To ensure compatibility between fuel and fuel tank weight, the equation can be reduced by specifying the tank weight per gallon of fuel. Hence, by assuming a tank weight of 0.5 lb. per gallon of fuel (50% self-sealing tanks) and further assuming a fuel weight of 6.0 lbs. per gallon, the available fuel weight ratio becomes:

$$R_F = \frac{1}{1 + k_F}\left(1 - R_P - R_C - \phi\right) \qquad 3\text{-}1$$

where $\frac{1}{1+k_F}$ = the ratio of fuel weight to fuel plus fuel tank weight: 6.0/6.5 = .923 for purposes of transport helicopter evaluations. This equation is referred to as the generalized weight equation in which the term R_F provides the link between weight and aerodynamic characteristics. Use of the equation in obtaining values of R_F and in combining with the aerodynamic analysis is straightforward providing that the function ϕ is known. The major effort in the weight analysis was therefore the derivation of ϕ as a function of the significant helicopter design parameters.

SECTION 3 - WEIGHT ANALYSIS TECHNIQUES

3. Methods and Assumptions

For each of the twenty-seven major empty weight components, the analysis of Reference 13 presents an analytical expression correlated to the available statistical weight data. Generally the component weights are shown to be functions of a significant dimension and/or the design power, torque loading or, for items of lesser importance, functions of design gross weight where these items may be directly related to the size of the helicopter. Thus, as examples, fuselage weight is a function of overall length and gross weight, mechanical drive shafting is a function of length and design torque, and power plant weight is a function of the installed take-off power. From these expressions, it would be possible to formulate an empty weight equation by determining each of the pertinent dimensions, design torques and installed power rating. However, to avoid this cumbersome procedure, it was postulated that each of the parameters could be expressed in terms of one or more of the major design parameters, which would then allow the reduction of the equation to fewer terms resulting in rapid and more accurate preliminary weight estimation. The initial steps in the weight analysis are therefore the establishment of (1) generalized dimensions, relating each significant dimension to rotor radius, and (2) assumed power distributions, relating mechanical drive loadings to the total installed power.

The generalized dimensions established for the purpose of the transport helicopter are shown in Figure 3-1. These dimensions were based on current design practice for the most part with some modifications in overall fuselage length necessary to maintain adequate cargo compartment length for special items of military equipment. These sketches are shown as an illustration of the helicopter parameters which are required to obtain the empty weight equation, and the derivation of the weight equation is subsequently presented in sufficient detail to allow variation of the dimensions. Of the various dimensions shown, the fuselage length factor alone is independent of the aerodynamic analysis insofar as the fuselage typifies reasonable fineness ratio and aerodynamic cleanliness. Therefore, the fuselage length factor may be altered within limits depending upon the cargo compartment length required for a particular payload specification. Tail rotor and tail rotor moment arm dimensions for the single rotor helicopters are consistent with the assumed power distributions and variation in these factors would require concurrent variation of the tail rotor power required. The tail rotor dimensions shown for the shaft powered single rotor helicopter are typical of current design practice, and for the single rotor tip powered configuration are based on the maneuvering requirements of Reference 17, consistent with the assumed power distribution for this type.

The assumed power distributions, shown in Figure 3-2, are determined from the aerodynamic analysis for the transport helicopter. As an example of the use of this data: knowing the percent power from Figure 3-2, the design torque for a transmission can be written as a function of installed take-off power, tip speed and rotor radius.

From the two sets of assumptions described above, the weight expressions given by Reference 13 can be reduced to approximately eight terms each of which is a function of gross weight, (W), disk loading, (w), tip speed, (V_T), take-off power loading, (l_{pm}), the number of installed engines, (n), or rotor overlap in the case of tandem rotor helicopters. The final empty weight equations presented in Part C are shown as functions of the first four variables, with alternate terms where applicable for various numbers of installed engines. The

TRANSPORT HELICOPTER DESIGN ANALYSIS METHODS

Single Rotor
Shaft Powered

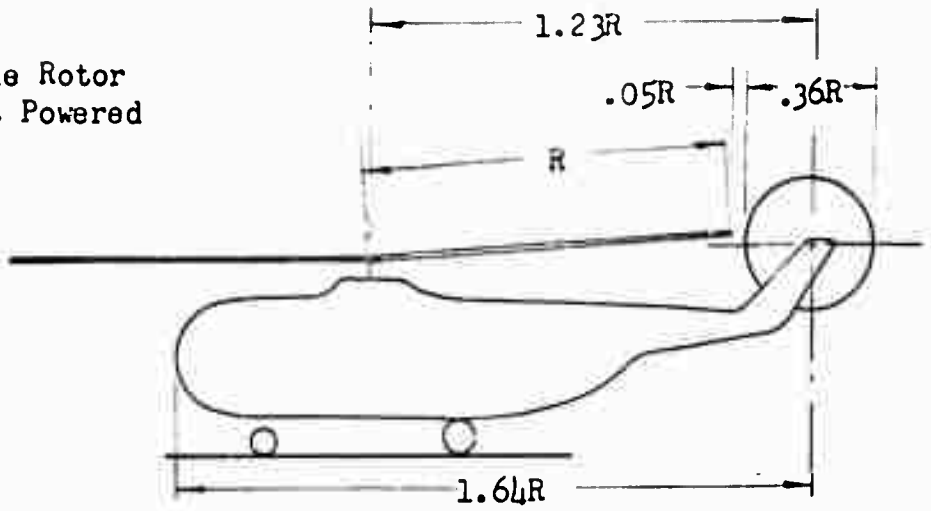

Tandem Rotor
Shaft Powered

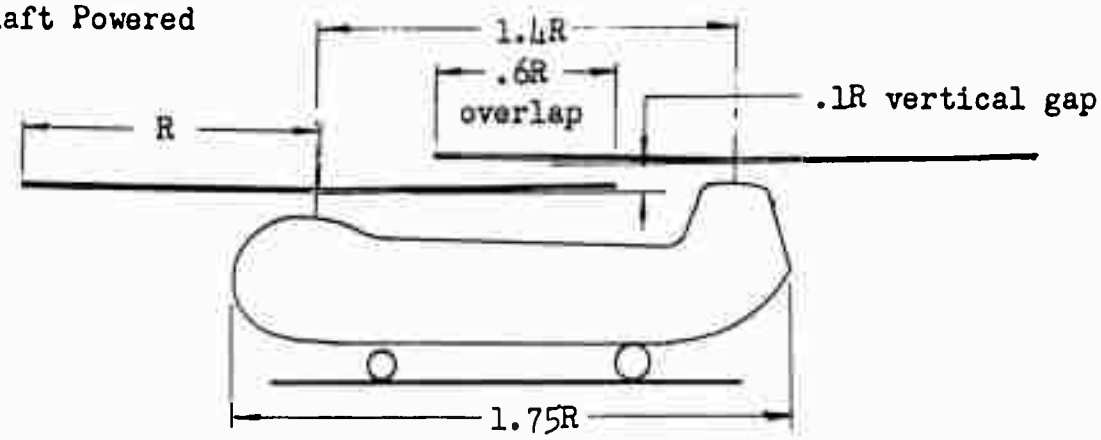

Single Rotor
Tip Powered

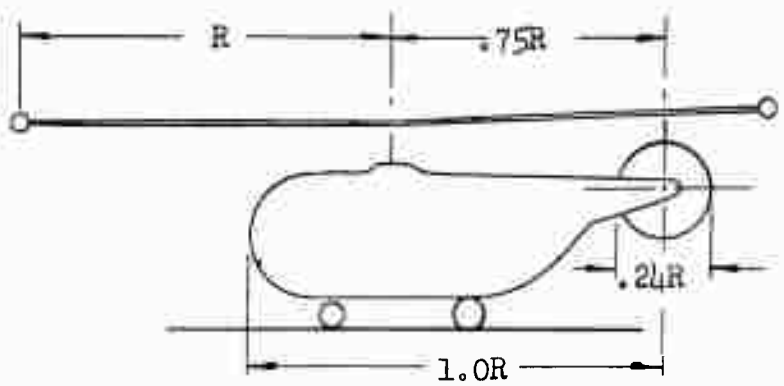

Figure 3-1 Generalized Dimensions for Various Transport Helicopter Configurations

SECTION 3 - WEIGHT ANALYSIS TECHNIQUES

POWER DISTRIBUTION TO	ROTOR AND POWER PLANT TYPE				
	Single Rotor			Tandem Rotor	
	Reciprocating	Geared Turbine	Tip Powered	Reciprocating	Geared Turbine
Main Rotor,	84.3	89.3	97.7	91.0	96.0
Tail Rotor,	7.7	7.7	2.3	0	0
Gear Loss	3.0	3.0		4.0	4.0
Cooling Loss	5.0	0	0	5.0	0

Figure 3-2: Assumed Power Distribution in Percent of Total Installed Power

tandem rotor helicopter empty weight equations are shown for a rotor overlap of 60%, the value chosen for the comparisons made in the report "Military Helicopter Transport Systems, 1956 to 1961".

For the evaluation of a single aircraft, the calculation of empty weight from the equations is straightforward provided that the parameters listed above are known. For purposes of optimization studies or preliminary design, however, where the payload, range and hover ceiling are specified and the minimum design gross weight is desired, it is necessary to combine the weight analysis and aerodynamic analysis by the procedure described in Section 4 of this report. Further detail on the procedure for this type of analysis is presented in Part C.

B. HELICOPTER COMPONENT WEIGHTS

1. Rotor Group

Considerable effort has been expended in various helicopter rotor studies to obtain a reliable method of predicting preliminary rotor weights on the basis of rotor parameters. The type of analysis which utilizes the strength-weight approach has been found to be cumbersome due to the inherent difficulty in analytically determining rotor blade loading which by itself is often not the weight determinant. Statistical analysis of rotor weight has therefore been utilized to a greater extent as the data and methods have become available. The statistical correlation of blade weight functions with statistical data from Reference 13 was deemed adequate for purposes of the study although in certain aspects of the investigation modifications were made in the basic expressions. The expressions used are functions of disk loading, tip speed and rotor radius, and although other variables such as solidity or ultimate load factor could be included in the correlation, the greater refinement of the expressions was not considered to be warranted by the scope of the investigation. Deviations from the basic expressions are noted in the following sections where applicable.

Weight data was available for both rigid (or teetering) and for articulated types of rotor blade systems. To select one of the two systems for use in the present study, a comparison was made between the total weight of blades plus hub and hinge of both types. Figure 3-3 shows the comparison of the two types and it will be noted that for any given radius, disk loading and tip speed, the articulated rotor system exhibits a lower weight on the basis of the statistical data. Hence for all the shaft powered configurations, the relatively lighter articulated system weight was used in developing the weight equation. For tip powered helicopters, the only data available represented weights of two blade teetering rotor systems.

a) Rotor Blade

Rotor blade weight for single rotor, shaft powered helicopters is given by the expression:

$$\text{Blade weight} = 28.1 \frac{\omega_r R^{2.41}}{V_T} \qquad \text{for } R < 40 \text{ ft.}$$

SECTION 3 - WEIGHT ANALYSIS TECHNIQUES

$$\text{Blade weight} = 14.0 \frac{w R^{2.60}}{V_T} \qquad \text{for } R > 40 \text{ ft.}$$

Since $R = \sqrt{\frac{W}{\pi w}}$

$$\left.\begin{aligned} \text{Blade weight} &= 7.07 \frac{W^{1.205}}{V_T w^{.205}} && \text{for } \frac{W}{w} < 4680 \\ &= 3.16 \frac{W^{1.30}}{V_T w^{.30}} && \text{for } \frac{W}{w} > 4680 \end{aligned}\right\} \qquad 3\text{-}2$$

The preceding total blade weight expressions are valid for three blade, articulated rotor systems and it was further assumed that they are representative of rotors with a mean solidity of .045. For variation of solidity as an extension of the parametric study, the weight expressions were modified by the factor $(\sigma /.045)^{.33}$ in the manner of Reference 18.

Rotor blade weight for tandem rotor, shaft powered helicopters: the data of Reference 13 indicates that the rotor blade weight expression is valid for both single and tandem rotor weights, if, when utilizing the weight function, the tandem rotor disk loading is defined as

$$w_s = \frac{W}{2\pi R^2}$$

Since the tandem rotor disk loading for purposes of this study was defined as:

$$w = \frac{W}{2\pi R^2 - \text{OVERLAP AREA}}$$

the tandem rotor blade weight function is modified by the factor k, to allow for variation of blade weight with rotor overlap at constant effective disk loading.

$$\left.\begin{aligned} \text{Blade weight} &= 6.15k \frac{W^{1.205}}{V_T w^{.205}} && \text{for } R < 40' \\ &= 2.57k \frac{W^{1.30}}{V_T w^{.30}} && \text{for } R > 40' \end{aligned}\right\} \qquad 3\text{-}3$$

The variations of k with rotor overlap for the two ranges of rotor radius are given in Figure 3-4.

For tip powered helicopters, based on the limited data of Reference 13 it was possible to combine the expressions for blade weight and hub and hinge weight into the expressions:

$$\left.\begin{aligned} \text{Rotor group weight} &= .0362 \frac{W^{1.21}}{w^{.21}} && \text{for } \frac{W}{w} < 5030 \\ &= .0256 \frac{W^{1.25}}{w^{.25}} && \text{for } \frac{W}{w} > 5030 \end{aligned}\right\} \qquad 3\text{-}4$$

Figure 3-3: Comparison of Rotor System Types - Rotor Weight vs. Radius for Various Tip Speeds

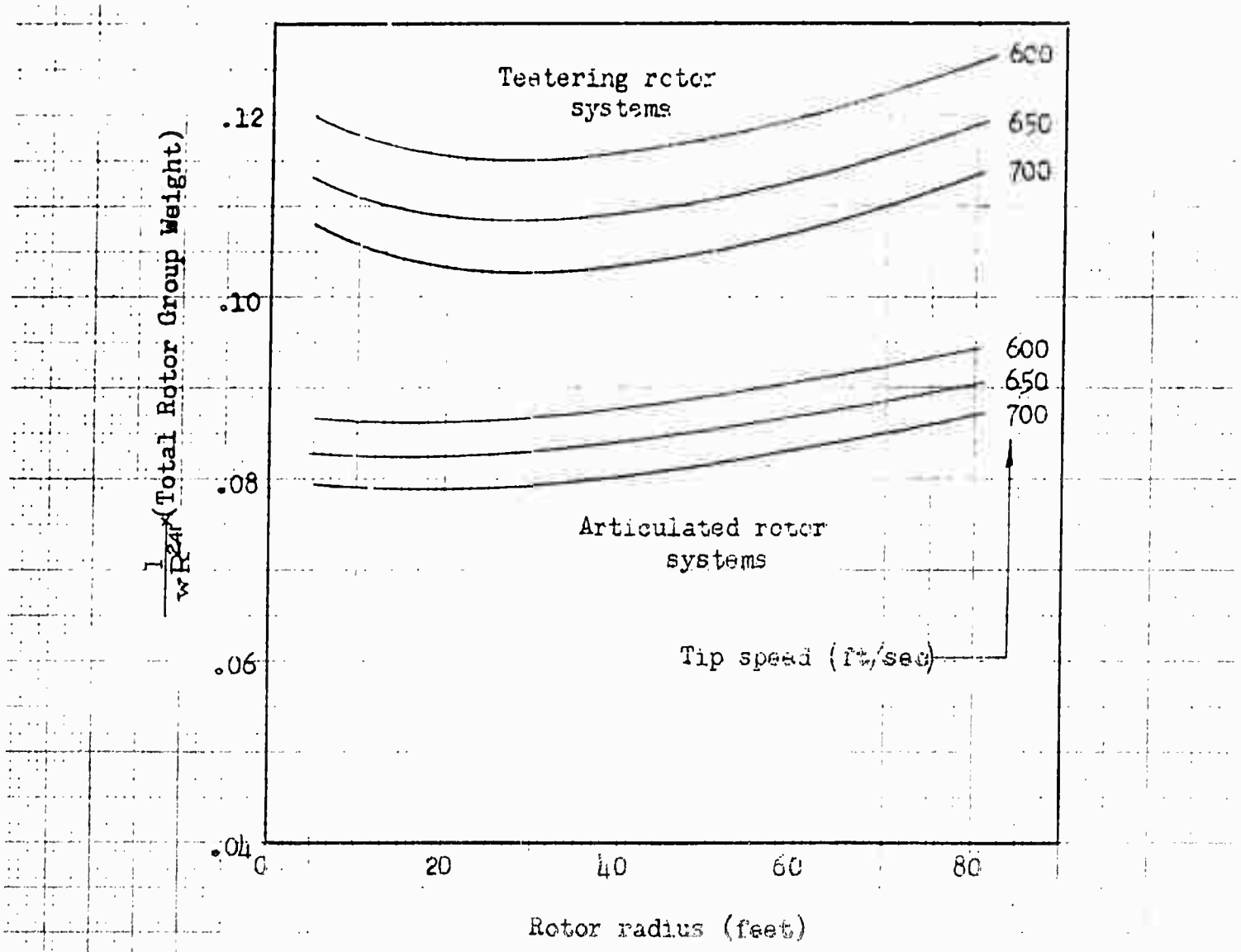

Figure 3-4: Tandem Rotor Blade Weight Correction Factor (Equa.3-3) vs. Percent Rotor Overlap

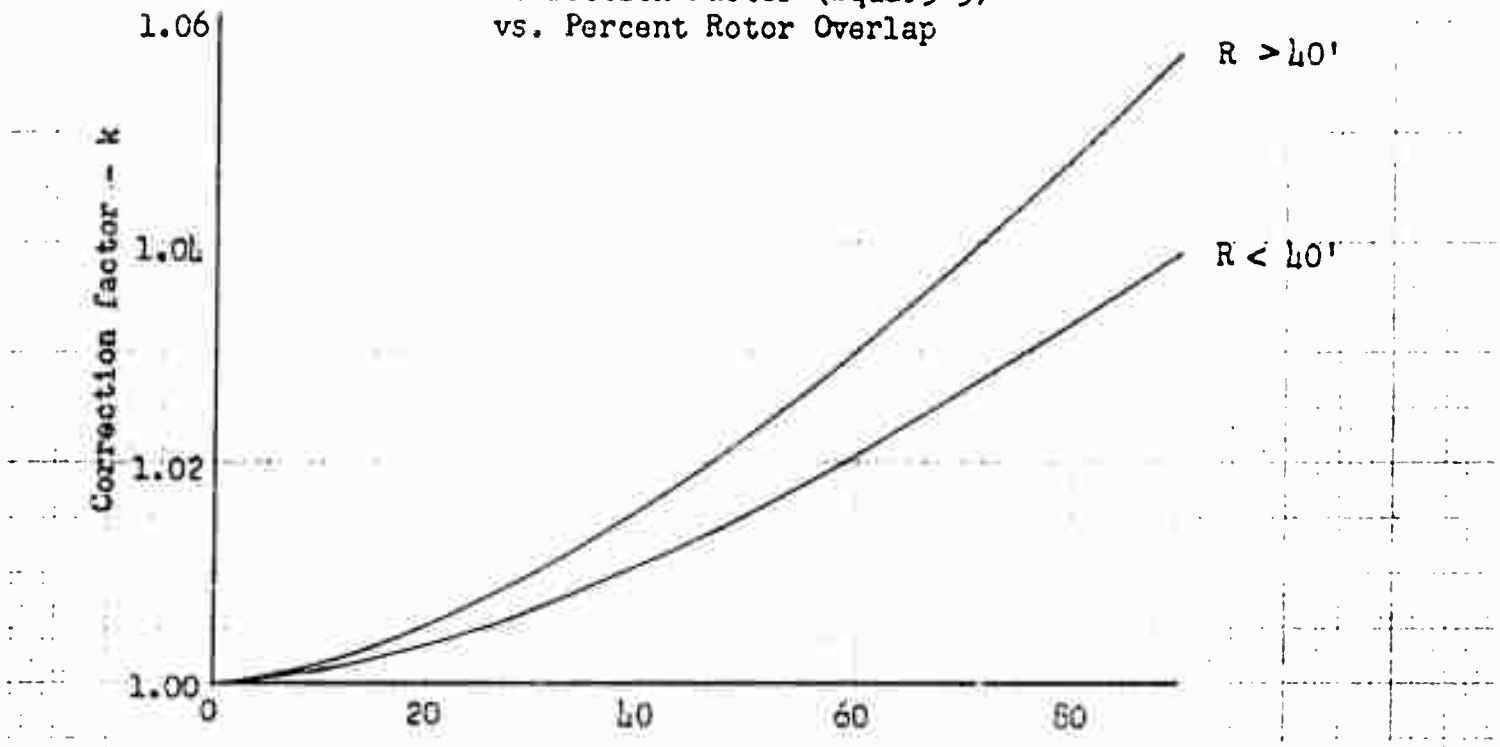

Figure 3-5: Tandem Rotor Hub Assembly Weight Correction Factor (Equa. 3-6) vs. Percent Rotor Overlap

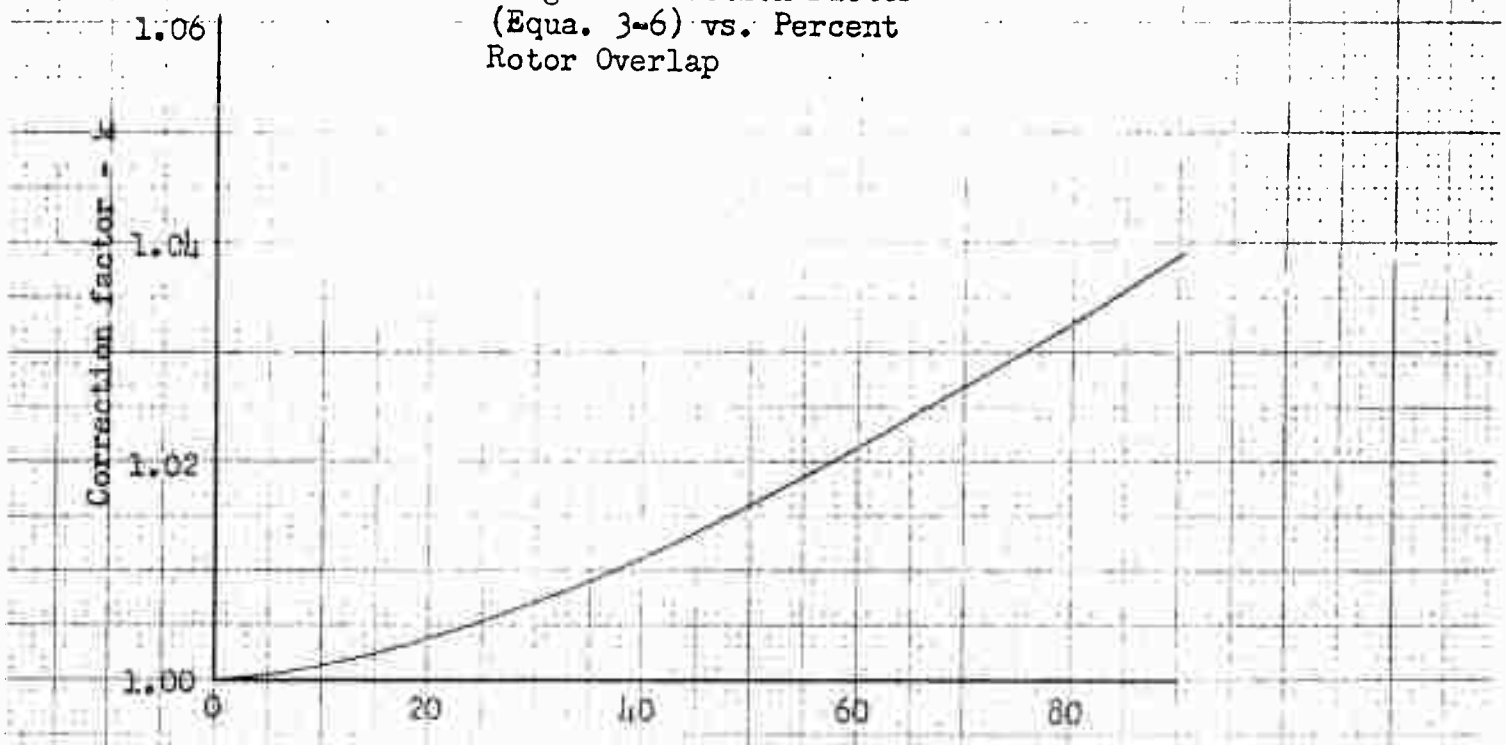

This weight expression was assumed to account for the weight of additional fuel lines or ducting for the tip mounted power plants and to include the weight of tip burners in the case of pressure jet power plants.

b) Rotor Hub Assembly

Rotor hub and hinge weight for single rotor, shaft drive helicopters are given as:

$$\text{Hub and hinge weight} = .00975 \frac{W^{1.21}}{w^{.21}} \qquad 3\text{-}5$$

Rotor hub and hinge weight for tandem rotor, shaft drive helicopters:

$$\text{Hub and hinge weight} = .00839\,k \frac{W^{1.21}}{w^{.21}} \qquad 3\text{-}6$$

where k is the correction factor for variation of rotor overlap shown in Figure 3-5.

Rotor hub and hinge weight for single rotor tip powered helicopters is included with blade weight, paragraph 1(a).

2. Tail Group

a) Stabilizer

For all single rotor helicopters with shaft drive or tip mounted power plants, stabilizer weight was assumed to be:

$$\text{Stabilizer weight} = .002\,W \qquad 3\text{-}7$$

and for tandem rotor helicopters:

$$\text{Stabilizer weight} = .006\,W \qquad 3\text{-}8$$

b) Tail Rotor Weight

The statistical data of tail rotor weight shows considerable scatter, however, the net effect of an average curve for weight was found to induce little error in the final weight since tail rotor weight itself is a small percentage of empty weight. Tail rotor weight can be represented by the expression

$$\text{Tail rotor weight} = 53 \frac{w_t\, r^3}{V_{T_t}}$$

For single rotor, shaft drive helicopters, the tail rotor thrust ($T_t = w_t \pi r^2$) can be related to main rotor torque by the expression

$$T_t = \left[\eta \frac{550\,HP_m \times R}{V_T}\right] \times \frac{1}{1.23R}$$

where the term in brackets is the design rotor torque at engine take-off power, and (1.23 R) is the assumed tail rotor moment arm. Assuming that tail rotor tip speed is equal to main rotor tip speed and noting from the general dimensions (Figure 3-1) that $r = .18R$, the weight expression reduces to the following:

$$\text{Tail rotor weight} = 1360\,\eta\,\frac{HP \cdot R}{V_T^2}$$

From the propulsive efficiency factors shown in Figure 3-2:

$\eta = .843$ single rotor - recipr. powered

$\eta = .893$ single rotor - geared turbine powered

the final weight expressions are therefore:

$$\text{Tail rotor weight} = 646\,\frac{W^{1.50}}{l_{pm}\,V_T^2\,w^{.50}} \qquad 3\text{-}9$$

for single rotor-reciprocating powered helicopters

$$= 685\,\frac{W^{1.50}}{l_{pm}\,V_T^2\,w^{.50}} \qquad 3\text{-}10$$

for single rotor-geared turbine powered helicopters

Tail rotors for directional control of tip powered helicopters have been included in the weight analysis for these configurations since it was assumed that a simple rudder would not afford sufficient control in certain flight regimes. An analysis of tail rotor parameters (see Section 2, Aerodynamics Analysis) was made based on the requirements of Reference 17. From this analysis, tail rotor radius,

$$r = .12R$$

and tail rotor maneuvering thrust in terms of gross weight and main rotor disk loading,

$$T_t = \frac{.13W}{\sqrt{w}}$$

Using the expression for tail rotor weight and making the substitutions indicated previously

$$\text{Tail rotor weight} = .148\,\frac{W^{1.50}}{w\,V_T} \qquad 3\text{-}11$$

3. Body Group Weight

The statistical data of Reference 13 shows a correlation of body group weight with the expression:

$$\text{Body weight} = .159(WL)^{.69}$$

in which L = overall fuselage length. This expression was found to predict reasonable values for fuselage weights of both single and tandem rotor helicopters.

For the single rotor shaft drive helicopters considered in the study, it was

noted that the fuselage weight function held considerable influence over the selection of the optimum disk loading. Since the overall fuselage length was determined by rotor radius, it followed that decreasing radius (increasing disk loading) decreased body weight for constant gross weight. The net effect of using this body weight expression when summing all the helicopter weights therefore, was that minimum empty weights were obtained at a relatively low rotor radius hence low fuselage length. In some cases it was found that for minimum gross weight the resulting fuselage length was inadequate for the design payload - a prior consideration. Therefore, a study was made to redefine the body group weight expression to lessen the apparent weight advantage of high disk loading - low fuselage length.

As a rational basis for this study it was postulated that, for a given payload or cargo compartment size, the effect of increasing disk loading was to decrease only the tail boom length and weight and that the average ratio of weights per unit length of cargo compartment and tail boom was 4:1. It was further assumed that the statistical data represented helicopters with an average disk loading of 4.0 lbs/ft^2. Based on these assumptions the revised body weight expression for single rotor, shaft powered helicopters took the form:

$$\text{Body weight} = .108 W^{.94} L^{.20}$$

Using the relationship, $L = 1.64R$, which is the statistical average of overall single rotor fuselage lengths (Reference 13) the expression reduces to:

$$\text{Body weight} = .106 \frac{W^{1.035}}{w^{.098}} \qquad 3\text{-}12$$

If weight function given by Reference 13 and shown previously is similarly reduced the

$$\text{Body weight} = .151 \frac{W^{1.036}}{w^{.345}}$$

By comparison of the two expressions for body weight it can be seen that the same trend of body weight with gross weight is maintained, however the effect of disk loading is reduced by use of the revised form of the function. Figure 3-6 illustrates this change in body weight ratio with varying disk loading. This relationship then predicts conservative values of body group weight for disk loadings greater than 4.0.

Tandem rotor body weight is based on the data of Reference 13 without revision.

$$\text{Body weight} = .159(WL)^{.69}$$

The body length, shaft to shaft, is related to the rotor overlap by the following:

$$\beta R = \left(2 - \frac{\% \text{ overlap}}{100}\right)$$

where βR = body length, shaft to shaft. The body overhang is assumed to be $1.25 \beta R$ as is shown in Figure 3-7.

Thus the body weight expression becomes

$$\text{Body weight} = .185(\beta R W)^{.69}$$

Figure 3-6: Body Weight Ratio vs.
Disk Loading

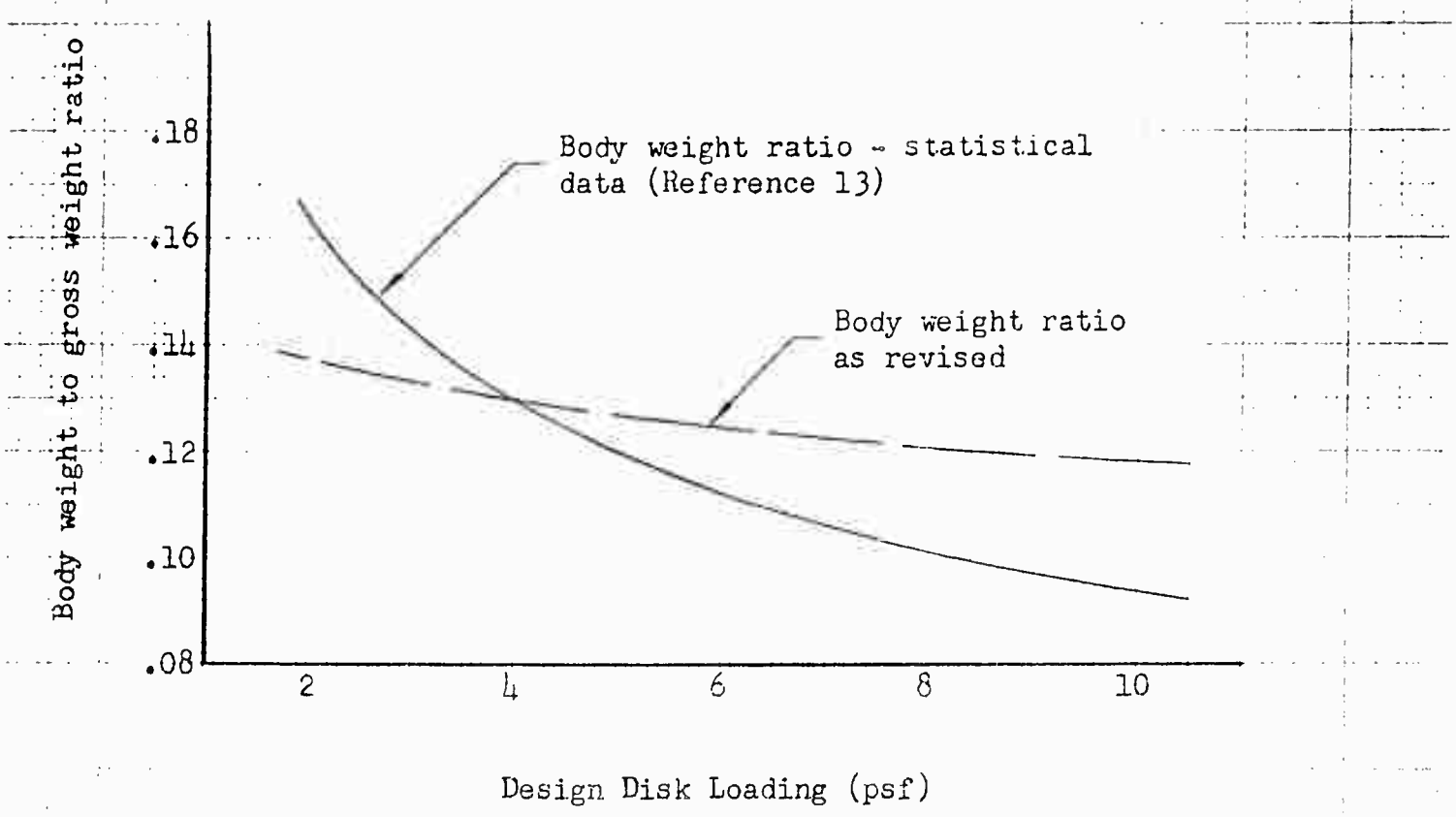

Figure 3-8: Tandem Rotor Body Weight Correction Factor (Equa. 3-13) vs. Percent Rotor Overlap

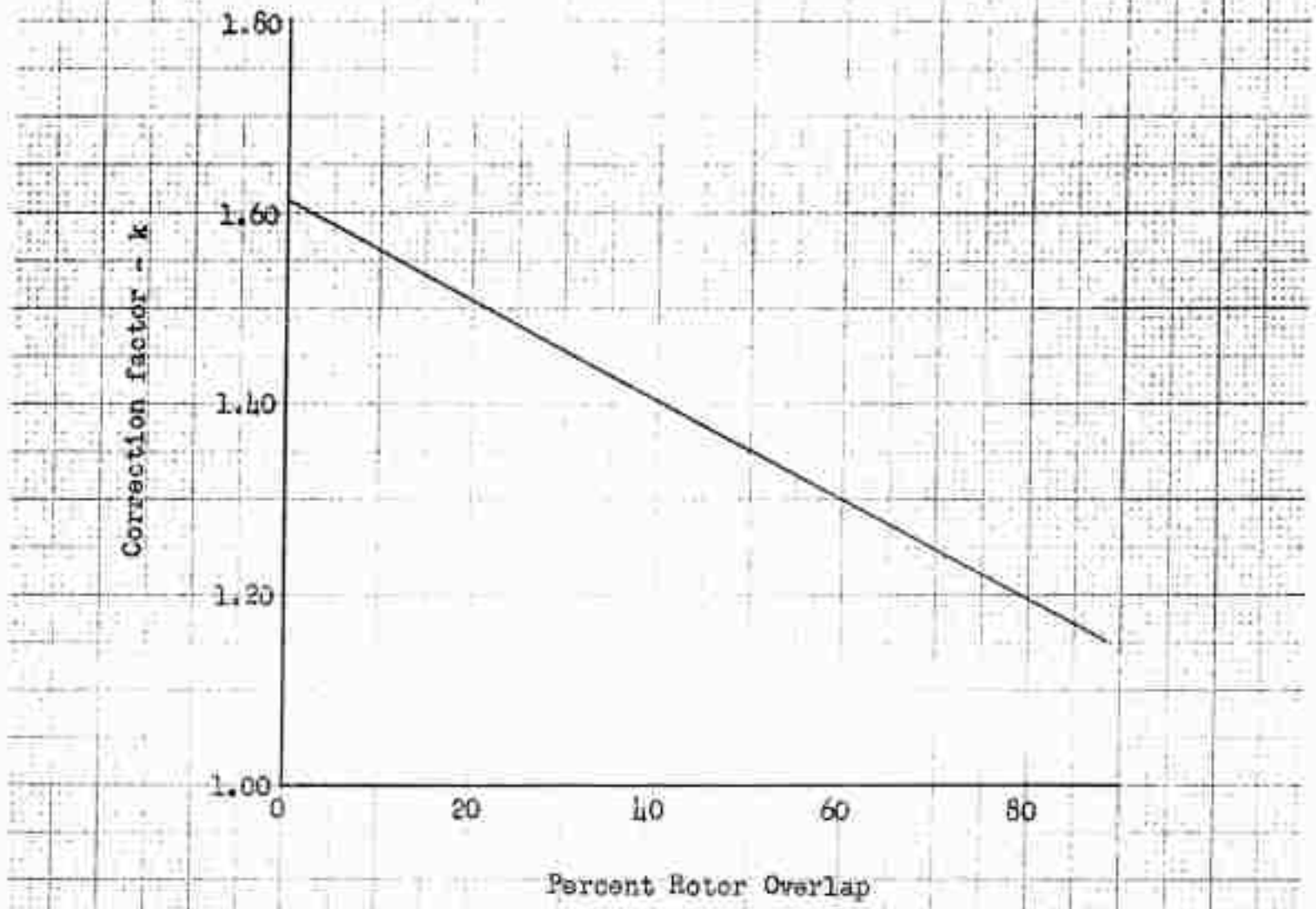

SECTION 3 - WEIGHT ANALYSIS TECHNIQUES

Since the term βR is a function of rotor overlap, the expression can be written in final form:

$$\text{Body weight} = .0983\, k\, \frac{W^{1.035}}{w^{.345}} \qquad 3\text{-}13$$

in which the term k, the overlap correction factor, is shown in Figure 3-8 as a function of percent rotor overlap.

Figure 3-7

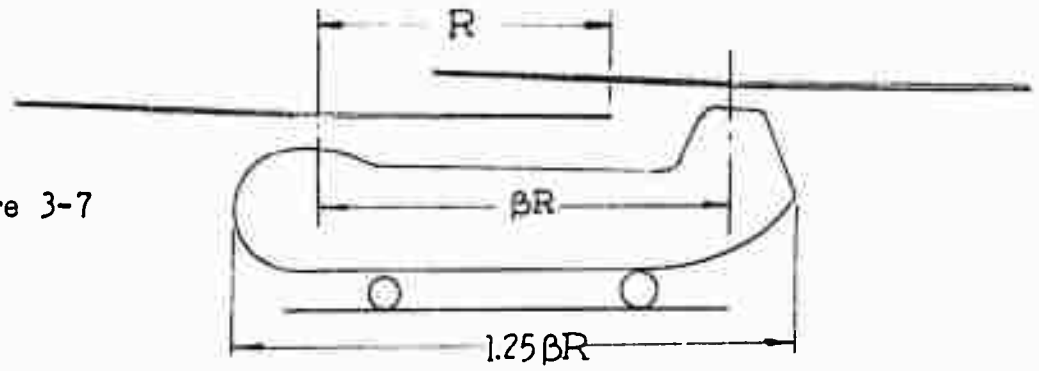

Body group weight for single rotor tip powered helicopters is based on the basic body weight expression from Reference 13. Since the tip powered helicopters allow the use of smaller tail rotor diameters and tail rotor moment arms, the fuselage length was fixed at 1.0 x main rotor radius. The statistical average body length for single rotor tip powered helicopters is .76 x main rotor radius, however, in view of the cargo compartment length required by the transport mission, the value of 1.0R was chosen.

Body group weight is therefore expressed by the equation,

$$\text{Body weight} = .107 \frac{W^{1.035}}{w^{.345}} \qquad 3\text{-}14$$

4. Landing Gear Weight

For fixed landing gear consisting of 3 or 4 wheels, the statistical data shows landing gear weight:

$$= .0337\, W^{1.02} \qquad 3\text{-}15$$

A consideration of retractable landing gear has been made to provide a comparison in operational studies between transport helicopters with fixed and retractable gear, however, due to lack of data on the increase in weight of retractable gear for similar classes of aircraft, the retractable type was arbitrarily assumed to weigh 40% more than the fixed gear for a given gross weight. This weight increase was assumed to account for the additional weight of fuselage structural modification as well as the additional weight of the retracting mechanisms.

5. Engine Section Weight

The engine section weight includes engine mounts, firewall, vibration isolation systems and cowlings. The weight of these items for a reciprocating en-

gine powered helicopter is

$$.124\,HP_m^{1.07}$$

To reflect the change in engine section weight for a multiple engine installation the weight was assumed to change by a factor of

$$n^{-.07}$$

where n = number of installed engines. The final expression for engine section weight for reciprocating engine powered helicopters becomes:

$$\text{Engine section weight} = .124\left(\frac{W}{l_{pm}}\right)^{1.07} n^{-.07} \qquad 3\text{-}16$$

For geared gas turbine powered helicopters the following expression for engine section weight was used:

$$= .053\left(\frac{W}{l_{pm}}\right)^{1.07} n^{-.07} \qquad 3\text{-}17$$

6. Power Plant Weights

a) Engine Weight
Reciprocating engine weight is given by the expression

$$\text{Engine weight} = 4.46\,HP_m^{.822}$$

where HP_m is the military take-off power rating and the weight represents dry engine weight. For multiple engine installation the total dry engine weight is modified by a factor

$$n^{.178}$$

where n = number of installed engines for a total installed take-off power, HP_m . Total reciprocating engine weight then reduces to:

$$\text{Engine weight} = 4.46\,n^{.178}\left(\frac{W}{l_{pm}}\right)^{.822} \qquad 3\text{-}18$$

Geared gas turbine weights given by Reference 13 include the weight of the basic turbine-compressor unit, primary reduction gear box, fuel and lubrication systems and power plant controls. It does not include the weight of starting systems, fuel and oil tanks and necessary plumbing. As a function of take-off equivalent shaft power,

$$\text{Engine weight} = 75 + .89(ESHP_m)^{.908}$$

Since shaft output is of primary interest, a statistical survey of existing geared turbine engines indicated the following relationships

$$ESHP_m = 1.095\,HP_m$$

and $$ESHP_m = 1.167\,ESHP$$

These expressions were derived from the data noted above and are shown in Figures 3-9 and 3-10. Utilizing these relationships and introducing the

Figure 3-9: Equivalent Shaft HP (Take-off) vs. Shaft HP (Take-off) - Geared Gas Turbines

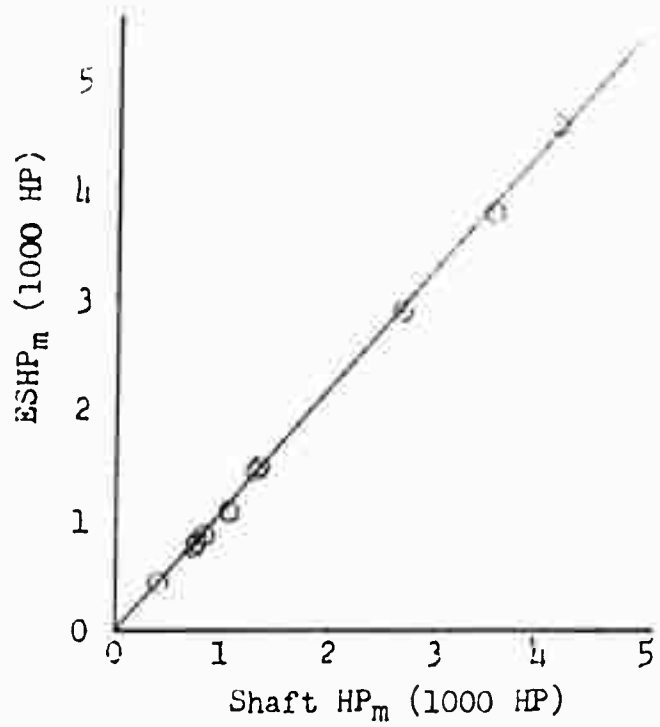

Figure 3-10: Equivalent Shaft HP (Take-off) vs. Equivalent Shaft HP (Normal Rated) - Geared Gas Turbines

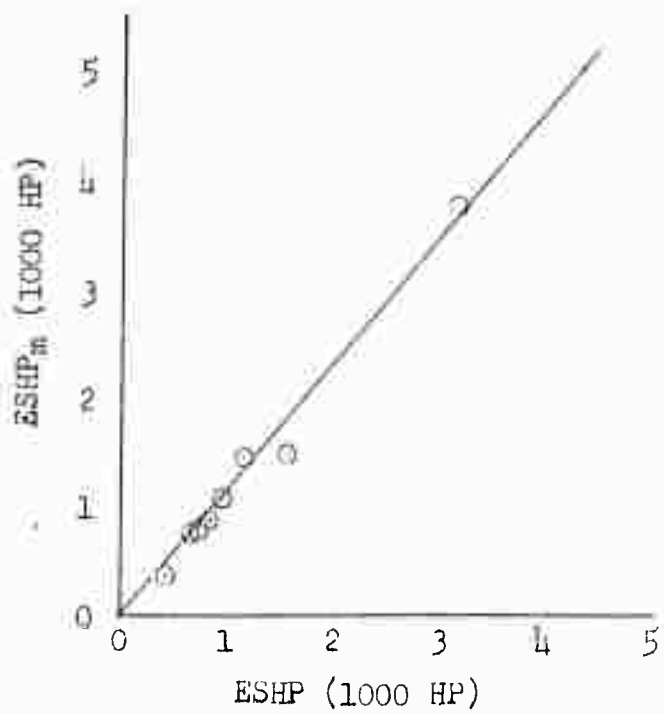

Figure 3-11: Variation of Ramjet Engine Weight with Sea Level Net External Thrust and Mach Number

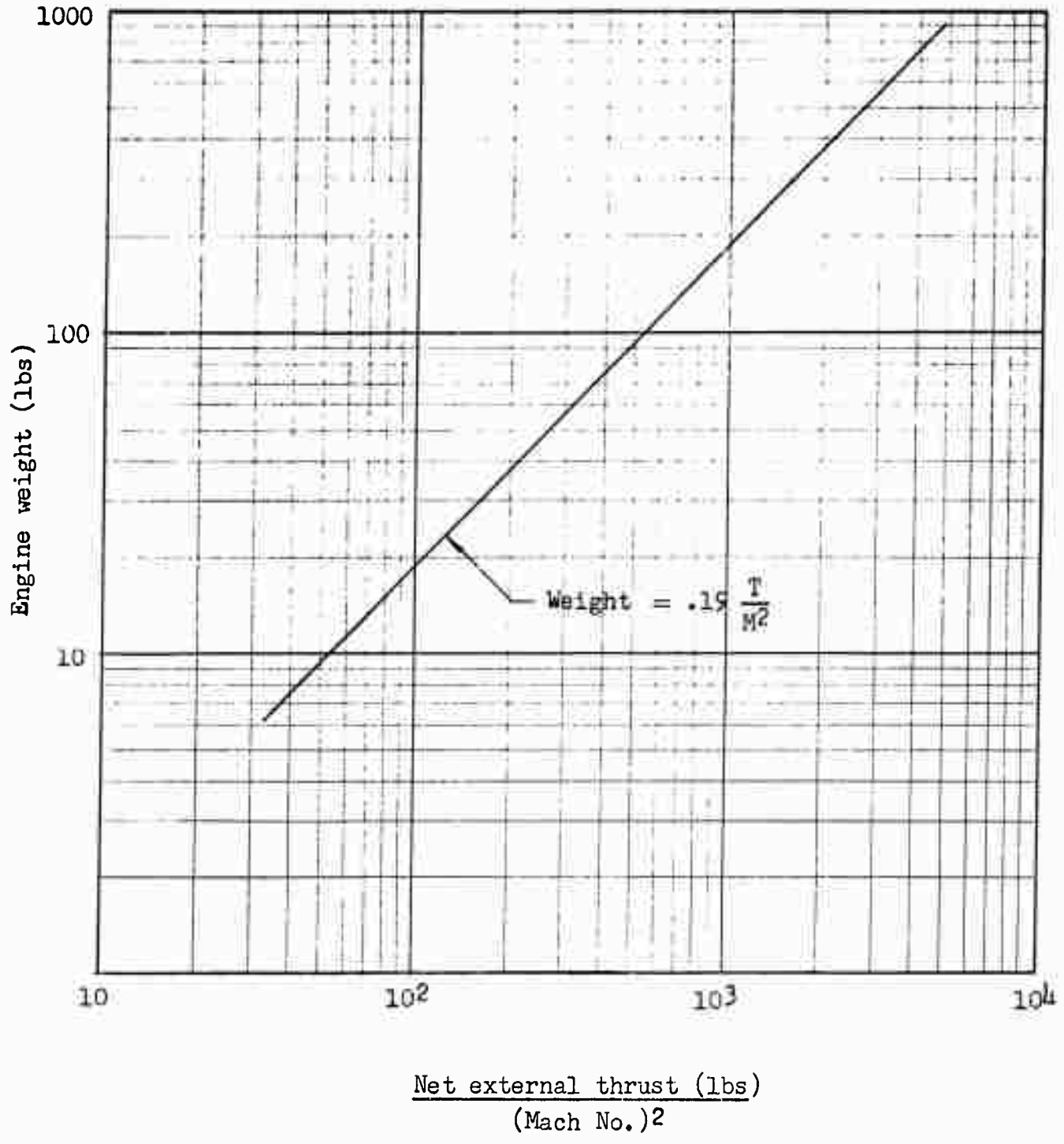

term designating the number of installed engines, the geared gas turbine engine weight becomes:

$$\text{Engine weight} = 75n + .966\, n^{.092}\left(\frac{W}{l_{pm}}\right)^{.908} \qquad 3\text{-}19$$

Ramjet engine weights were based on the available statistical data of Reference 13 augmented by previous analyses (Reference 19) made by the contractor. The latter analysis indicated a higher slope for the engine weight vs. net external thrust based upon a detailed consideration of centrifugal loading, engine diameter and material properties at high temperature, and were also, by necessity, based on proven design principles. Therefore, the resulting weight-thrust relationship used in the present study may be somewhat conservative in light of further development in ramjet performance and structural design. Figure 3-11 shows the final trend of weight as a function of sea level net external thrust and tip speed Mach number. From this, converting Mach number to tip speed, the total ramjet engine weight function:

$$\text{Engine weight} = 1.33 \times 10^{8}\,\frac{W}{l_{pm}\, V_T^{3}} \qquad 3\text{-}20$$

in which the power loading is determined from the sum of main rotor, tail rotor, and accessory power required. This expression includes the weight of two engines plus the weight of engine accessories at the rotor tip.

Tip mounted turbojet engine weight estimates were derived principally from Packard Motor Car Co. data (Reference 12) and the thrust-weight relationship is presented in Figure 3-12 for a single tip speed of 700 feet per second. The slope of this curve was based on data from a number of proposed tip turbojet designs and in addition, on thrust-weight trends for existing pure turbojet designs. The level of the curve as well as the variation of the thrust-weight expression with design tip speed were derived from Packard data. From these considerations:

$$\text{Engine weight} = .08\, T^{1.234}$$

in which T = net take-off thrust at sea level (total thrust less nacelle drag)

The expression is based on a rotor tip speed of 700 feet per second, however, as Reference 12 indicates, variation in tip speed within 5% of the design value can be expected to cause negligible change in the data considering the present stage of development.

The total rotor power for a tip turbojet installation in terms of the total power (HP_m), number of engines (n) and thrust per engine (T):

$$HP_m = \frac{n\, T\, V_T}{550}$$

Utilizing the thrust-weight expression the total tip turbojet engine weight:

$$\text{Engine weight} = 188\, n^{-.234}\left(\frac{W}{l_{pm}\, V_T}\right)^{1.234} \qquad 3\text{-}21$$

The weight predicted by the equation includes the basic turbojet unit, nacelle, starting and lubrication systems and fuel regulator.

TRANSPORT HELICOPTER DESIGN ANALYSIS METHODS

Figure 3-12: Gas Turbine Engine Weight vs. Thrust

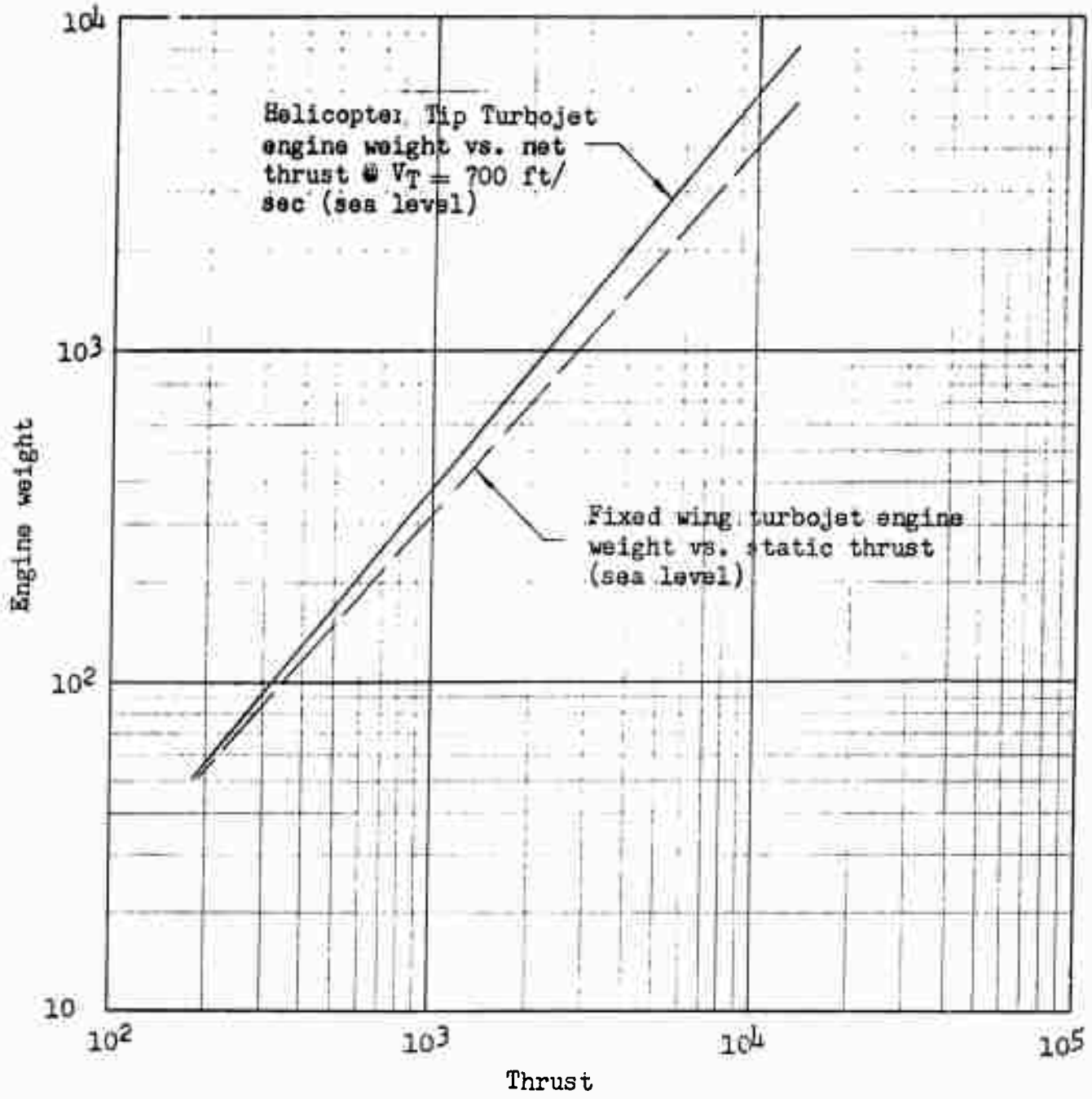

SECTION 3 - WEIGHT ANALYSIS TECHNIQUES

Engine weight for the pressure jet helicopters considered in the study were based on the analysis shown in the Appendix. Accordingly, the weights of the basic turbine, secondary compressor, accessories and engine section were assumed to be adequately predicted by the expression:

$$\text{Engine weight} = .464 \frac{W}{lpm} \qquad 3\text{-}22$$

b) Engine Accessories and Controls
For the reciprocating engine, the power plant accessories and controls weight:

$$= 2.69(W_E - 260)^{.54}$$

where W_E = engine dry weight. Substituting the expression for engine weight from paragraph 6(a), the accessories and controls weight becomes:

$$\text{Accessories and controls weight} = 6.03\left[n^{.178}\left(\frac{W}{lpm}\right)^{.822} - 58.3\right]^{.54} \qquad 3\text{-}23$$

where n = number of engines installed for a total power loading of lpm.

For geared gas turbine and tip mounted power plants the accessories and controls weight is included in the engine weight.

c) Rotor Mast Weight
As a function of maximum torque transmitted:

$$\text{Rotor mast weight} = .108\,Q^{.70}$$

For single rotor, shaft drive configurations the maximum torque at the "design" condition of sea level take-off engine power

$$Q = \eta\left(550 \frac{HP_m \cdot R}{V_T}\right)$$

Substituting the values of η , the propulsive efficiency, obtained from Figure 3-2, the torque expressions:

$Q = 464 \frac{HP_m \cdot R}{V_T}$ single rotor - reciprocating

and $Q = 491 \frac{HP_m \cdot R}{V_T}$ single rotor - geared turbine

The rotor mast weights for single rotor shaft powered helicopters become:

$$\text{Rotor mast weight} = 5.32 \frac{W^{1.05}}{(lpm\, V_T)^{.70}\, w^{.35}} \qquad 3\text{-}24$$

for single rotor - reciprocating

$$= 5.56 \frac{W^{1.05}}{(lpm\, V_T)^{.70}\, w^{.35}} \qquad 3\text{-}25$$

for single rotor - geared turbine

Figure 3-13: Tandem Rotor Mast Weight Correction Factor (Equas. 3-27 and 3-28) vs. Percent Rotor Overlap

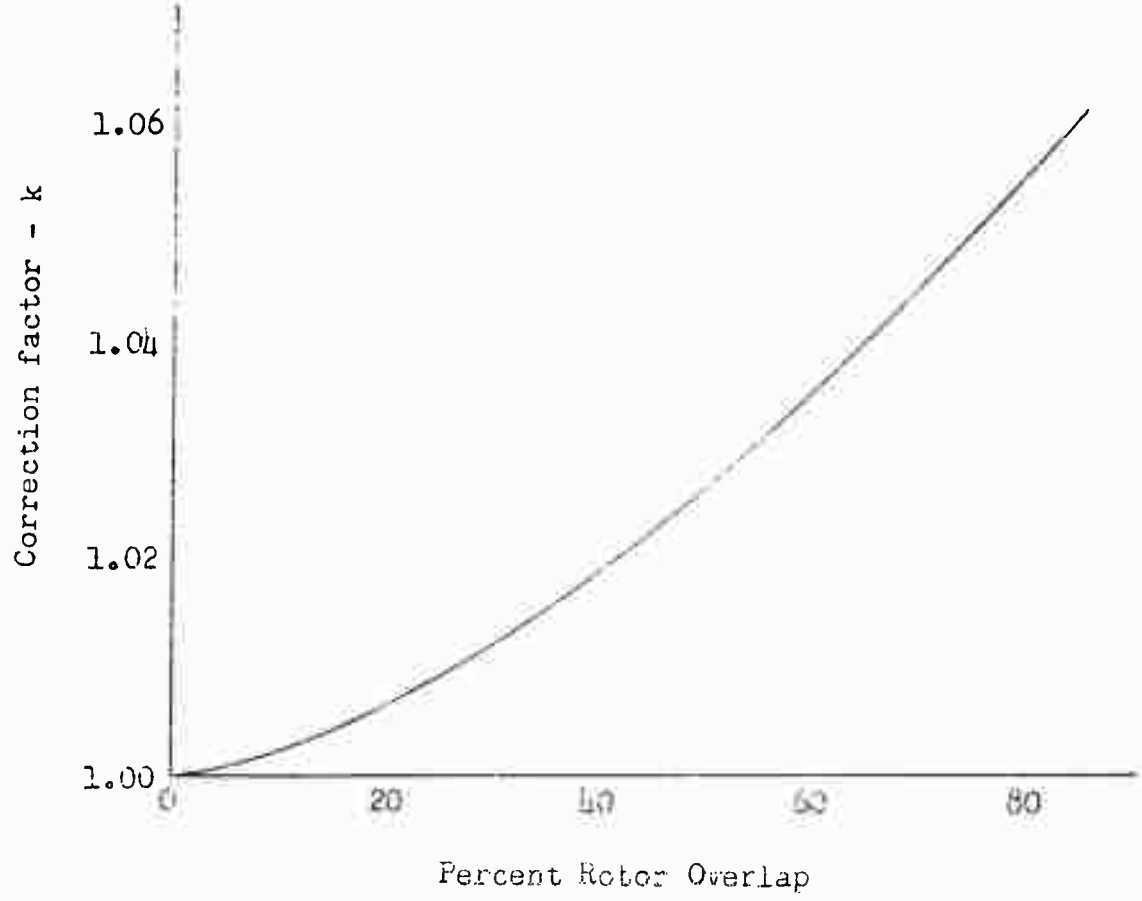

SECTION 3 - WEIGHT ANALYSIS TECHNIQUES

For the single rotor tip powered configurations, the rotor mast serves secondarily as a means of transmitting power, since the shaft torque is determined by the tail rotor and accessory drives power required. Due to the lack of statistical weight data on this component type, the rotor mast weight for tip powered helicopters was assumed to be conservatively predicted by equation 3-24, hence:

$$\text{Rotor mast weight} = 5.32 \frac{W^{1.05}}{(l_{pm} V_T)^{.70} \omega^{.35}} \qquad 3\text{-}26$$

Tandem rotor mast weight was based on the assumption that 60% of the available rotor power could be transmitted to either rotor. Accordingly, the design shaft torque was:

$$Q = \eta (.60)(550 \frac{HP_m R}{V_T})$$

The propulsive efficiencies for tandem rotor configurations from Figure 3-2 are .91 and .96 for reciprocating and geared turbine engines, respectively. Using the previous expression for rotor mast weight in terms of the "design" rotor torque, the weight of two shafts becomes:

$$\text{Rotor mast weight} = 6.13\,k \frac{W^{1.05}}{(l_{pm} V_T)^{.70} \omega^{.35}} \qquad 3\text{-}27$$

for tandem rotor - reciprocating

$$= 6.35\,k \frac{W^{1.05}}{(l_{pm} V_T)^{.70} \omega^{.35}} \qquad 3\text{-}28$$

for tandem rotor - geared turbine

in which the factor "k" is determined as a function of rotor overlap from Figure 3-13.

d) Tail Rotor Drive Shaft Weight

The weight of this component is expressed in terms of the torque transmitted and the shaft length, and includes the weight of the shaft plus bearings and supporting structure.

$$\text{Shaft weight/foot} = .104\, Q^{.57}$$

Tail rotor drive shaft torque can be expressed in terms of the helicopter parameters as follows:

$$Q = 550\, \eta_t \frac{(HP_m)(.18R)}{V_{T_t}}$$

in which η_t = maximum tail rotor power/HP_m from Figure 3-2

$.18R$ = tail rotor radius

V_{T_t} = tail rotor tip speed (assumed equal to main rotor tip speed)

From Figure 3-1, the shaft length is taken as 1.23 x main rotor radius, hence the final weight expression becomes:

$$\text{Tail rotor drive shaft weight} = .166 \frac{W^{1.355}}{(l_{pm} V_T)^{.57}\, \omega^{.785}} \qquad 3\text{-}29$$

for single rotor - shaft powered helicopters

For the tip powered configurations the maximum tail rotor power required for maneuver has been determined to be: .009W; and tail rotor radius corresponding to this required power is: .12 x main rotor radius. The analysis, based on the maneuvering requirements of MIL-H-8501 (Reference 6), and shown in the aerodynamics section of this report, also assumed a tail rotor moment arm of .70 times main rotor radius and a gear loss of 3% of power transmitted to the tail rotor. It was further assumed that the tail rotor gear box effects a direction change only, hence tail rotor rpm equals tail rotor drive shaft rpm. Based on these assumptions maximum drive shaft torque

$$Q = (1.03)(550 \times .009W)\left(\frac{12R}{V_T}\right) = .611 \frac{WR}{V_T}$$

and tail rotor drive shaft weight by use of the weight - torque relationship:

$$\text{Tail rotor drive shaft weight} = .0223 \frac{W^{1.355}}{V_T^{.57}\, \omega^{.785}} \qquad 3\text{-}30$$

for tip powered helicopters

e) Interconnect Shaft Weight
For tandem rotor helicopters, the interconnect shaft weight-torque expression:

$$\text{Shaft weight/foot} = .104\, Q^{.57}$$

and the design torque, statistically, is

$$Q = 2.67\, HP_m \quad \text{(Reference 13)}$$

The length of the shaft is determined by the rotor overlap as defined in part 3. From this:

$$\text{Interconnect shaft weight} = .0725\, k \frac{W^{1.07}}{l_{pm}^{.57}\, w^{.50}} \qquad 3\text{-}31$$

where the factor, k, is the rotor overlap correction factor shown in Figure 3-14 as a function of percent rotor overlap.

f) Engine-Transmission Drive Shaft Weight
The weight of this item in terms of the installed power and number of engines (n)

$$= .14\, n^{.12}\left(\frac{W}{l_{pm}}\right)^{.88} \qquad 3\text{-}32$$

Figure 3-14: Tandem Rotor Interconnect Shaft Weight Correction Factor (Equa.3-31) vs. Percent Rotor Overlap

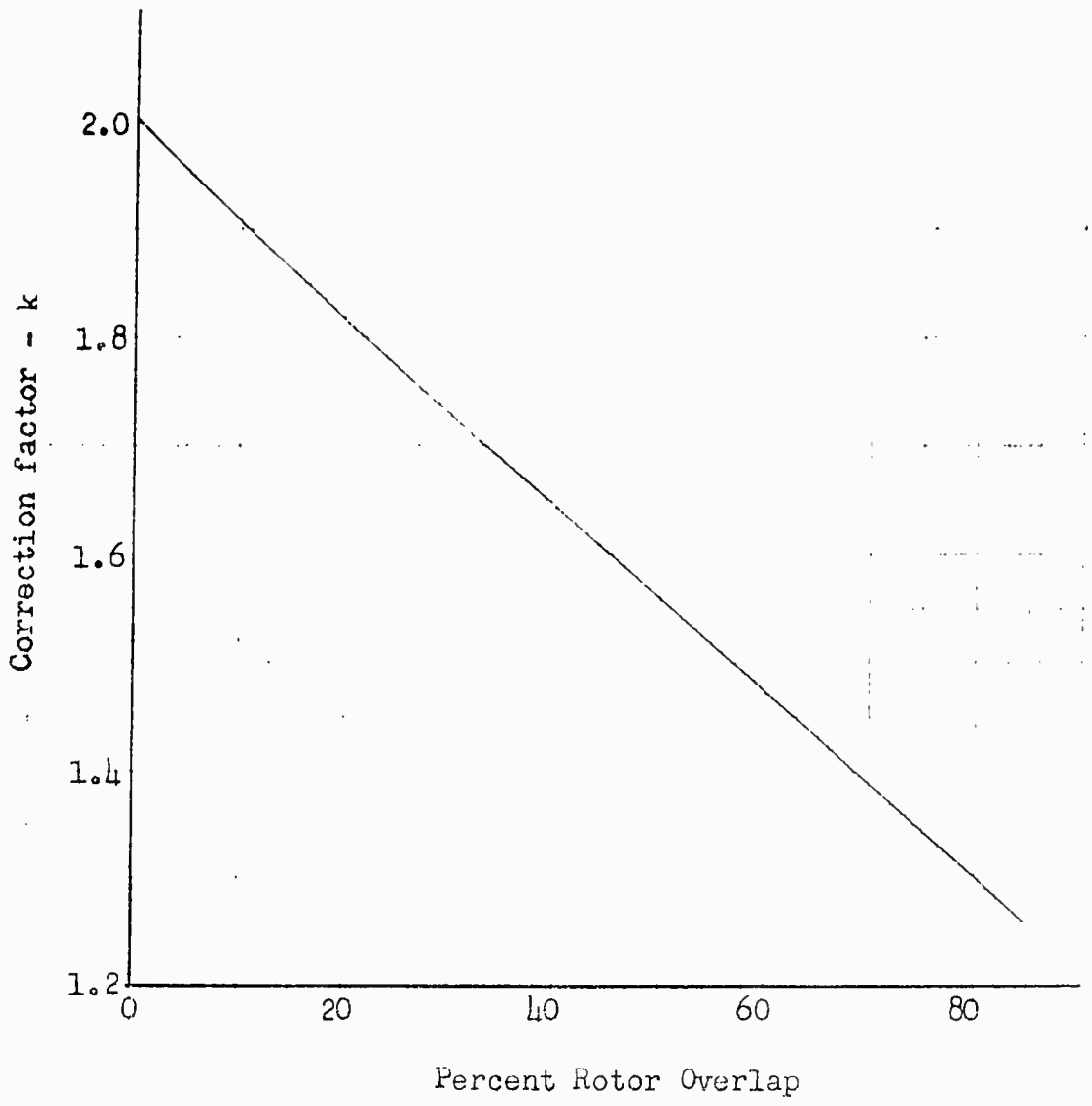

Figure 3-15: Tandem Rotor Main Transmission Weight Correction Factor (Equas. 3-35 and 3-36) vs. Percent Rotor Overlap

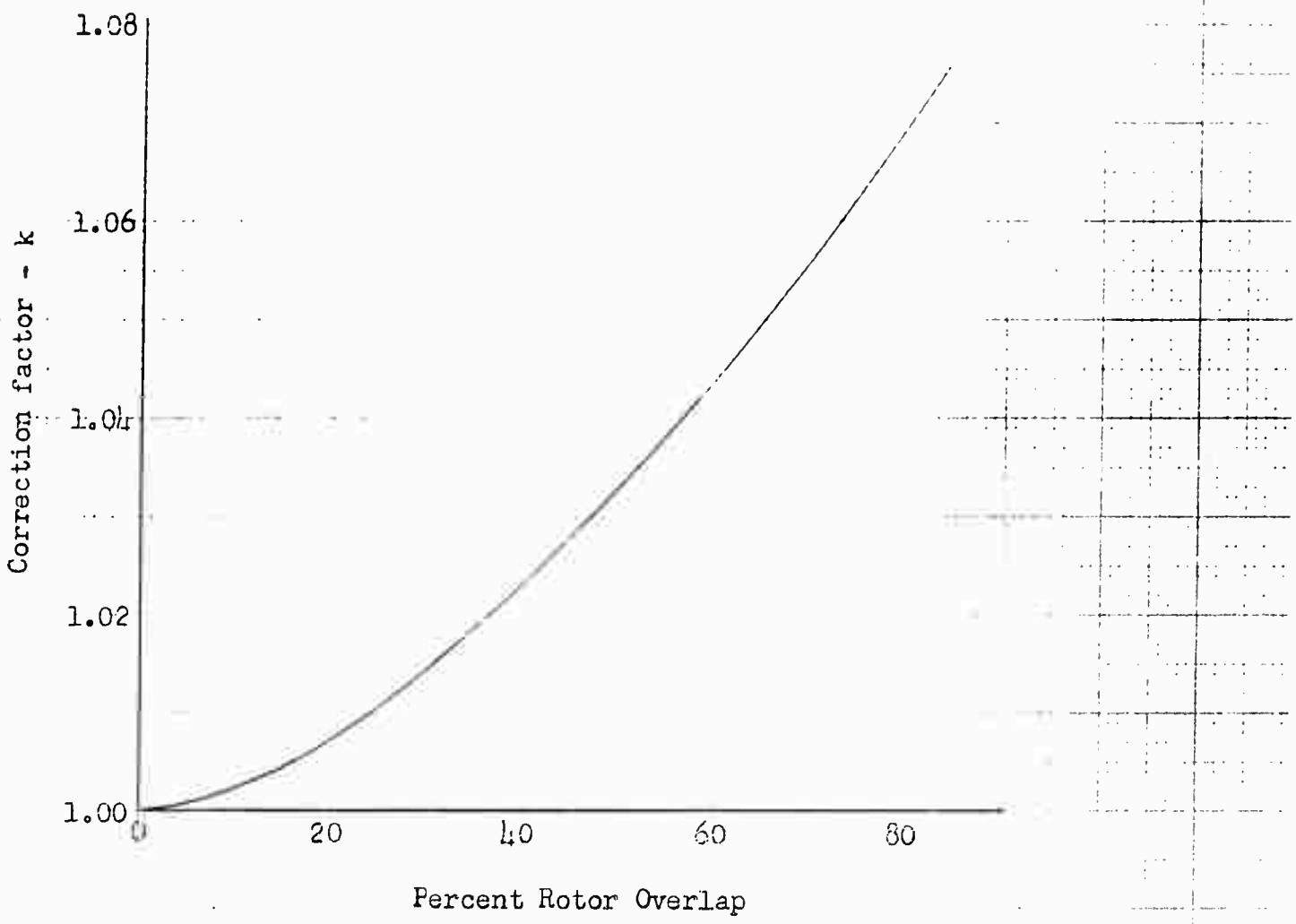

This expression is then applicable to both single and tandem, shaft powered configurations.

g) Main Transmission Weight

The statistical data for main transmission weights includes the weights of the gear box, centrifugal clutch and the over-running clutch. Planetary gearing has been used for the majority of helicopter reduction gear boxes due to their lighter weight and greater efficiency. Planetary transmission weight as a function of maximum torque on the low speed output:

$$\text{Transmission weight} = .081\, Q^{.88}$$

For single rotor, shaft powered helicopters, the maximum torque (same as maximum rotor mast torque - paragraph 6c)

$$Q = 464\,\frac{HP_m \times R}{V_T} \qquad \text{for single rotor, reciprocating}$$

$$Q = 491\,\frac{HP_m \times R}{V_T} \qquad \text{for single rotor, geared turbine}$$

Since multiple engine installations were assumed to require additional clutches and direction change gear sets, the transmission weight would increase accordingly. The basic weight data did not include multi-engine helicopter transmission weights, however, from a recent transmission study, Reference 15, it was found that there is a statistical correlation between transmission weight and the number of power inputs and outputs. Based on the assumption that the basic data represented helicopter transmissions with one input and one output, a factor was developed which would account for increasing transmission weight with number of installed engines. Hence the factor:

$$k_n = \left(\frac{n+1}{2}\right)^{.375}$$

where n = number of installed engines.

The main transmission weight for <u>single rotor, shaft powered</u> helicopters becomes:

$$\text{Transmission weight} = .081\, Q^{.88}\left(\frac{n+1}{2}\right)^{.375}$$

and, substituting in this, the torque expressions:

$$\text{Transmission weight} = 10.9\left(\frac{n+1}{2}\right)^{.375}\frac{W^{1.32}}{(l_{pm}V_T)^{.88}\,\omega^{.44}} \qquad 3\text{-}33$$

for single rotor, reciprocating

$$= 11.4\left(\frac{n+1}{2}\right)^{.375}\frac{W^{1.32}}{(l_{pm}V_T)^{.88}\,\omega^{.44}} \qquad 3\text{-}34$$

for single rotor, geared turbine

TRANSPORT HELICOPTER DESIGN ANALYSIS METHODS

Since two main transmissions are required for tandem rotor helicopters, the assumption was again made that "design" power transmitted through either transmission was 60% of total power available at the rotors. "Design" torque may then be expressed as:

$$Q = 300 \frac{HP_m \times R}{V_T} \qquad \text{tandem - reciprocating}$$

$$Q = 317 \frac{HP_m \times R}{V_T} \qquad \text{tandem - geared turbine}$$

Utilizing the weight-torque relation the final weight of both main transmissions for tandem rotor helicopters:

$$\text{Transmission weight} = 10.9\, k \frac{W^{1.32}}{(l_{pm} V_T)^{.88}\, w^{.44}} \qquad 3\text{-}35$$

for tandem - reciprocating

$$= 11.5\, k \frac{W^{1.32}}{(l_{pm} V_T)^{.88}\, w^{.44}} \qquad 3\text{-}36$$

for tandem - geared turbine

in which the factor, k, accounts for variation of rotor overlap and is given in Figure 3-15.

Main transmissions for tip powered helicopters considered in the study were assumed to effect the increase in rpm from main rotor to tail rotor and to provide take-offs for the accessory drives. The basic weight-torque expression for this transmission was assumed to be the same as the planetary gear box relationship. Maximum torque (rotor shaft side) was assumed to vary with the main rotor - tail rotor radius ratio, hence the maximum torque:

$$Q = \frac{R}{.12R}\left(.611 \frac{WR}{V_T}\right)$$

in which the term within parentheses is the "design" tail rotor drive shaft torque derived previously. Substituting the design torque in the weight function:

$$\text{Main transmission weight} = .204 \frac{W^{1.32}}{V_T^{.68}\, w^{.44}} \qquad 3\text{-}37$$

h) Tail Rotor Transmission

Tail rotor transmissions were assumed to be direction change gear boxes. Thus the weight in terms of maximum torque:

$$\text{Tail rotor transmission} = 2.2\, Q^{.50} \qquad \text{(Reference 13)}$$

Maximum tail rotor transmission torque for shaft powered configurations was assumed equal to tail rotor drive shaft torque, paragraph 6(d):

$$Q = 7.62 \frac{HP_m \times R}{V_T}$$

[illegible]

Intermediate Gear Box Weight

[illegible] intermediate gear box weight [illegible]

[illegible]

$$\text{Intermediate transmission weight} = .325\left(\frac{N_e - 2}{3}\right)^{.375}\left(\frac{W}{\text{rpm}}\right)^{.35}$$ [illegible]

f) Starting System Weight

For reciprocating engine powered helicopters the starting system weight including electrical accessories and wiring

$$\text{Weight} = .79\, N_e^{[illegible]}\left(\frac{W}{\text{rpm}}\right)^{.60}$$ [illegible]

and tail rotor transmission weight:

$$= 4.56 \frac{W^{.75}}{(l_{pm} V_T)^{.50} \omega^{.25}} \qquad 3\text{-}38$$

for single rotor - shaft powered helicopters

Tail rotor gear boxes for tip powered helicopters were based on the same weight-torque expression, using the torque expression from paragraph 6(d):

$$Q = .611 \frac{WR}{V_T}$$

The resulting weight equation becomes:

$$\text{Tail rotor gear box weight} = 1.29 \frac{W^{.75}}{V_T^{.50} \omega^{.25}} \qquad 3\text{-}39$$

for tip powered helicopters

i) Intermediate Gear Box Weight
For the tandem rotor helicopters the intermediate gear box weight was assumed as:

$$\text{Intermediate gear box weight} = .137 Q^{.88}$$

Considering that this weight would be a function of the number of engine power inputs, i.e., increased weight due to additional bearings and gear sets, the method of analysis used in obtaining single rotor main transmission weight increase was employed. Based on the assumption that the statistical data represented intermediate gear boxes with one input and two power take-offs, the factor

$$k_n = \left(\frac{n+2}{3}\right)^{.375}$$

was deemed adequate to account for the weight variation with number of installed engines (n).

Using the expression for maximum torque based on statistical data (Reference 13)

$$Q = 2.67 HP_m$$

the final form of the weight expression:

$$\text{Intermediate transmission weight} = .325 \left(\frac{n+2}{3}\right)^{.375} \left(\frac{W}{l_{pm}}\right)^{.88} \qquad 3\text{-}40$$

j) Starting System Weight
For reciprocating engine powered helicopters the starting system weight including electrical accessories and wiring

$$\text{Weight} = .79 n^{.40} \left(\frac{W}{l_{pm}}\right)^{.60} \qquad 3\text{-}41$$

and for geared gas turbine powered helicopters, starting system weight:

$$= .29 n^{.40} \left(\frac{W}{l_{pm}}\right)^{.60} \qquad 3\text{-}42$$

Ramjet and pressure jet powered helicopters were assumed to have the same starting system weight as the geared gas turbine powered machine. Tip mounted turbojet engine starting systems, however, are included in the engine weight.

k) Cooling System
Cooling system weight for reciprocating engine installations includes the weight of fans, radiators, tanks, plumbing and coolant. For any number installed engines:

$$\text{Cooling system weight} = .04 n^{-.07} \left(\frac{W}{l_{pm}}\right)^{1.07} \qquad 3\text{-}43$$

Geared gas turbine engines normally require no cooling systems and for purposes of this study it was assumed that the cooling system weight, if required, would be accounted for in the engine weight.

l) Lubrication System
Lubrication system weights include the weight of oil pumps, coolers, plumbing but excludes the weight of oil and oil tanks. The latter are treated separately in paragraph 8. Lubrication system weight as a function of the total installed power and number of engines (for reciprocating engines):

$$\text{Lubrication system weight} = .27 n^{.19} \left(\frac{W}{l_{pm}}\right)^{.81} \qquad 3\text{-}44$$

Geared turbine and tip powered helicopters were considered to have lubrication system weight included in the weight of the engine.

m) Fuel System
The weight of fuel systems includes all necessary plumbing, fittings and filters but does not include fuel tank weight. For reciprocating engine installations:

$$\text{Fuel system weight} = .05 n \left(\frac{W}{l_{pm}}\right) \qquad 3\text{-}45$$

For geared turbine and tip powered configurations the fuel system weight was assumed to be included in the engine weight.

7. Fixed Equipment Group

The various items of fixed equipment are given in Reference 13 as follows:

a) Instrument weight $= .104\ W^{.71}$

b) Flight Controls weight $= .512\ W^{.68}$

c) Hydraulic and Electrical Systems weight $= .381\ W^{.71}$

d) Furnishings weight $= .682\ W^{.65} - 50$

e) Communications Equipment weight $= 5.55(W - 1200)^{.35}$

Calculation of the total weight of these items for a range of gross weights yields a single expression for Fixed Equipment Group weight as:

$$\text{Total Fixed Equipment weight} = 1.93\ W^{.672} \qquad 3\text{-}46$$

8. Oil and Oil Tank Weight

For reciprocating engine powered helicopters the ratio of engine and transmission oil weight to engine weight was assumed to be .096 (Reference 13). Further assuming oil weight of 7.5 lbs/gallon and tank weight as 2.0 lbs/gallon, the total weight of oil and oil tanks:

$$= .122 \times \text{engine weight}$$

From paragraph 6(a) the expression for reciprocating engine weight

$$= 4.46\, n^{.178} \left(\frac{W}{l_{pm}}\right)^{.822}$$

hence the weight of oil and oil tanks

$$= .542\, n^{.178} \left(\frac{W}{l_{pm}}\right)^{.822} \qquad 3\text{-}47$$

Oil weight for geared gas turbine power plants was assumed to be .04 x the engine weight. By use of the geared turbine engine weight, the expression for oil and oil tank weight:

$$= 3.8n + .049\, n^{.09} \left(\frac{W}{l_{pm}}\right)^{.908} \qquad 3\text{-}48$$

C. EMPTY WEIGHT EQUATIONS FOR SPECIFIC HELICOPTER CONFIGURATIONS

1. Procedure

The analysis presented in this part of the design analysis concerns the integration of the individual component weight expressions derived in Part B, to formulate empty weight equations for specific rotor and power plant configurations. Since the weight expressions were derived on the basis of assumptions for the most part considered applicable to the transport helicopter, the equations of this part of the analysis are based on similar assumptions as an example of the techniques employed. As a review of the major assumptions on which the component weight expressions were derived the following steps may be summarized:

a) establishment of certain fixed dimensions shown in Figure 3-1 for the transport helicopter configuration, and

b) establishment of assumed power distribution to rotors and mechanical drives similar to that shown in Figure 3-2.

TRANSPORT HELICOPTER DESIGN ANALYSIS METHODS

In addition, the further assumptions are made in presenting the empty weight equations in this part that:

c) tandem rotor overlap is fixed at 60% of rotor radius, and

d) Communications Equipment weight is fixed at 273 lbs, which includes the equipment considered requisite for the transport mission as outlined in Reference 1, p.90.

On the basis of the preceding assumptions, the individual weight expressions may be combined to form weight equations for given configurations. Figure 3-16 shows the equation number for each component of various configurations as an aid in locating specific items of empty weight. The weight equation terms consist in part, of three groups of terms each of which may be combined:

a) Terms which are functions of gross weight or which are fixed weight items, i.e., Communications Equipment weight in the following analysis. The items which can be combined are: Stabilizer, Landing Gear, and Fixed Equipment weight.

b) Terms which are functions of the total installed take-off power, (HP_m)

c) Terms which are functions of or have the units of torque, $\frac{W^{1.50}}{(l_{pm})(V_T)\ w^{.50}}$

In the empty weight equations which follow, the three groups of terms indicated above have been combined by the process of calculating the values of the individual weight items for a range of the particular variable, replotting the total of the group weight against the applicable parameter and determining a new functional relationship for the total group weight. Obtaining the total weight function in this manner is approximate at the extreme limits of the function but well within the range of probable error incurred by use of the statistical data itself. The final empty weight equations for the seven rotor-power plant configurations are shown in the following paragraphs, and a typical plot of the variation of empty weight with gross weight is shown in Figure 3-22 for a single rotor, twin geared ga. turbine powered helicopter (n=2) with a design hover ceiling of 5000' and a tip speed of 700 feet/sec.

Rotor tip speed has been established as 700 feet per second on the basis of preliminary investigation of the aerodynamic and weight effects. Weightwise, increasing tip speed decreases rotor and mechanical drives weight due to greater centrifugal relief for rotor blades and decreased design torque for transmissions and drives, other factors remaining constant. Aerodynamically, higher rotor speed requires increased installed power and weight for a given disk loading and design hover ceiling. The net effect of these opposing trends is to decrease design gross weight with increasing tip speed. The limiting tip speed of 700 ft/sec was selected on the basis of tip compressibility limits, therefore, as the best compromise between aerodynamic and weight efficiency.

Power loadings are established by the aerodynamic analysis from the criterion of power required per pound of gross weight for a given hover ceiling. Since the hover power required is a function of altitude and design disk loading primarily, the values of take-off power loading for various hover ceilings are plotted in Figures 3-17 through 3-21.

SECTION 3 - WEIGHT ANALYSIS TECHNIQUES

COMPONENT GROUP	COMPONENT WEIGHT EQUATION NO.						
	Single Rotor		Tandem Rotor		Single Rotor		
	Recip. Eng.	Geared Turb.	Recip. Eng.	Geared Turb.	Ram-jet	Tip Turbo Jet	Press. Jet
Rotor Group							
Blades	3-2	3-2	3-3	3-3	3-4	3-4	3-4
Hub Assembly	3-5	3-5	3-6	3-6			
Tail Group							
Stabilizer	3-7	3-7	3-8	3-8	3-7	3-7	3-7
Tail Rotor	3-9	3-10			3-11		
Body Group	3-12		3-13		3-14		
Alignting Gear	3-15						
Engine Section	3-16	3-17	3-16	3-17			
Power Plant Group							
Engine	3-18	3-19	3-18	3-19	3-20	3-21	3-22
Access. and Controls	3-23		3-23				
Rotor Mast	3-24	3-25	3-27	3-28	3-26		
T.R. Drive Shaft	3-29				3-30		
Interconn. Shaft			3-31				
Eng-Trans.Drive Shaft	3-32						
Main Transmission	3-33	3-34	3-35	3-36	3-37		
T.R. Transmission	3-38				3-39		
Inter. Gear Box			3-40				
Starting System	3-41	3-42	3-41	3-42	3-42		
Cooling System	3-43		3-43				
Lubr.System,less tanks	3-44		3-44				
Fuel System,less tanks	3-45		3-45				
Fixed Equipment	3-46						
Oil and Oil Tanks	3-47	3-48	3-47	3-48			

Figure 3-16 Resume' of Component Weight Expressions for Various Configurations

TRANSPORT HELICOPTER DESIGN ANALYSIS METHODS

The fuel weight to gross weight ratio (R_F) can be readily calculated from equation 3-1, having the suitable trends of ϕ vs. gross weight.

$$R_F = .923(1 - R_P - R_C - \Phi) \qquad 3\text{-}1$$

The generalized weight equation, repeated above, can be seen to be a function only of payload and crew weight and the empty weight less fuel tank weight ratio, ϕ. Since the latter expression can be reduced to a function of gross weight and disk loading for any given hover ceiling, the calculation of R_F is relatively straightforward. The section entitled "Configuration Selection Techniques" discusses the graphical procedure of combining this expression with the aerodynamic range equation to obtain compatible gross weight solutions.

SECTION 3 - WEIGHT AND [illegible]

Figure 3-17: Power Loading vs. Disk Loading for various design hover ceilings
Single rotor, reciprocating powered helicopters
V_T = 700 feet/sec
Note: for tandem rotor, counter-rotating powered helicopters multiply by 1.076

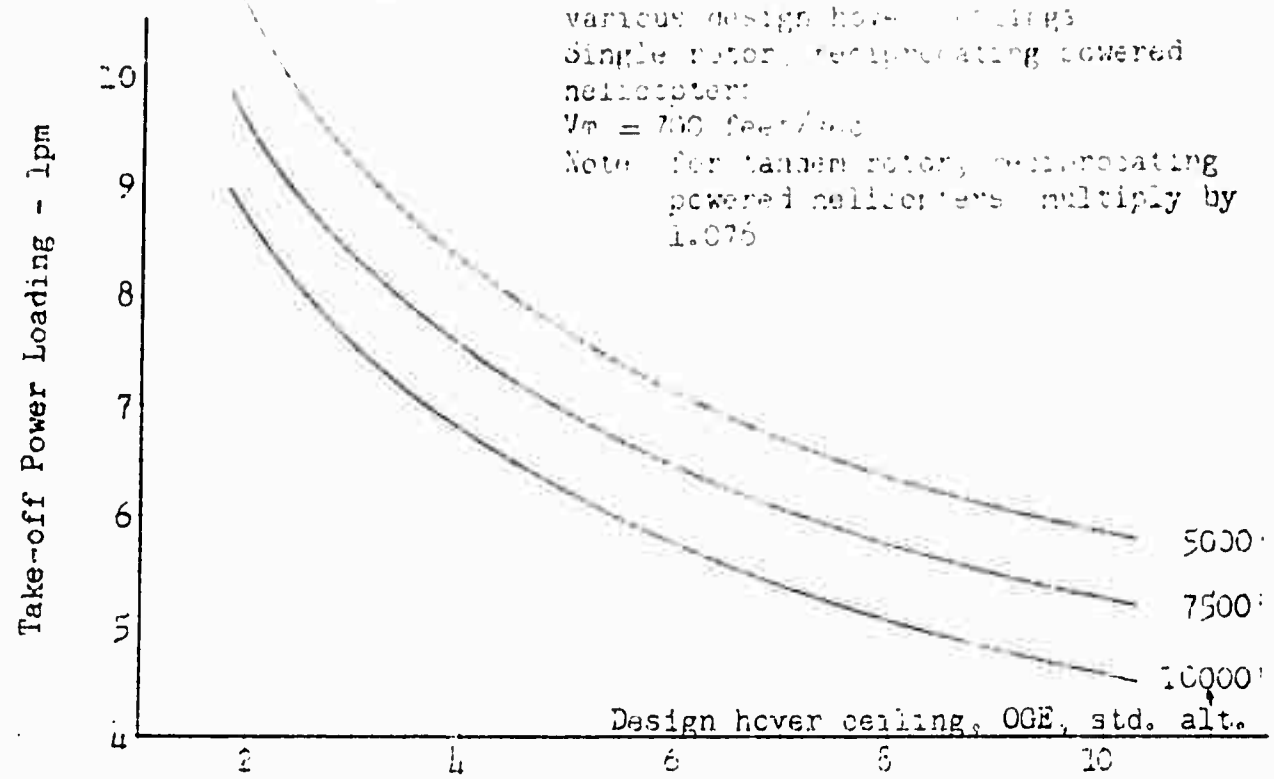

Figure 3-18: Power Loading vs. Disk Loading for various design hover ceilings
Single rotor, geared turbine powered helicopters
V_T = 700 feet/sec
Note: for tandem rotor, geared turbine powered helicopters, multiply by 1.076

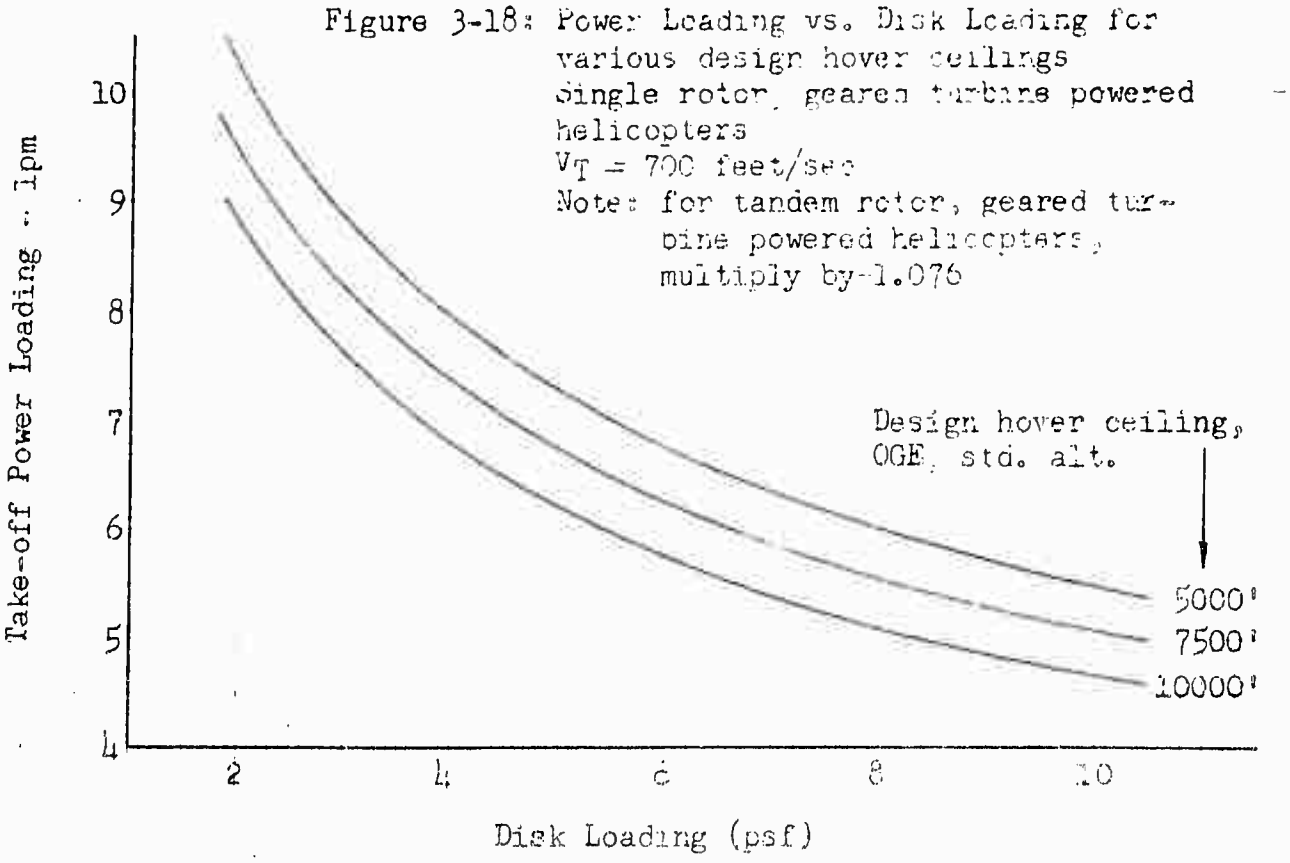

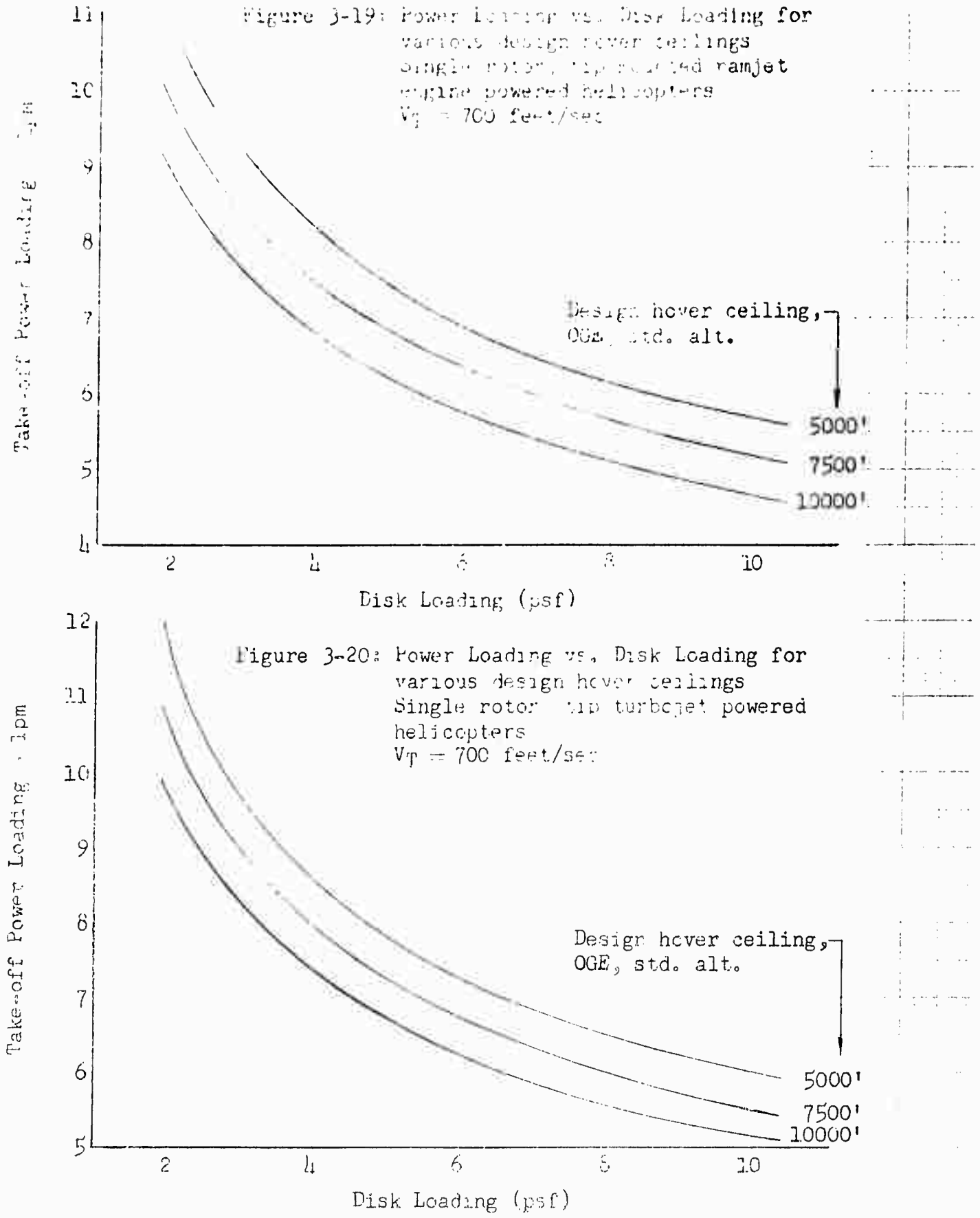

Figure 3-19: Power Loading vs. Disk Loading for various design hover ceilings Single rotor, tip mounted ramjet engine powered helicopters V_T = 700 feet/sec

Figure 3-20: Power Loading vs. Disk Loading for various design hover ceilings Single rotor tip turbojet powered helicopters V_T = 700 feet/sec

Figure 3-21: Power Loading vs. Disk Loading for various design hover ceilings
Single rotor, pressure jet powered helicopters
V_T = 700 feet/sec
Power loadings based on installed gas turbine shaft HP with 2000°F tip burner temperature and 2.5 pressure ratio in hover.

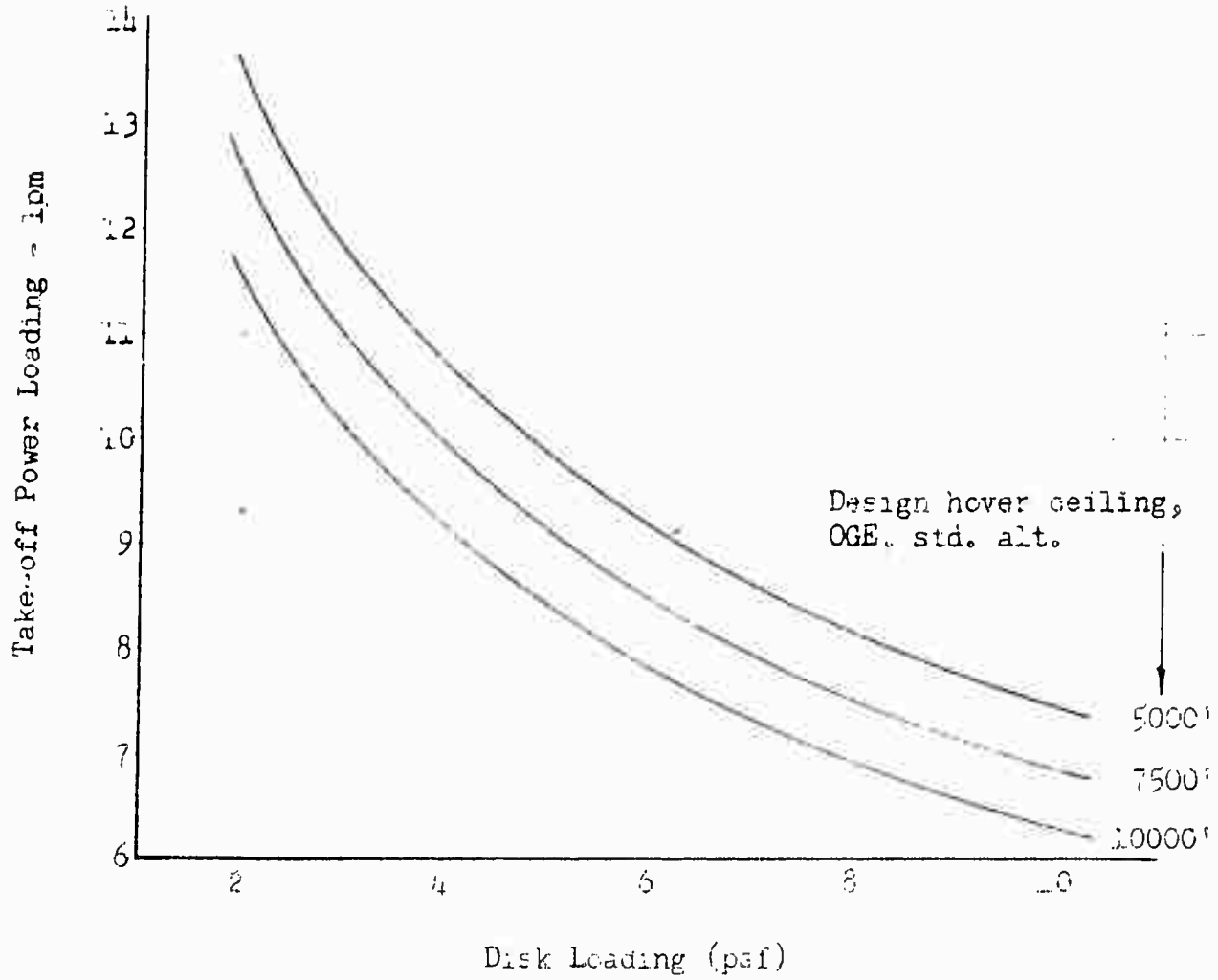

TRANSPORT HELICOPTER DESIGN ANALYSIS

Figure 3-22: Typical variation of θ with gross weight for various disk loadings
Single rotor, twin geared gas turbine powered helicopter
5000' design hover ceiling OGE, std. alt.
Tip speed = 700 feet/sec
From equation 3-60

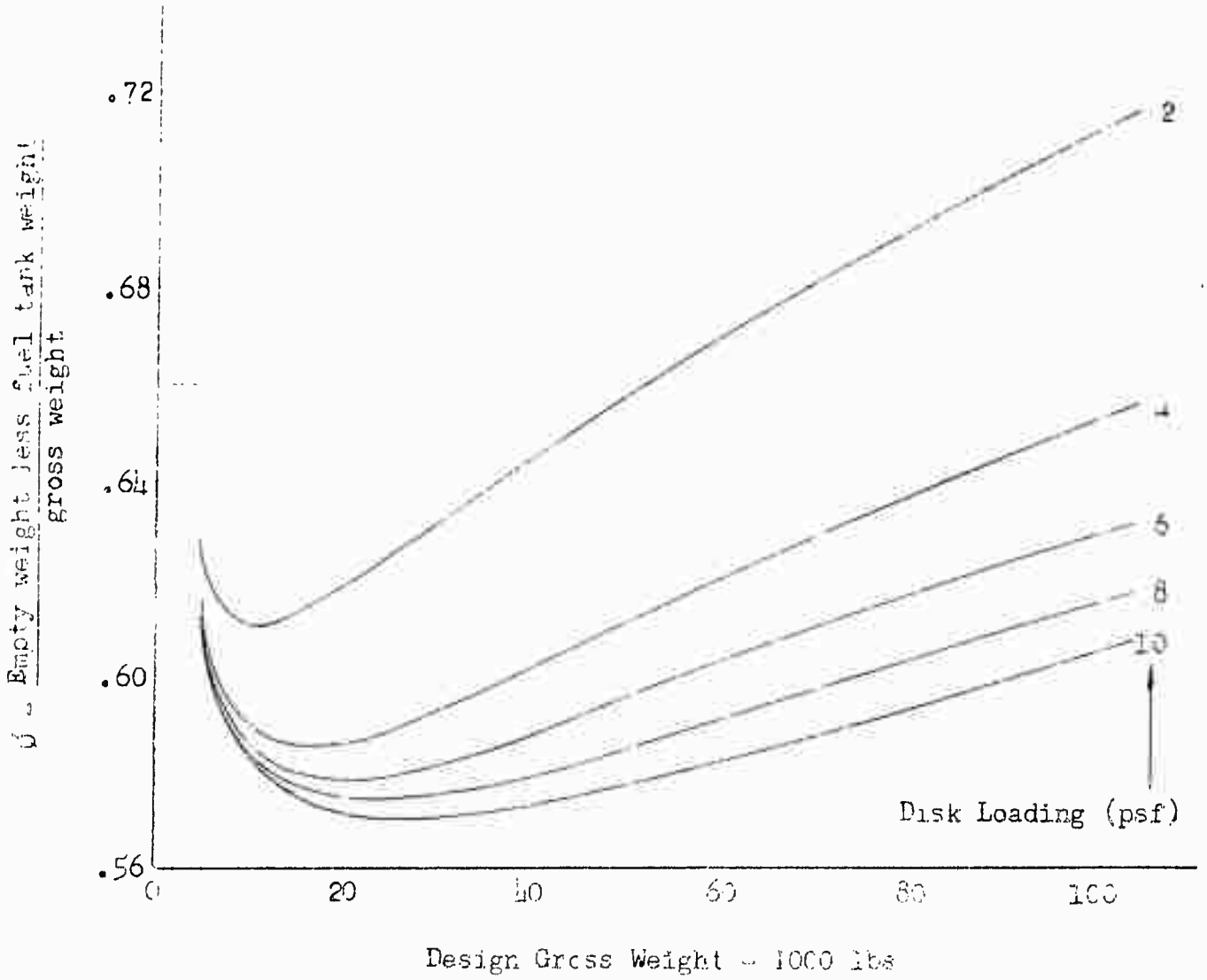

SECTION 3 - WEIGHT ANALYSIS TECHNIQUES

2. Example Weight Equations for Transport Helicopter Configurations

a) Single Rotor, Reciprocating Engine Powered

$$\phi = .106\frac{W^{.035}}{w^{.098}} + 3.86W^{-.341} + 7.07\frac{1}{V_T}\left(\frac{W}{w}\right)^{.205}$$

(Body) (Stabilizer, Land'g Gear and Fixed Equipment) (Rotor blades) ①

$$+.0097\left(\frac{W}{w}\right)^{.21} + \frac{K_2}{l_{pm}^{.862}\,W^{.138}} + \frac{K_3\,W^{.251}}{(l_{pm}V_T)^{.834}\,w^{.417}}$$

(Rotor hub assembly) (Power plant) ② (Transmissions and drives) ③

$$+\frac{.166\,W^{.355}}{(l_{pm}V_T)^{.57}\,w^{.785}} + \frac{646}{l_{pm}\,V_T^{2}}\left(\frac{W}{w}\right)^{.50}$$

(Tail rotor drive shaft) (Tail rotor)

① For values of $\frac{W}{w} > 4680$, this term $= 3.16\frac{1}{V_T}\left(\frac{W}{w}\right)^{.30}$

② For single engine installations: $K_2 = 5.26$
2 engines, $K_2 = 5.93$
3 engines, $K_2 = 6.40$
4 engines, $K_2 = 6.83$

③ For single engine installations: $K_3 = 17.25$
2 engines, $K_3 = 19.5$
3 engines, $K_3 = 21.3$
4 engines, $K_3 = 22.9$

TRANSPORT HELICOPTER DESIGN ANALYSIS METHODS

b) Single Rotor, Geared Gas Turbine Powered

$$\phi = .106\frac{W^{.035}}{w^{.098}} + 3.86W^{-.341} + \text{①}\ 7.07\frac{1}{V_T}\left(\frac{W}{w}\right)^{.205}$$

(Body) (Stabilizer, Land'g Gear and Fixed Equipment) (Rotor blades)

$$+ .0097\left(\frac{W}{w}\right)^{.21} + \text{②}\ R_s + \text{③}\ \frac{K_3 W^{.248}}{(l_{pm}V_T)^{.832} w^{.416}}$$

(Rotor hub assembly) (Power plant) (Transmissions and drives)

$$+ \frac{.166 W^{.355}}{(l_{pm}V_T)^{.57} w^{.785}} + \frac{685}{l_{pm}V_T^2}\left(\frac{W}{w}\right)^{.50}$$

(Tail rotor drive shaft) (Tail rotor)

3-50

① For values of $\frac{W}{w} > 4680$, this term = $3.16\frac{1}{V_T}\left(\frac{W}{w}\right)^{.30}$

② For single engine installations, $R_s = \frac{1.52}{l_{pm}^{.90} W^{.10}}$

2 engines, $R_s = \frac{2.08}{l_{pm}^{.872} W^{.128}}$

3 engines, $R_s = \frac{2.71}{l_{pm}^{.85} W^{.15}}$

4 engines, $R_s = \frac{3.20}{l_{pm}^{.836} W^{.164}}$

③ For single engine installations, $K_3 = 18.6$
2 engines, $K_3 = 20.8$
3 engines, $K_3 = 22.6$
4 engines, $K_3 = 24.1$

SECTION 3 - WEIGHT ANALYSIS TECHNIQUES

c) Tandem Rotor, Reciprocating Engine Powered

$$\phi = .128\frac{W^{.035}}{w^{.345}} + 3.78\,W^{-.335} + 6.28\,\frac{1}{V_T}\left(\frac{W}{w}\right)^{.205}\ ①$$

(Body) (Stabilizer, Land'g Gear and Fixed Equipment) (Rotor blades)

$$+.00857\left(\frac{W}{w}\right)^{.21} + \frac{K_2}{l_{pm}^{.855}\,W^{.145}}\ ② + \frac{17.0\,W^{.262}}{(l_{pm}V_T)^{.841}\,w^{.42}}$$

(Rotor hub assembly) (Power plant) (Transmissions and drives)

$$+\frac{.1066\,W^{.07}}{l_{pm}^{.57}\,w^{.50}}$$

(Interconnect shaft)

3-51

① For values of $\frac{W}{w} > 5550$, this term $= 2.65\,\frac{1}{V_T}\left(\frac{W}{w}\right)^{.30}$

② For single engine installations, $K_2 = 6.0$
2 engines, $K_2 = 6.67$
3 engines, $K_2 = 7.29$
4 engines, $K_2 = 7.75$

TRANSPORT HELICOPTER DESIGN ANALYSIS METHODS

d) Tandem Rotor, Geared Gas Turbine Powered

$$\phi = .128\frac{W^{.035}}{w^{.345}} + 3.78\,W^{-.335} + 6.28\frac{1}{V_T}\left(\frac{W}{w}\right)^{.205}\ ①$$

(Body) (Stabilizer, Land'g Gear and Fixed Equipment) (Rotor blades)

$$+.00857\left(\frac{W}{w}\right)^{.21} + \frac{K_2}{l_{pm}^{.84}\,W^{.16}}\ ② + \frac{17.5\,W^{.268}}{(l_{pm}V_T)^{.845}\,w^{.422}}$$

(Rotor hub assembly) (Power plant) (Transmissions and drives)

$$+ \frac{.1066\,W^{.07}}{l_{pm}^{.57}\,w^{.50}}$$

(Interconnect shaft)

3-52

① For values of $\frac{W}{w} > 5550$, this term $= 2.65\frac{1}{V_T}\left(\frac{W}{w}\right)^{.30}$

② For single engine installations, $K_2 = 2.93$
2 engines, $K_2 = 3.21$
3 engines, $K_2 = 3.44$
4 engines, $K_2 = 3.66$

SECTION 3 - WEIGHT ANALYSIS TECHNIQUES

e) Single Rotor, Tip Mounted Ramjet Engines

$$\phi = .107\frac{V_T^{.035}}{W^{.345}} + 3.86\,W^{-.341} + .0362\left(\frac{W}{W}\right)^{.21}\ ①$$

(Body) (Stabilizer, Land'g Gear and Fixed Equipment) (Rotor group)

$$+ \frac{1.35\times10^{8}}{l_{pm}\,V_T^{3}} + \frac{.29}{l_{pm}^{.60}\,W^{.40}} + \frac{.716\,W^{.15}}{V_T^{.766}\,W^{.303}}$$

(Engines) (Starting system) (Main transmission)

$$+ \frac{.0223\,W^{.355}}{V_T^{.57}\,W^{.785}} + \frac{.148\,W^{.50}}{V_T\,W} + \frac{5.32\,W^{.05}}{(l_{pm}V_T)^{.70}\,W^{.55}}$$

(Tail rotor drive shaft) (Tail rotor) (Rotor mast)

3-53

① For values of $\frac{W}{W} > 5030$, this term = $.0256\left(\frac{W}{W}\right)^{.25}$

TRANSPORT HELICOPTER DESIGN ANALYSIS METHODS

f) Single Rotor, Tip Mounted Turbojet Engines

$$\Phi = .107\frac{W^{.035}}{w^{.345}} + 3.86\,W^{-.341} + .0362\left(\frac{W}{w}\right)^{.21}\text{①}$$

(Body) (Stabilizer, Land'g Gear and Fixed Equipment) (Rotor group)

$$+ \frac{160\,W^{.234}}{(l_{pm}V_T)^{1.234}} + \frac{.716\,W^{.15}}{V_T^{.766}\,w^{.383}} + \frac{.0223\,W^{.556}}{V_T^{.57}\,w^{.785}}$$

(Power plant group) (Main transmission) (Tail rotor drive shaft)

$$+ \frac{.148\,W^{.50}}{V_T\,w} + \frac{5.32\,W^{.05}}{(l_{pm}V_T)^{.70}\,w^{.35}}$$

(Tail rotor) (Rotor mast)

3-54

① For values of $\frac{W}{w} > 5030$, this term $= .0256\left(\frac{W}{w}\right)^{.25}$

SECTION 3 - WEIGHT ANALYSIS TECHNIQUES

g) Single Rotor, Pressure Jet Power Plant

$$\phi = .107\frac{W^{.035}}{w^{.345}} + 3.86\,W^{-.341} + .0362\left(\frac{W}{w}\right)^{.21}\text{①}$$

(Body) (Stabilizer, Land'g Gear and Fixed Equipment) (Rotor group)

$$+ \frac{464}{l_{pm}} + \frac{.716\,W^{.15}}{V_T^{.766}\,w^{.383}} + \frac{.0223\,W^{.355}}{V_T^{.57}\,w^{.785}}$$

(Power plant group) (Main transmission) (Tail rotor drive shaft)

$$+ \frac{.148\,W^{.50}}{V_T\,w} + \frac{5.32\,W^{.05}}{(l_{pm}V_T)^{.70}\,w^{.35}}$$

(Tail rotor) (Rotor mast)

3-55

① For values of $\frac{W}{w} > 5030$, this term $= .0256\left(\frac{W}{w}\right)^{.25}$

SECTION 3 - WEIGHT ANALYSIS TECHNIQUES

D. SYMBOLS

A_e...tandem rotor effective disk area ($2\pi R^2$ - overlap area)

ESHP.S.L. normal rated equivalent shaft HP; geared gas turbine engines

$ESHP_m$..S.L. military take off rating equivalent shaft HP; geared gas turbines

HP...normal rated power, S.L.

HP_m..military take-off power assumed as 1.167 times HP, S.L.

k....tandem rotor overlap weight correction factor

kF...ratio of fuel tank weight per gallon to fuel weight per gallon

l_{pm}..W/HP_m

l_p...W/HP

L....overall fuselage length

n....number of installed engines

Q....design torque for mechanical drive component; corresponds to torque developed at engine take-off power, sea level rating

r....tail rotor radius

R....main rotor radius

R_P...payload to gross weight ratio

R_C...crew weight/W

R_F...fuel weight/W

R_{FT}..fuel tank weight/W

V_T...main rotor tip speed (feet/sec)

V_{T_t}..tail rotor tip speed (feet/sec)

w....disk loading (lbs/ft^2)
$W/\pi R^2$ for single rotor configurations
W/A_e for tandem rotor configurations

w_t...tail rotor disk loading

W....design gross weight

W_i...a component weight; i referring to:
P...payload
C...crew
F...fuel
FT..fuel tank
E...empty weight

β...tandem rotor fuselage length (shaft to shaft) $\div$ R

$$= \left(2 - \frac{\% \text{ rotor overlap}}{100}\right)$$

η...main rotor power/ installed power

η_t..tail rotor power/ installed power

ϕ....empty weight less fuel tank/ gross weight

σ...main rotor solidity

CONFIGURATION SELECTION

SECTION 4 - CONFIGURATION SELECTION TECHNIQUES

CONTENTS

SECTION 4 - CONFIGURATION SELECTION TECHNIQUES

A. OPTIMUM DESIGN PARAMETER SELECTION

1. Introduction

This section presents the methods of determining the characteristics of the optimum helicopter for a given specification and the design parameters which both satisfy the specification and determine the design characteristics. These methods, developed in the course of the study, are based in part upon unpublished methods used in the fixed wing aircraft industry to optimize single variables for a particular configuration and have been extended for the study to allow the optimization of many design parameters and the determination of the corresponding design gross weight. With little modification, the methods may be applied to any aircraft or vehicle type which by its nature requires considered judgement and compromise between performance and weight efficiencies.

The number of variables typical of problems of this type require a rational and organized approach to their proper selection. The type of parametric analysis presented in this section has been termed the R_F Method: derived from the basic link between aerodynamic and weight characteristics, the fuel weight to gross weight ratio. The approach, therefore, requires the feasibility of analytically determining the aerodynamic and weight characteristics of a vehicle type as preliminary steps. These have been described in Sections 2 and 3 and the analyses have shown the derivation of the fuel weight ratio in terms of the significant design parameters.

The data and methods of aerodynamic performance prediction have become sufficiently crystallized to allow this determination, however, the analysis of the attendant component weights must rely upon projection of statistical data which has recently become available. The final degree of accuracy is therefore primarily dependent upon the validity of the assumptions required by the relatively more complex performance analysis and upon the reliability of the extrapolation of the existing helicopter component weight data. Since the ultimate proof of the analysis depends upon the verification of predictions with actual operational characteristics of future helicopters, it is necessary that improved performance and weight prediction techniques be incorporated in the analyses to assure continued reliability.

2. The R_F Graphical Method

The parameter, R_F, the fuel weight to gross weight ratio, is common to the aerodynamic and weight analyses. It is readily defined from the aerodynamic analysis as:

R_F = the required fuel weight ratio for a given radius of action

and from the weight analysis as:

R_F = the available fuel weight ratio for a given payload

In addition to the mission specifications: radius of action and payload, which are unique to the aerodynamic and weight R_F functions respectively, both R_F terms are primarily functions of the design parameters: gross weight, disk loading, power loading and tip speed. Consistent with the assumptions noted in the

performance analysis, however, the power loading can be expressed as a function of design hover ceiling and disk loading, and tip speed, as will be shown, may be assigned a fixed value. For a specified hover ceiling the R_F functions reduce to the following:

R_F = required fuel weight ratio

= f (radius of action, W, w)

and R_F = available fuel weight ratio

= f (payload, W, w)

The R_F graphical method consists of equating the two functions to provide a compatible solution for gross weight and disk loading satisfying the specified payload and radius of action. Figure 4-1 illustrates this procedure for a single disk loading, and shows the characteristic forms of the functions. The aerody-

Figure 4-1

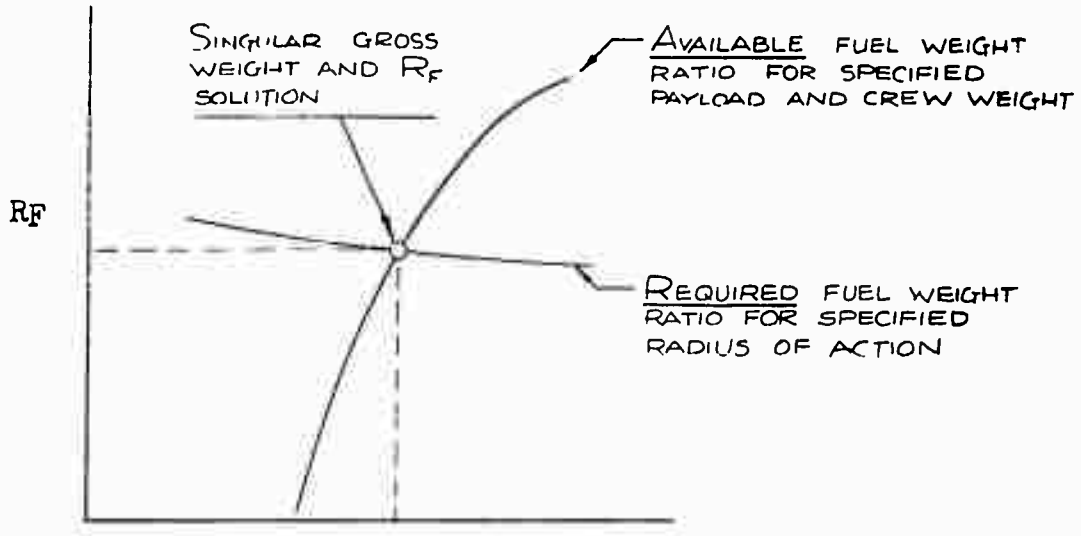

namic, required R_F function decreases with increasing gross weight due to the inherent "square-cube" (area-volume) law by which the larger helicopters become progressively "cleaner" aerodynamically. The weight, available R_F shows a tendency to approach a limiting value asymtotically or to maximize at some point depending upon the combined effects of the decreasing payload-gross weight ratio and the increasing empty weight ratio. The resulting intersection of the two functions defines a singular solution which indicates the design gross weight and fuel weight ratio which satisfy both the payload and radius of action specified.

Extending this procedure, the available and required R_F may be plotted for a range of disk loading as in Figure 4-2.

Figure 4-2

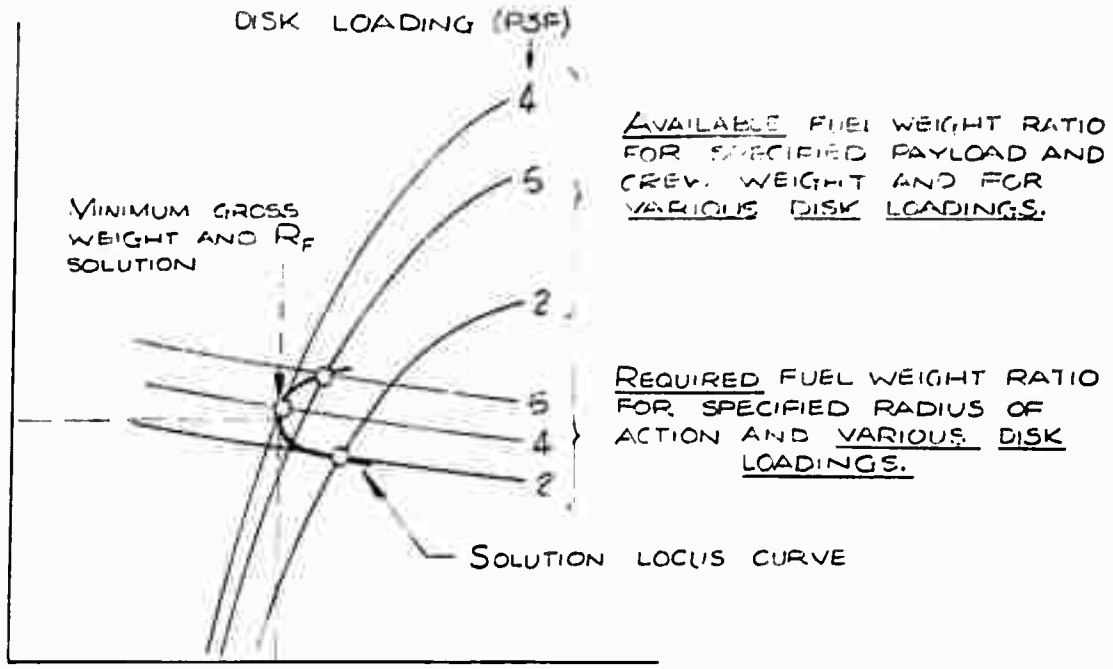

The intersection of each pair of equal disk loading R_F curves defines the singular gross weight solution for that disk loading, and the locus of these intersection points defines the variation of gross weight with disk loading. From this solution locus curve may be selected the minimum gross weight for the specified payload-radius of action mission, and by interpolation, the optimum disk loading and fuel weight ratio.

Figure 4-3 shows a typical set of intersections for a single design payload (available R_F), combined with various design radii of action (required R_F). The intersections shown are for mission and performance specifications of a 2-ton payload single rotor helicopter with twin geared gas turbine engines and a design hover ceiling of 5000 feet OGE, standard altitude. From a series of such intersection charts for additional design payloads, the minimum design gross weight, optimum disk loading and fuel weight ratio may be determined for a complete matrix of design payloads and radii of action. The data thus obtained is presented in a typical Design Characteristics Chart, Figure 4-6, for the mission specifications outlined above.

3. Extensions to the "R_F Method"

For the following discussion the term mission and performance specifications are defined as the design payload, crew requirement, radius of action and hover ceiling; and design parameters are defined as gross weight, disk loading, rotor tip speed, and power loading.

Figure 4-4 shows a sequential analysis of the configuration selection technique starting with the mission and performance specifications and ending with the solution locus curve defining the design parameters. The procedure has been simplified considerably for presentation and has been included primarily to show

Figure 4-3

Typical Simultaneous Solutions for Minimum Gross Weight Helicopters, for single rotor geared gas turbine power plant:

Payload = 2 tons
Crew weight = 600 lbs
Tip speed = 700 ft/sec
Design hover ceiling = 5000', OGE, std. alt.
Various design radii of action (R)

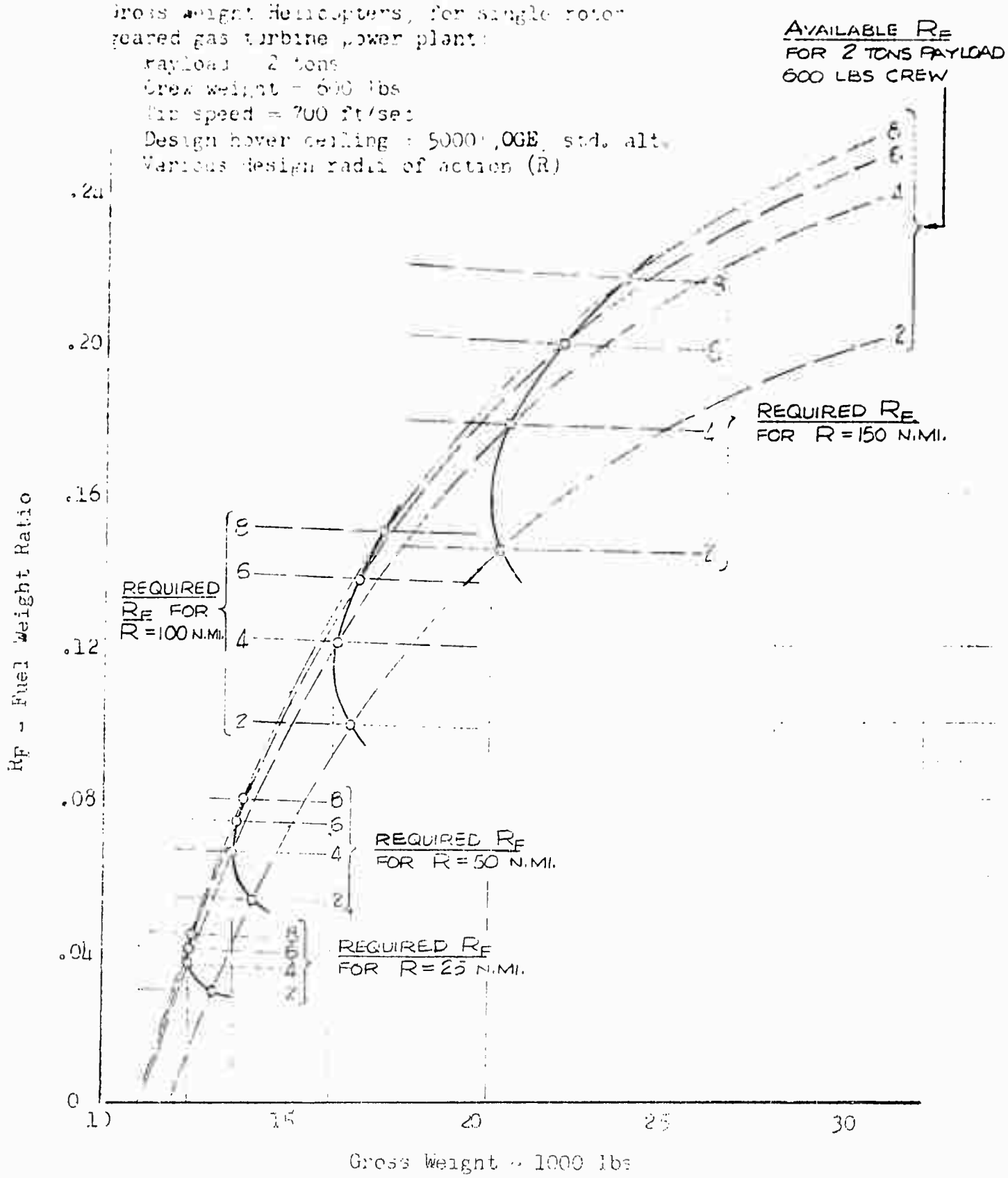

SECTION 4 - CONFIGURATION SELECTION TECHNIQUES

Figure 4-4: Schematic Diagram of Optimum Parameter Selection Technique

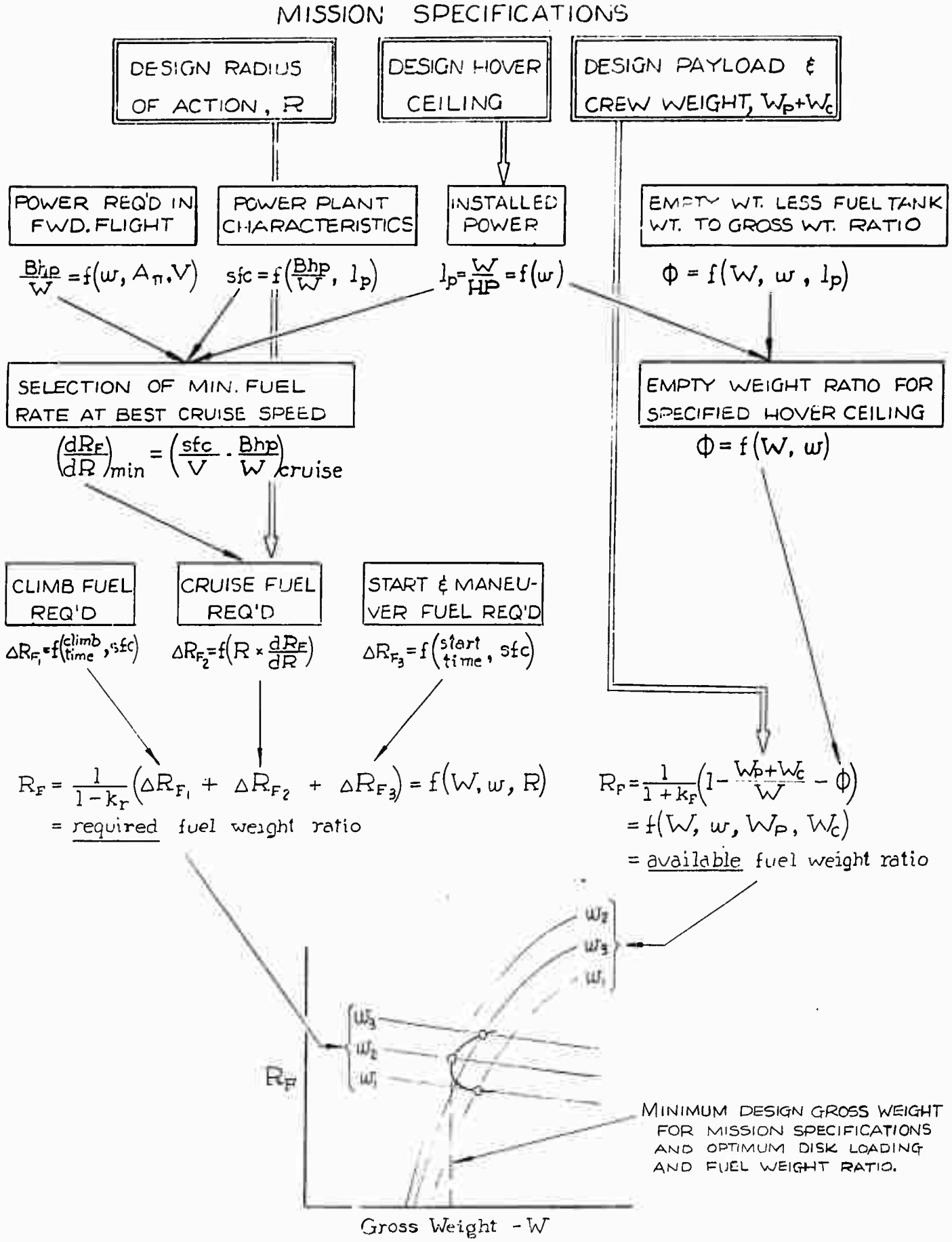

the interaction of various components of the "R_F Method", and of the aerodynamic and weight analyses shown on the left and right hand sides, respectively. Of the mission and performance specifications, the design hover ceiling immediately determines power loading for both weight and aerodynamic analyses. In the aerodynamic analysis, the power loading, combined with the power plant characteristics and the power required in forward flight allow the selection of best cruise speed and corresponding minimum fuel rate per nautical mile. By this procedure, discussed in detail in Section 2, paragraphs D.5 and D.6, the minimum fuel rate is determined as a function of gross weight and disk loading. The mission specifications and minimum fuel rate then determine the aerodynamic <u>required</u> R_F.

In the weight analysis, establishing power loading from the design hover ceiling reduces the empty weight expression to a function of gross weight and disk loading which can then be combined with payload and crew specifications to determine the <u>available</u> R_F. It will be noted that the mission specifications of payload and radius of action enter the procedure in the final steps of calculating R_F. Thus, the aerodynamic and weight analyses for a given configuration and design hover ceiling can be combined with a broad range of payloads and radii of action with little additional effort.

If "optimum" values are required for additional design parameters, they must be included throughout the sequence. By this procedure, the effect of rotor tip speed and tandem rotor overlap were determined for the helicopter configurations considered for the transport mission. Figure 4-5 shows typical solution locus curves for the optimization of rotor tip speed, in which the available and required R_F curves have been omitted for clarity.

Figure 4-5

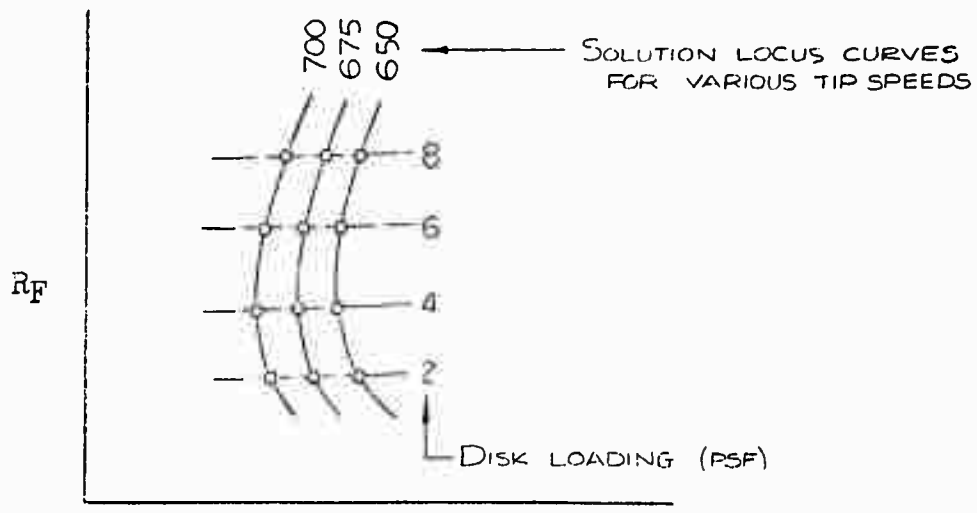

In this particular case, increasing rotor tip speed resulted in shifting the solution locus curve to the left, i.e., increasing tip speed resulted in decreasing gross weight solutions. A similar result was found in attempting to optimize tandem rotor overlap: increasing overlap resulted in decreasing gross weight. For design parameters which resisted optimization in this manner it was necessary to resort to establishing their limiting value by operational or per-

formance criteria. Thus, tip speed was fixed at 700 feet per second as an upper limit based on the restrictions of tip compressibility drag divergence at maximum flight speed, and the value of tandem rotor overlap established at 60% of rotor radius, limited by the minimum cargo compartment or fuselage length.

As may be derived from the preceding discussions, the R_F Graphical Method is dependent upon the development of equations expressing the aerodynamic, performance and weight characteristics of the helicopter in terms of the significant specifications and design parameters. As a corollary of this it may be stated that all design parameters entering the optimization must be common to both aerodynamic and weight analyses. If, for example, a design parameter appears in the aerodynamic analysis only and cannot be expected to affect the concurrent weight analysis, the best or optimum value of the parameter is defined as that which minimizes the aerodynamic required fuel weight ratio, R_F, within the restrictions inposed by reasonable design practice.

[illegible]

[illegible] al De[illegible] Char[illegible]

Figure [illegible]-6 [illegible] Design Characteristics Chart, Design [illegible] of [illegible] vs. Minimum Design Gross Weight for Various Payloads
[illegible] turbine engines
[illegible] OGE, std. alt.
[illegible]

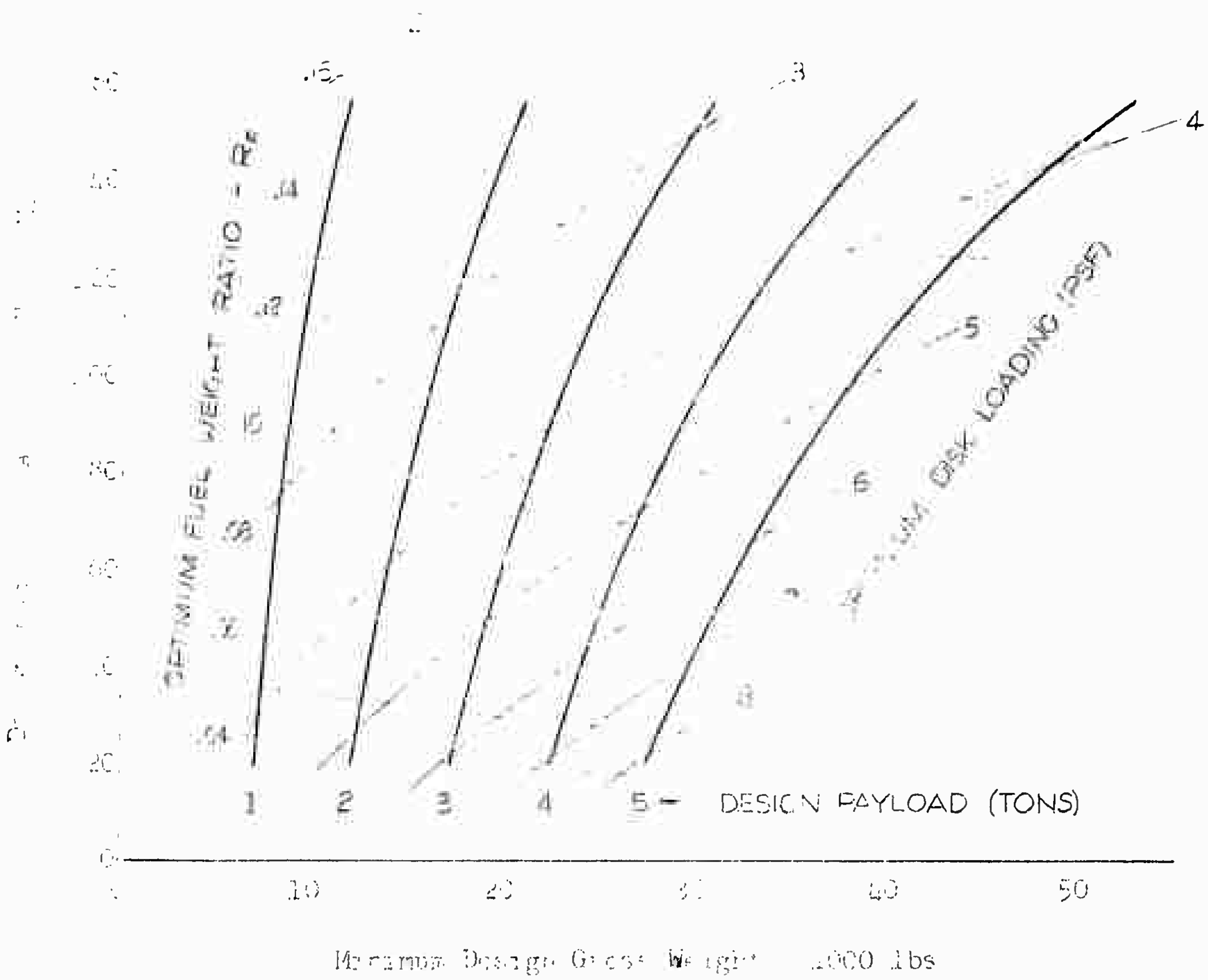

SECTION 4 - CONFIGURATION SELECTION TECHNIQUES

B. COST ANALYSIS PROCEDURES

The following discussion concerns the methods used to determine the total military flight hour cost of the various helicopters considered by the study. The scope and assumptions of the cost analysis have been discussed in the Summary Report No. 350.1, Military Helicopter Transport Systems (Reference 1) and the detail cost trends for helicopter components are presented in Hiller Report No. 360.1, Transport Helicopter Operating Cost Analysis Methods (Reference 2).

The purpose of the discussion is to show the methods of evaluating the flight hour cost of the helicopter configurations obtained from the parametric analyses described in the preceding sections and from their combination by the "R_F Graphical Method" in this section. The components of the problem involved in cost analysis are dependent upon both the operational and technical aspects of the problem, and these in turn are determined by the specified mission. Therefore, although the flight hour costs are not determined directly by the type of mission, the mission requirements are implicit in the cost determining technical design parameters.

The basic data required for the cost analysis of a given rotor type and power plant configuration are given by the Design Characteristics Charts or equivalent data yielding gross weight, disk loading, and fuel weight ratio for a given payload-range combination. In addition, the computation requires the tabulation of:

1) cruise speed
2) average rate of climb
3) climb speed

which, for a given radius of action, determine the mission time and block speed, and:

4) percent normal rated power in cruise
5) component group weights
   a) rotors
   b) airframe
   c) engine
   d) transmissions and drives
   e) "other" (radio & instruments)
6) aircraft utilization (hours/year)

Example calculation forms are shown on the following pages. For the various terms the following notes apply and are referenced by number:

(1) A discussion of the methods of predicting helicopter utilization is contained in Reference 1, pp 29-30. From this the aircraft utilization:

$$U = \frac{A}{1 + K_1 P V_B / R}$$

in which A = aircraft availability, assumed to be 1825 hrs/year for the transport helicopter

K_1 = loading rate

Sample Table for Total Operating Cost Calculation

Configurations: Rotor type _____ Power Plant type _____ Design Hover Ceiling _____

(1)	(2)	(3)	(4)	(5)	(6)	(7)	(8)	(9)	(10)	(11)	(12)	(13)	(14)
DESIGN PAY LOAD	DESIGN RAD OF ACTION	GROSS WEIGHT	DISK LOADING	FUEL WEIGHT RATIO	FUEL WEIGHT	CREW WEIGHT	EMPTY WEIGHT	NO. OF MECHANICS PER SHIP	TRAING COST/YR.	UTILIZATION	TRAING COST	BLOCK SPEED	MISSION TIME RECIPROCAL
P	R	W	w	R_F	W_F	W_C	W_E	N_M		U	C_T	V_B	$V_B/2R$
TONS	NAUT. MI.	LBS	LB/FT^2		③×⑤	LBS	③ − ⑥ − ⑦ − 2000·①		20000 + 2440·⑨	HRS/YR.	⑩ / ⑪	KNOTS	⑬ / 2·②
		FROM "DESIGN CHARACTERISTICS" CHARTS						FROM REF. 2 P. 71		SEE NOTE 1		SEE NOTE 2	

(15)	(16)	(17)	(18)	(19)	(20)	(21)	(22)	(23)	(24)	(25)	(26)	(27)	(28)	(29)
FUEL COST FACTOR	FUEL & OIL COST	TOT. FLT. OPERATION COSTS	ROTOR WEIGHT RATIO	ROTOR WEIGHT	TRANS & DR. WEIGHT RATIO	TRANS & DRIVES WEIGHT	AIRFRAME WEIGHT RATIO	AIRFRAME WEIGHT	ENGINE WEIGHT RATIO	ENGINE WEIGHT	'OTHER' WEIGHT RATIO	'OTHER' WEIGHT	CRUISE % L/D	ROTOR MAINT. COST
K_{fo}	C_{fo}	$C_c+C_T+C_{fo}$	R_{RS}	W_{RS}	R_{TD}	W_{TD}	R_A	W_A	R_{EN}	W_{EN}	R_o	W_o		C_{MRST}
$/LB	⑥ × ⑭ × ⑮	*15.37 + ⑫ + ⑯		③ × ⑱		③ × ⑳		③ × ㉒		③ × ㉔		③ × ㉖		$/HP
FROM REF. 2 P. 5		*SEE NOTE 3											SEE NOTE 4	FROM REF. 2 P. 24

Sample Table for Total Operating Cost Calculation (Continued)

Configuration: Rotor type _____ Power Plant type _____ Design Hover Ceiling _____

(30)	(31)	(32)	(33)	(34)	(35)	(36)	(37)	(38)	(39)	(40)	(41)
TRANS. & DRIVES MAINT. COST	AIRFRAME MAINT. COST	ENGINE MAINT. COST	"OTHER" MAINT. COST	TOT. MAINT. COST PER HR.	TOTAL MILITARY MAINT. COST/HR	PRODUCTION QUANTITY CORR. FACTOR		OVERHAUL PERIOD			
								ENGINES	TRANS. & DRIVES		
$C_{M_{TDT}}$	$C_{M_{AT}}$	$C_{M_{ET}}$	$C_{M_{OT}}$	C_M	C_{M_T}	K_P	$\frac{.19 K_P W}{U}$	OHP_{EN}	OHP_{TD}	$28.5 R_R \left(1 + \frac{U}{4000}\right)$	$43 R_{TD} \left(1 + \frac{U}{4 \cdot OH_{TD}}\right)$
$/HR.	$/HR.	$/HR	$/HR	$\sum_{29}^{33}$ (11)	$K^*_{C_M} \cdot$ (34)		$\frac{.19 \cdot (3) \cdot (36)}{(11)}$			$28.5 (8) \left(1 + \frac{(11)}{4000}\right)$	$43 (20) \left(1 + \frac{(11)}{4 \cdot (39)}\right)$
REF. 2 P. 92	REF. 2 P. 46	REF. 2 PP. 40 44 OR 45	REF. 2 P. 54		* $K_{C_M} = 2.5$	SEE NOTE 5		FROM REF. 2 P. 21, CHART #5			

(42)	(43)	(44)	(45)	(46)	(47)	(48)	(49)	(50)	(51)	(52)
				TOTAL DEPR. COST/HR.	NO. OF SHIPS PROCURED		DEVELOPMENT COSTS			TOTAL DEVELOPM'T COST/HR.
							AIRFRAME	ENGINES		
$C_{M_{21}} R_{EN} \left(1 + \frac{U}{4 C_H R_{EN}}\right)$	$34.5 R_A \left(1 + \frac{U}{8000}\right)$	$17.25 R_E \left(1 + \frac{U}{4000}\right)$		C_{O_T}	N_S	$5 N_S U$	C_{DEV_A}	$C_{DEV_{EN}}$		C_{DEV_T}
$C^*_{M_{21}}$ (28) $\left(1 + \frac{(11)}{4 \cdot (38)}\right)$	34.5 (22) $\left(1 + \frac{(11)}{8000}\right)$	17.25 (26) $\left(1 + \frac{(11)}{4000}\right)$	$\sum_{40}^{44}$ (11)	(37) · (45)		5 · (11) · (47)	$	$	(49) + (50)	$\frac{(51)}{(48)}$
* FROM REF. 2 P. 65,					SEE NOTE 5		FROM REF. 2 P. 70			

CONFIDENTIAL

Sample Table for Total Operating Cost Calculation (Continued)

Configuration: Rotor type _____ Power Plant type _____ Design Hover Ceiling _____

(53)	(54)	(55)	(56)	(57)
ADJ. TOTAL MAINT. COST/HR.	ADJ. TOTAL DEPR. COST/HR.	ADJ. TOTAL DEVEL. COST/HR.	ADJ TOTAL FLT. OR COST/HR.	ADJ. TOTAL FLT. HR. COSTS
C_{M_T}	C_{D_T}	C_{DEV_T}	C_{FO}	C_{TOT}
$K_1^* \times$ (35)	$K_2^* \times$ (46)	$K_2^* \times$ (52)	$K_2^* \times$ (17)	$\sum_{53}^{56}$ (n)

*SEE NOTE 6

SECTION 4 - CONFIGURATION SELECTION TECHNIQUES

K_1 = .133 hrs/ton for payload carried outbound only

= .266 hrs/ton for payload carried out and inbound legs

P = mission payload (tons)

V_B = block speed (knots)

R = mission radius (naut. mi.)

(2) Block speed, as defined herein

$$V_B = \frac{2R}{(\text{total mission time}) - (\text{total loading time})}$$

(3) Flight crew costs ($15.37/hr) are based on the assumptions as noted in Reference 1, p.40, for a three man crew.

(4) Cruise percent power may be determined from the aerodynamic analysis as a function of gross weight and disk loading. This is most readily determined at the same point in the analysis at which best cruise speed is found (see Figure 4-4) and is defined as:

$$\% \text{ NRP} = 100 \frac{\text{Power req'd @ Mission Alt.}}{\text{Power Available @ Alt.}}$$

(5) The production quantity correction factor is given in chart form in Reference 2, p.66. For purposes of the major portion of the study, presented in the Summary Report (Reference 1), the first costs of components were adjusted such that $K_P = 1.0$ for a production quantity (N_S) of 200. The chart noted above gives values of K_P for alternate production quantities.

(6) K_1 and K_2 in the columns noted are factors which allow the adjustment of costs to any desired time period. Figure 4-7 shows the variation of K_1 and K_2 versus time period based on the single curve of Reference 1, Appendix H. The factor K_1, applies to maintenance data which is representative of 1953 operation, whereas K_2 applies to all other costs which are representative of 1954 operation.

Having the total flight hour costs for a given configuration the transport efficiency in terms of ton-nautical miles per dollar can be calculated from the expression:

$$E = \frac{PV_B}{C_T}$$

TRANSPORT HELICOPTER DESIGN ANALYSIS METHOD

Figure 4-7
Price Level Adjustment Factors vs. Time Period

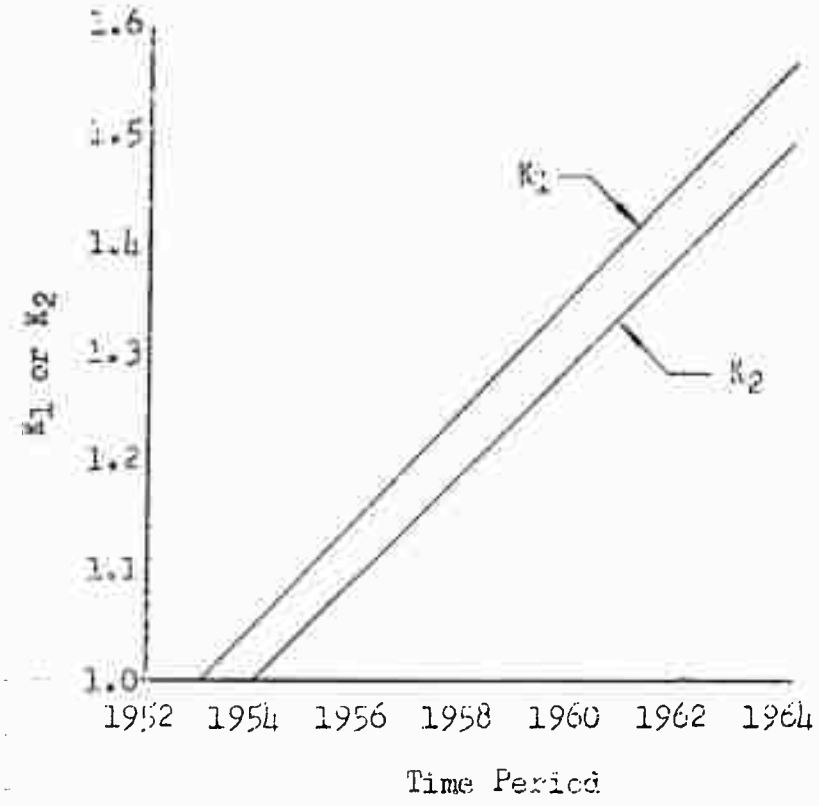

or in terms of the notation used on the sample calculation chart:

$$E = \frac{(1) \cdot (13)}{(57)}$$

The cost analysis procedure is expressly designed for the analysis of helicopters operating at design payload and range. Hence, a rigorous analysis of operating cost for off-design conditions, (for example, reduced payload and extended radius of action) would entail the alteration of fuel costs to reflect the reduced range. However, the fuel costs constitute only a small portion of total cost. Therefore, calculation of total cost per flight hour for design payload and radius operation can be considered, with negligible error, to remain constant within the boundaries of the payload-radius diagram. In the measure of transport effectiveness, therefore, only the payload and block speed will be altered by off-design point operation.

REFERENCES

1. "Military Helicopter Transport Systems"; Hiller Report No. 350.1

2. "Transport Helicopter Operating Cost Analysis Methods"; Hiller Report No. 360.1

3. Wiesner, W.; "A Chart Method for Calculating Helicopter Performance and Parameters", Kellett Report No. 130.9, 15 April 1944

4. Hughes Performance Handbook, Hughes Aircraft Co., Report No. 220

5. Gessow, A., and Myers, G. C. Jr.; "Aerodynamics of the Helicopter", MacMillan, 1952

6. Coleman, R. P., Feingold, A. M., and Stempin, C. W.; "Evaluation of the Induced-Velocity Field of an Idealized Helicopter Rotor". NACA WRL-126, 1945. (Formerly NACA ARR L5E10)

7. Carpenter, Paul J.; "Effects of Compressibility on the Performance of Two Full-Scale Helicopter Rotors"; NACA TN 2277, January 1951

8. J. Stuart III; "Helicopter Performance Possibilities"; Proceedings, Seventh Annual Forum, American Helicopter Society, April 26, 27, 1951

9. Amer, Kenneth B.; "Effect of Blade Stalling and Drag Divergence on Power Required by a Helicopter Rotor at High Forward Speed"; Proceedings, Eleventh Annual Forum, American Helicopter Society, April 27 to 30, 1955

10. "Generalized Power Plant Characteristics for Reciprocating Engines"; Douglas-Rand study, Douglas Aircraft Co., 14 October 1947

11. "Proposal for the Improvement of the Ramjet Engine for Helicopter Propulsion"; Hiller Report No. 545.3, 30 November 1954

12. Helicopter Tip Turbojet Brochure, Packard Motor Co., Aircraft Engr. Div. Report No. 7JE-103, 27 September 1954

13. "Helicopter Propulsion System Study"; Thermal Research and Engineering Corporation, Conshohocken, Pa.; September 1952

14. Corning, Gerald; "Airplane Design"; Edwards Brothers, Inc., Ann Arbor, Mich. 1953

15. Carlson, R. M., and Schnebly, F. D.; "The Price of Helicopter Transmission Service Life"; presented at Army Transportation Corps Conference and Symposium on Spare and Replacement Parts; May 1954

16. Military Specification MIL-C-5011A; "Charts; Standard Aircraft Characteristics and Performance, Piloted Aircraft"; 5 November 1951

17. Military Specification MIL-H-8501; "Helicopter Flying Qualities, Requirements For"; 5 November 1952

18. Holzmeier, George R.; "Application of Statistical Weight Analysis Methods to Helicopter Preliminary Design", presented at the SAWE Conference, May 1955

19. "Optimum Ramjet Engine Weight", Hiller Report No. 250.7, October, 1952

APPENDIX

PRESSURE JET POWER PLANT CONSIDERATIONS

Prepared For

MILITARY HELICOPTER TRANSPORT STUDY

Contract No. Nonr-1340(00)

By

J. B. Nichols
Chief Research Engineer
Hiller Helicopters

APPENDIX

PRESSURE JET POWER PLANT CONSIDERATIONS

Prepared For

MILITARY HELICOPTER TRANSPORT STUDY

Contract No. Nonr-1340(00)

By

J. B. Nichols
Chief Research Engineer
Hiller Helicopters

APPENDIX - PRESSURE JET POWER PLANTS

SUMMARY

This report has been prepared to provide the operations analysis group with sufficient pressure-jet power plant data to evaluate helicopters employing this form of propulsion.

The wide variety of pressure jet cycles and the mass of available data have been narrowed down, on the basis of actual practical experience, to an extremely small amount of information on a single pressure jet cycle which, for purposes of operational studies, represents a generalized picture of all pressure jets falling within the scope of this analysis.

The information has been presented in a form similar to that for more conventional power plants so that the same operational techniques can be applied as for the geared type reciprocating engine or turbine drives.

TRANSPORT HELICOPTER DESIGN ANALYSIS METHODS

INTRODUCTION

The scope of Contract Nonr 1340(00) provides for a limited amount of consideration of pressure-jet propulsion systems for the period of 1960 - 1970.

The consideration of the pressure-jet must of necessity be limited because the actual application of the pressure-jet has itself been of such limited extent that the little design and statistical data available is not a satisfactory foundation upon which to build a set of conclusions for establishing an accurate operations analysis.

The primary attempt of this report is to digest the work which has been done on pressure-jets and by the injection of a considerable amount of judgment to deduce the real limits of applicability of the pressure-jet for transport helicopters.

The true limitation of really applicable data is obscured by the tremendous amount of literature produced on pressure-jets, well out of proportion to the actual practical activities in the field. It would be only a slight exaggeration to state that the paperwork outweighs the hardware.

The tremendous theoretical activities in the pressure-jet field are easily explainable by the following facts:

1. The pressure-jet is one of the most versatile of all aircraft power plants, having so many degrees of freedom that an almost infinite variety of combinations and permutations of components can be considered, studied, and synthesized into cycles.

2. The various cycles, no matter how practical or impractical, are amenable to analysis and this makes the pressure-jet a seductive subject to anyone analytically inclined.

3. The popularity of the helicopter and the unpopularity of helicopter gears, drives, and tail rotors has fostered a continuing general interest in jet drives, possibly out of proportion to their real value for general application.

The above statements are not intended to set up a pessimistic atmosphere for the reader, but are the attempt to dispel undue optimism to the extent that the following sections can be reviewed with a realistic attitude and a realization that, for the purposes of this study, there must be a clear understanding of the division between the practical and theoretical results of various pressure-jet study and development programs.

APPENDIX - PRESSURE JET POWER PLANTS

HISTORICAL REVIEW

The results of this study would appear to be best introduced by a review of the history of pressure-jet propulsion. This historical review is intended not so much as an interesting sidelight as it is to assist the reader in firmly establishing the division between the analytical and hardware developments in the field because, as we have stated, the difference between the two is important in establishing the building blocks for our ultimate aim -- an accurate operations analysis.

About thirty or so years ago, Pescara, in France, did some of the original work on helicopters. Many of the basic control methods and constructional techniques of the modern helicopter were anticipated by his original patents. He never produced a successful helicopter, however he correctly attributed most of the failure to the power plants. In setting out to improve the power plant situation, he invented the free piston hot gas generator. This type power plant lent itself best to pressure-jet propulsion and this was Pescara's stated intent. He never continued his work on helicopters but devoted all his time up to the present on development of the hot gas generator.

During World War II, Doblhoff, in Austria, developed a series of pressure-jet compound helicopters which employed reciprocating engine driven compressors and tip burners for rotor propulsion in hovering and a propeller for forward flight, during which time the pressure-jet was inoperative and the rotor was to operate in the autorotative regime.

After the war, Doblhoff came to the United States and continued his work with McDonnell Aircraft. Their XV-1 is a modernized version of the Doblhoff ship. Many of the old Doblhoff team moved to Sncaso, in France, where the basic Doblhoff pressure-jet structural developments were put to work on the Djinn cold jet helicopter. The basic blade retention and gas seal systems of the Djinn are direct evolutionary developments of the Austrian models.

Doblhoff also left his mark with Fairey, in England, where his pressure-jet enthusiasm was picked up and has resulted in the Gyrodyne and Rotodyne programs.

In 1945, Kellett Autogyro Company and General Electric were awarded an Air Force contract to construct a flying test stand (the XH-17) to study the rotor problems of a giant helicopter. The propulsion method was originally left open, and it is interesting now to realize that ramjets and gear type drives were considered for this ship as well as the pressure jet. The ramjet was eliminated because of the developmental time expected; and gear drives were eliminated because of the long manufacturing delays for such large gears. The pressure-jet drive was chosen, surprisingly enough, on the basis of earliest availability.

The original power plant chosen was a reciprocating engine driven compressor, but after further study, it was decided not to mix rotating and reciprocating components. Instead, two TG 180 (J-35) jet engines were converted to air bleed units to supply the air for the tip burners.

After a number of the airframe components were completed, financial difficulties at Kellett resulted in transfer of the airframe contract to Hughes Aircraft and the finished parts were moved to Hughes.

TRANSPORT HELICOPTER DESIGN ANALYSIS METHODS

In the meantime, G. E. continued development and construction of the air supply turbine units and development of the tip burners and blade tip section. While the original specifications called for a total of about 2600 HP at 1800 F tip burner temperature, airframe weight increases and other considerations required increased power and the tip burners were developed until finally they were satisfactory for 3000 F and the power plant system provided 4200 HP.

This practical power plant development work at G. E. was accompanied by an intensive analytical program to examine all aspects of pressure-jet propulsion. Scores of new cycles were studied and methods of improving the XH-17 power plant system were examined. This work was carried on by W. E. Wayman and J. B. Nichols under the direction of J. K. Salisbury.

As far as is known, the analytical work done at this time represents the most complete and detailed examination of pressure-jets available and covers all cycles proposed in the past and since by other investigators.

Shortly after delivery of the XH-17 power plants to Hughes in 1949, Mr. Wayman joined Hughes; and in 1952, Mr. Nichols joined Hiller.

It must be realized that the McDonnell and Hughes work represents the complete extent of hardware developments in this country and that both employ the same cycle - "cold" cycle (i.e,, unheated air from air generator) with tip burning.

In 1952, Thermal Research and Engineering Company (J. A. Johnson et al) completed, under Air Force contract, an analytical study of helicopter propulsion systems. The purpose of this report was to evaluate all the various propulsion means when actually integrated with their optimum matching airframes. One conclusion of this study was the determination of the area of greatest effectiveness for the pressure jet and reconfirmation of the potential of the Hot Ducted Pressure Jet. (Previously studied by both McDonnell and G. E.) Possibly as a result of this study, Thermal Research obtained another contract to study the Hot Ducted Pressure Jet Helicopter. This report issued in 1953 indicated the hot cycle (with additional tip burning for take-off) to be promising. Since the major problem appeared to be the blade which has to conduct a large volume of hot gas out to the tip, a development program was undertaken on such a blade. No significant results are yet available from this program.

In 1954, the French Djinn Helicopter was announced and its major selling points were purported to be its extreme simplicity (cold gas and no tip burners) and its low noise level. Both of these points are of extreme importance when it is considered that the major objection to geared helicopters are their maintenance costs and the primary objection of jet helicopters, their noise.

Even after optimizing the performance of a pressure-jet helicopter which frequently requires the use of tip burning (at least for take-off in order to reduce installed power plant weights), one finds that design may still be far from acceptable on the basis of many such operational objections.

Because the pressure-jet is, at best, only about one half as efficient fuelwise as mechanical drive units it never attains a clear-cut victory over mechanical drives, even when a decision is made to use it. The Hughes studies on the XH-17 and XH-28 indicate that as helicopter sizes become larger, the tail rotor power

and structural considerations get out of hand for mechanical drives, and the pressure-jet actually starts to pay off.

The fact remains that the final machine is not an efficient transport, but a short range "crane" type, and its transport efficiency is not as high as a smaller cousin which is mechanically driven.

In other words, it does not appear as practical to scale up helicopters as it is to scale up airplanes. One is not forced to a less efficient design in bigger airplanes, but the helicopter appears to have inherited some of its characteristics from the dinosaur. It eats proportionately more as it gets bigger and is less and less able to earn its keep.

There is no question but that to lift a single large load vertically, the large helicopter is needed, but for efficient transportation of more conventional loads, it would appear that the transport helicopter has a maximum economical size. Even in the optimum size, the helicopter may have to compete with more efficient aircraft configurations — but this is another story.

As a result of the problems uncovered in the tip burning pressure-jet cycles and the ever present problems of the geared drive types, there has been a quickening interest in the non-tip burning hot cycles which provide greater efficiency than the tip burning types, higher power/weight ratio than the cold non-tip burning types (Djinn), and a reasonably low noise level.

At this writing, there is an Air Force competition under-way for a complete and detailed study of the Hot Gas Cycle Pressure Jet. Assuming an early award of a contract, it will be at least two or three years before an authoritative conclusion can be reached on this cycle. It is important to note, however, that Napier has produced a power plant for this type cycle (the Oryx), and Percival is building a helicopter employing these power plants. It is questionable, however, if this British program has been based upon an adequate background of experience, particularly after Fairey has had so much trouble with their Gyrodyne cold-pressure jet system for which a reasonable amount of experience and background is available.

In any case, it appears that reliable hot cycle information, based upon actual experience, whether from here or abroad, may be a long time in coming.

TRANSPORT HELICOPTER DESIGN ANALYSIS METHODS

GENERAL DESCRIPTION OF PRESSURE JET CYCLES AND NOMENCLATURE

1. Pressure Jet:

The pressure jet power plant is defined as one in which the propulsion is provided by jet nozzles at the helicopter rotor tip which are supplied by air or gas generators located in the fuselage. The tip jet nozzles may or may not be preceded by combustion chambers (tip burners) to augment the power. The primary difference between the various pressure jet cycles, excluding the variations in tip burning, is concerned with the propulsion gas generators. Since the propulsive efficiency of the pressure jet is poor at normal rotor tip speeds, it behooves one to compensate for this propulsive inefficiency by generating the propulsive air or gas with the maximum possible efficiency commensurate with the use of the lightest weight machinery.

2. Hot Vs. Cold Cycles:

For purposes of this report, the terms "hot" cycle and "cold" cycle refer to the temperature of the propulsive gas as it leaves the gas generator and are necessarily relative. In general, cycles which employ propulsive air directly from a compressor are termed "cold" cycles whether they employ tip burners or not; and cycles which employ propulsive gas which is obtained from a hot gas generator or by mixing compressor air with turbine exhaust air, etc., are termed "hot" cycles.

Obviously, there is an overlap where it is possible for the temperature of very highly compressed air to be higher than the temperature of gases from some mixed gas cycles. In actual usage, the division between hot and cold cycle definitions occurs at the temperature which requires a change in structural design concept for the rotor blades. For example, if the propulsive gas is of low enough temperature to allow the use of aluminum alloys without the need for excessive insulation around the rotor blade air ducts, the air is considered "cold"; whereas, if special blade design techniques are required because of the high temperature, then the cycle producing the gas is a "hot" cycle.

3. Cold Cycles:

The cold cycles are almost completely restricted to a simple mechanically driven compressor. As shown in Figure A following, the compressor may be driven by either a reciprocating engine or a gas turbine (turbo prop). The air from the compressor is ducted through the rotor blades and ejected at the tip (after passing through tip burners if desirable).

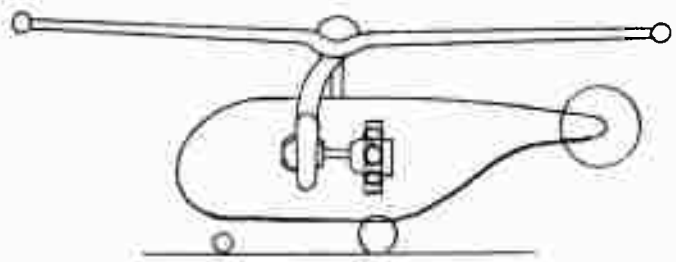

Figure A-1: Reciprocating Engine, Compressor, and Pressure-Jet Tip Burners

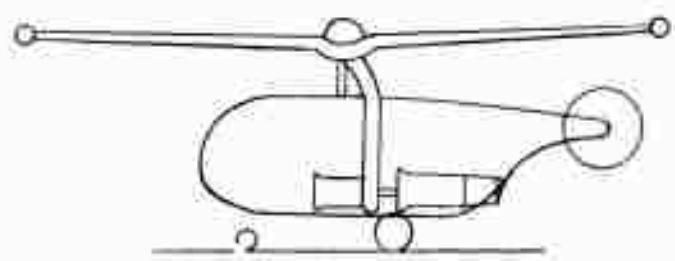

Figure A-2: Turboprop Engine, Compressor, Air Bleed and Pressure-Jet Tip Burners

APPENDIX - PRESSURE JET POWER PLANTS

4. Hot Cycles:

Figure B shows two intermediate temperature cycles ("hot" by our definition) which are obtained by alteration of the previous cold cycles. Basically, the engine or turbine exhaust heat is employed to increase the energy of the propulsive gas. The lower cycle is essentially a ducted fan. A helicopter power plant of this type, the Oryx, has been produced by Napier and this represents one of the most promising "hot" cycles. One primary difficulty of this cycle is the fact that the compressor air applies a back pressure to the turbine and lowers its capacity to do work. As a result, the compressor pressure must be kept low. This is good from a propulsive efficiency point of view, but the propulsive gas volume b comes so large as to require extraordinarily large blade ducts and, therefore, blade aerodynamic compromises.

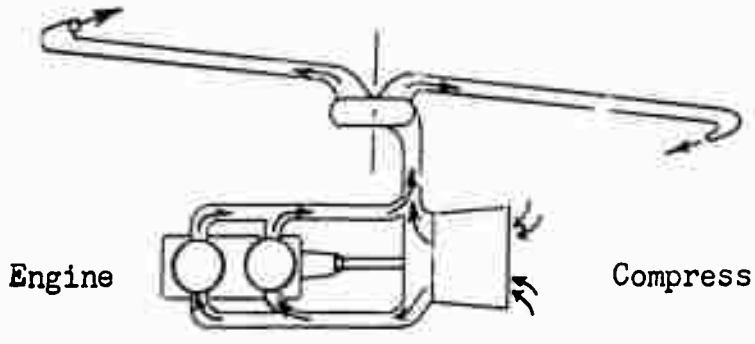

Figure B-1: Air from Recip. Engine Driven Comp. is Mixed with Engine Exhaust and Ducted to Rotor Tip Nozzles

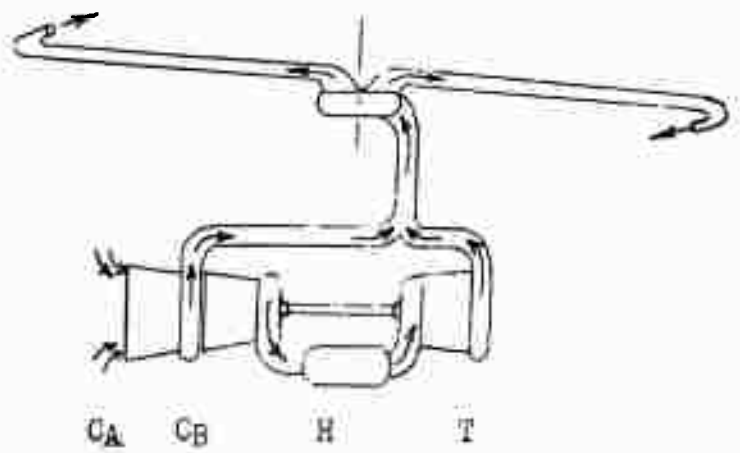

Figure B-2: Air Bled from Low Pressure Comp. is Mixed with Turbine Exhaust and Ducted to Rotor Tip Nozzles

Figure C shows one of many possible arrangements for employing a heat exchanger to improve the performance of the gas generator. In no studies accomplished so far has the high weight of a heat exchanger been shown to be worth the fuel saving.

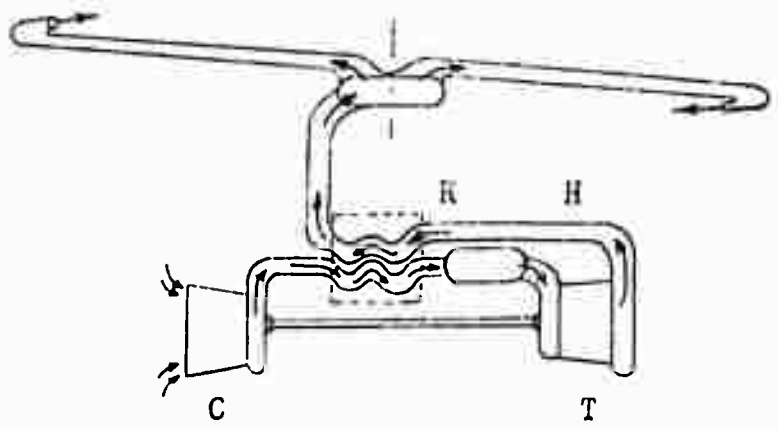

Figure C: Exhaust from Gas Turbine Helps Heat Air for its Own Drive Before Being Ducted to Rotor Tip Nozzles

Figure D shows the highest temperature cycle of all in which the exhaust from a standard gas turbine is ducted directly through the rotor blades. While the cycle is extremely simple and employs standard and available machinery, the blade design problems are presently overwhelming.

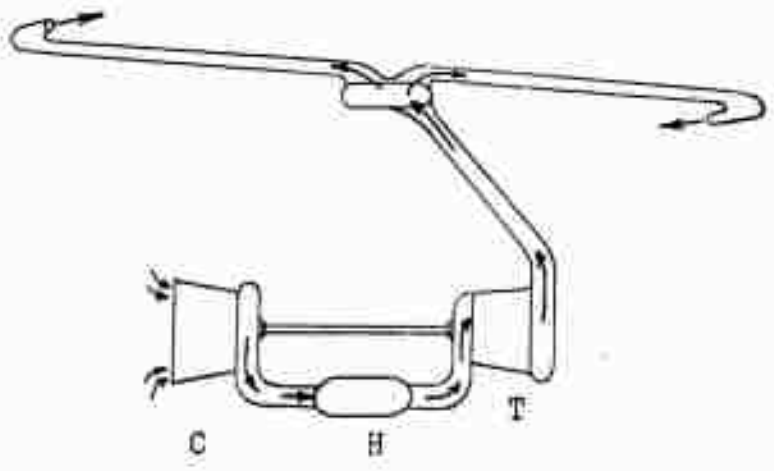

Figure D: Exhaust from Turbojet is Led Through Insulated Ducts to Rotor Tip Nozzles

APPENDIX - PRESSURE JET POWER PLANTS

DISCUSSION

The pressure jet differs from every other form of rotor propulsion in one basic respect. The rotor is a component of the power plant cycle and, as such, its design must be compromised not only aerodynamically and structurally, but thermodynamically as well.

It is possible to determine rotor parameters for a pressure jet helicopter which optimize the external aerodynamics and internal thermodynamic losses in the blade ducts, but it becomes extremely tedious to simultaneously account for structural weight as well. For some of the high volume flow cycles, a satisfactory aerodynamic design can be obtained only by ensuring that a major percentage of the rotor blade cross-sectional area is devoted to ducting. This entails a departure from the conventional constructional techniques which have been developed to allow a "natural" attainment of quarter-chord balance. Once quarter-chord balance is lost, it must be restored with heavy leading edge (or even external) counterweights. Needless to say, this results in re-examination of blade weights, external drag, and structural integrity.

During the XH-17 Project, a number of methods were developed for evaluating the effect of blade parameters on duct frictional losses and vice-versa. These methods are of general applicability and still valid. One discovery which was made at that time was the fact that the external aerodynamics of the cold pressure jet rotor were not at all compromised by thermodynamic considerations, compared to mechanically driven rotors. In other words, the design of a conventional rotor which provides for reasonable forward flight speeds and operating altitudes has sufficient blade cross-sectional area to provide ample duct area for the quantity of air required if it were to be cold pressure jet propelled.

The frictional losses for a given total solidity increases with the total number of blades, and, while the above conclusion is valid for a two-bladed rotor, it should be checked carefully for any design with a three or more bladed rotor. (It is interesting to note that the Fairey Rotodyne was originally planned to have five blades. Latest reports indicate that they have encountered duct "choking" and the latest model photograph now shows four blades.)

The XH-17 Helicopter has, in effect, a truly negligible blade duct frictional loss, and it employs far less blade area for ducting than is available. On the other hand, a hot cycle without tip burning requires such a high volume flow that the duct area requirements actually do infringe upon the external aerodynamic requirements.

The design problem here is to determine if the thermodynamic advantages of a more efficient cycle are worth the aerodynamic compromises in efficiency and the structural problems caused by the higher temperature.

For the purposes of this study, we are going to completely neglect the hot cycles. This is no condemnation of these cycles nor lack of confidence that more efficient systems will evolve from the developmental work now in progress (and planned over the next few years). The justification for this step is made necessary by the defined scope of this study:

TRANSPORT HELICOPTER DESIGN ANALYSIS METHODS

First, we are considering only those present, or near future, developments which can realistically be expected to show promise for production consideration within five or more years.

Secondly, we must integrate present design trends into the picture and one trend can be best described as follows: "users are getting impatient with under-powered helicopters". This trend alone tends to rule out any pressure jet developments in which increases in power available are obtainable only by increases in blade size (and increases in power requirements). The hot cycles, even through promising higher efficiencies are very dependent upon blade duct compromises. The cold cycles (by increasing pressure or by tip burning) can develop more power independently of the blade duct size. The hot cycles are quite limited in cycle pressure variation and the power output is very dependent on duct volume flow and, therefore, on blade duct size.

Thirdly, we are not intending to cover the entire helicopter picture, but are covering the transport helicopter exclusively. The work which has already been done for mechanically driven helicopters has indicated the importance of speed in transport efficiency. The helicopter is already speed limited by its rotor, even when this rotor is designed to favor every aerodynamic advantage.

A small aerodynamic compromise can prove rather costly in transport efficiency, so it would appear advantageous at this time to limit our pressure jet power plant choices to those which do not burden the designer with aerodynamic compromises — this points to the cold cycles.

APPENDIX - PRESSURE JET POWER PLANTS

ANALYSIS

Since we have chosen to limit ourselves to the cold cycles for various practical reasons our problems are resolved into the following:

1. What type of machinery is to be employed to provide the compressed air?

2. At what pressure should the air be supplied and should we or should we not employ tip burning?

MACHINERY CONSIDERATIONS

The question of compressor machinery is fairly easily resolved if a definite connection is desirable between this study and present practice. While it is not the intent of this study to be over-conservative, the rarity of practical pressure jet experience would indicate that we cannot expect an all-out, extensive, developmental effort to be supported in the near future. All American operational pressure jets have, to date, been dependent upon available machinery. The total helicopter market is still so small that development of specialized equipment is still uneconomical and it appears that special helicopter power plants will be considered only if they are also practical for other applications in addition to the helicopter.

A review of a few helicopter pressure jet programs will clarify this problem.

1. The McDonnell XV-1 employs a reciprocating engine driving a centrifugal compressor, shown schematically below. Both of these components were available, however, the compressor was altered.

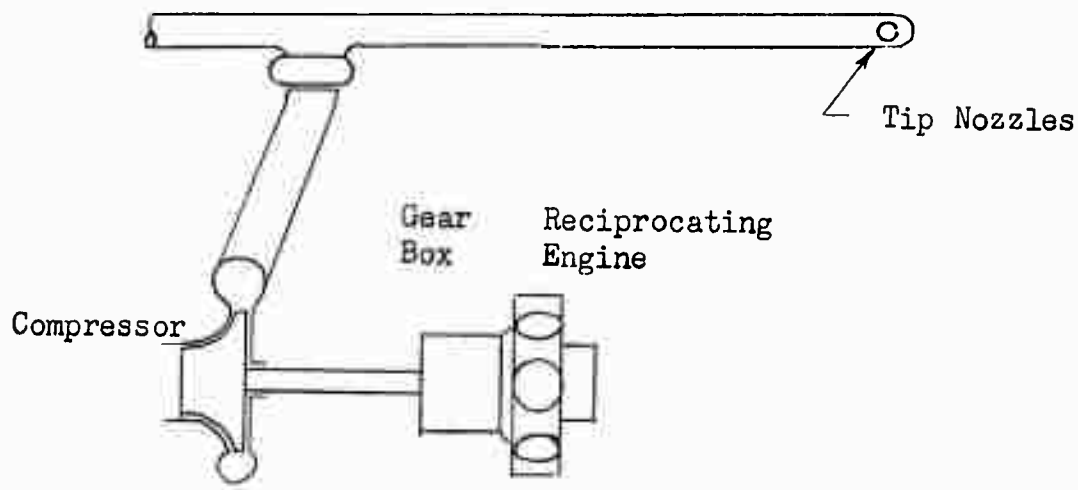

TRANSPORT HELICOPTER DESIGN ANALYSIS METHODS

2. The Hughes XH-17

This helicopter employs two J-35 turbojct engines which were converted to air supply units.

The standard J-35 employed eleven compressor stages to provide a compression ratio of approximately 4:1. The single stage turbine had a pressure drop of approximately 2:1, thereby leaving a pressure ratio of about 2:1 for the jet exhaust nozzle.

The converted units had the last three compressor stages removed to provide a pressure ratio of 2.5:1. The space provided by the removal of the last three stages allowed for the installation of an air bleed collection scroll at the aft end of the compressor case. The turbine wheel was unchanged, but the higher turbine pressure drop and the lower turbine air flow required an alteration of the turbine nozzle area.

Neither the cycle pressure (2.5:1) nor the turbine efficiency were optimized for this helicopter but were chosen to allow the minimum cost of power plant development. An additional problem of this power plant was the fact that the turbine air and the bleed air were obtained from the same compressor so that a variation of bleed air flow affected the turbine flow and temperature which required cautious control of the power plant.

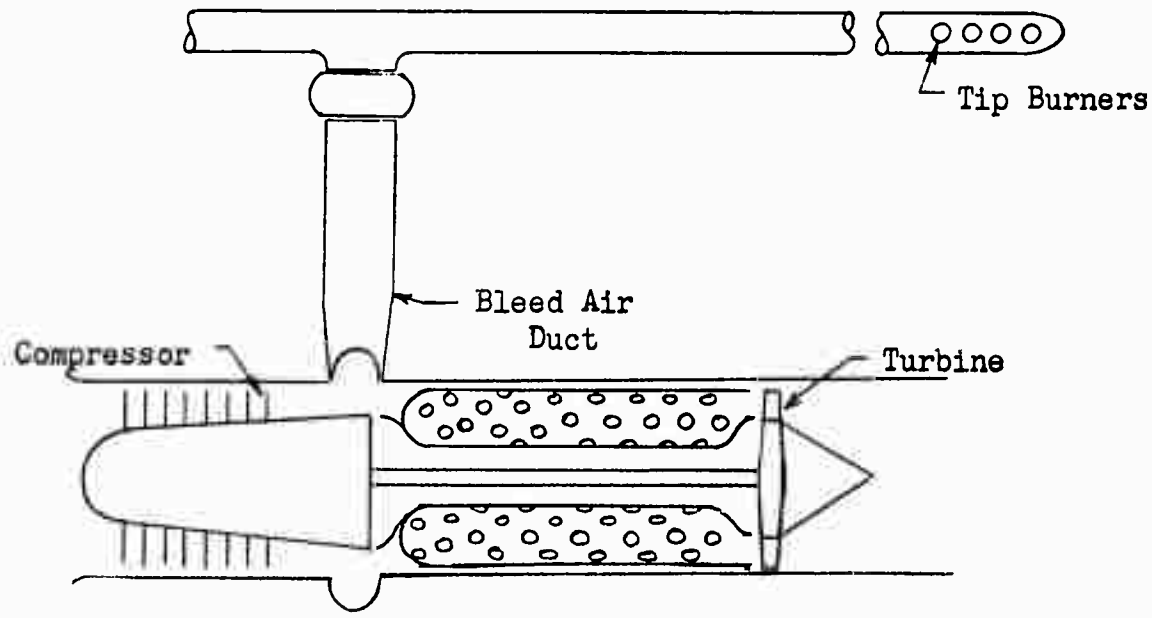

APPENDIX - PRESSURE JET POWER PLANTS

3. The Palouste air compressor unit (as used on the D n Helicopter) employs the same basic cycle as the XH-17 power plants and the same basic problems are evident. Again, this unit was employed in the Djinn because it was AVAILABLE.

The simplest solution to the cycle and control problems of the pressure jet power plant is to employ a different compressor for the air supply than is employed for supplying the turbine.

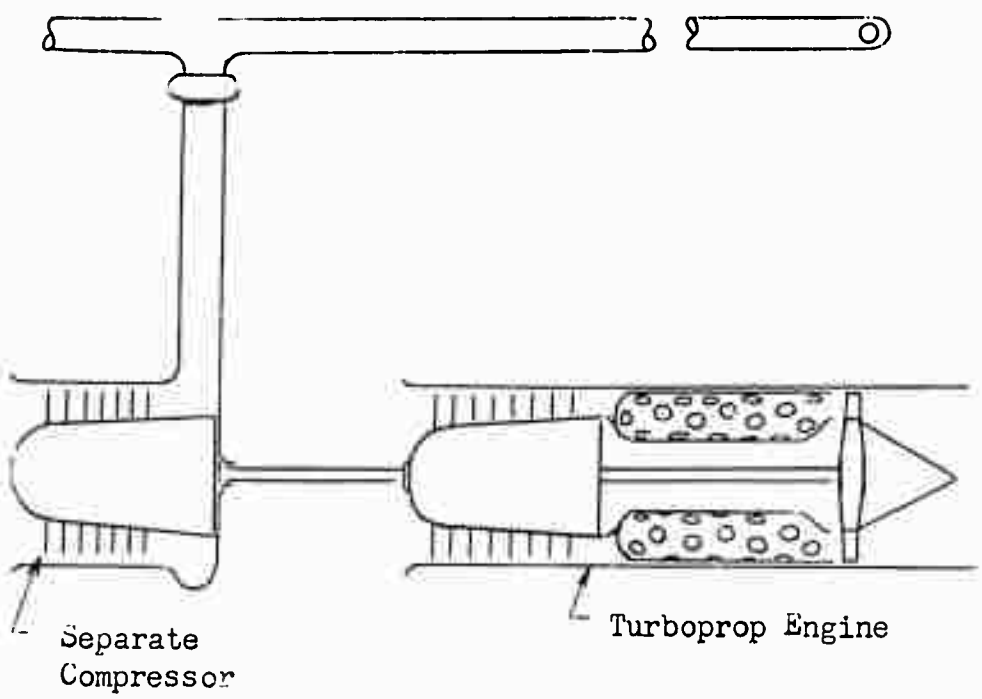

This type unit combines the advantages of the light weight of turbine machinery (XH-17 and Djinn) with the flexibility of the separate compressor (McDonnell).

The air supply compressor can be designed for the most desirable duct pressure without affecting the drive turbine compressor ratio. Furthermore, the gas turbine prime mover does not have to be of special design but may be an available turbo prop engine. The driven air supply compressor can be matched to the turbo prop engine speed so that no gear boxes will be necessary as for a reciprocating engine driven compressor.

While it might be reasonably expected that more advanced pressure jet cycles may ultimately prove applicable and special power plants produced, the immediate future points favorably to a gas turbine driven compressor.

TRANSPORT HELICOPTER DESIGN ANALYSIS METHODS

CYCLE CONSIDERATIONS

Having made a choice of air compression machinery, we are now faced with a choice of cycle pressure and the decision of whether or not to employ tip burning.

For preliminary analysis purposes, it is desirable to study the cycle independently of the application. For this reason, we would like to eliminate the effect of duct frictional losses from our consideration. We know that the duct area is limited by the external aerodynamic requirements of the helicopter rotor blades, however, and a definite frictional loss must be expected. There is also a pressure rise due to centrifugal pumping.

The pressure at the rotor tip may be represented by an equation of the following type:

$$P_{tip} = P_{hub} - \Delta P_{friction} + \Delta P_{pumping}$$

In order to simplify our cycle considerations without neglecting the general effect of frictional losses we shall assume that all frictional losses are just equalled by the centrifugal pumping or:

$$P_{tip} = P_{hub}$$

This assumption is quite conservative for a cold cycle since pressure losses are not expected to be quite this high, however, the assumption of a reasonably high friction loss is necessary if we are to assume that the duct requirements are not to interfere with normal structural or aerodynamic practice.

The assumption of frictional losses which increase in proportion with centrifugal pumping and are independent of tip burning is further justifiable because:

1. While tip burning cycles require less airflow, and therefore, less duct friction drop than a non-tip burning cycle, the saving in frictional loss is compensated by the tip burner pressure loss.

2. Higher tip speeds provide more centrifugal pumping but the higher tip speeds are also invariably associated with lower rotor blade solidities (to keep profile drag low) and therefore with reduced duct areas and higher frictional drops.

Since the actual frictional losses should, and will, be checked once a definite cycle and blade design is chosen, there does not appear to be a further need to justify the above assumptions for this preliminary analysis.

NON TIP BURNING CYCLE

Normally, the decision to employ tip burning is arrived at as a result of cycle analyses which show that there is an optimum tip burner temperature (SFC-wise) which is dependent upon cycle pressure. On the other hand, the greatest amount of tip burning provides the minimum power plant weight.

Independently of cycle considerations, there is a definite trend away from tip burning. The greatest antagonism against tip burning rests among those who are most experienced with tip burners and has probably been fostered as a result of

the mechanical and control problems and complexities which arise with the employment of tip burners. The most recent evidence of this antagonism has been the development of the French Djinn Helicopter by a group who had previously developed three tip burning types. There must be some merit to the claims of simplicity of this type power plant, since the Djinn, while the latest of all pressure jet helicopters, has probably accumulated more flying hours than all other pressure jet helicopters combined. It is also the only pressure-jet machine in production.

While the non-tip burning type helicopter can be shown to be theoretically less effective than the tip burning types, any operational analysis must properly evaluate greater simplicity and possibly reduced maintenance costs of the non-tip burning pressure jet.

Figure 1 which follows shows the effect of compressor pressure ratio and rotor tip speed on the installed power requirements of a non-tip burning pressure jet. It should be noted that the $\frac{\text{Rotor Power}}{\text{Installed Power}}$ ratio is rather insensitive to either pressure ratio or tip speed beyond pressure ratios of about 2. It can also be seen that a conventional tip speed of 700 ft/sec is as satisfactory for the pressure jet as it is for the mechanically driven rotor. Since increasing cycle pressure does not provide increased performance beyond a pressure ratio of about 3, the only advantage of increased pressure is reduced duct size. On the other hand, increasing air pressure is associated with increasing air temperature, and the problem here is primarily structural. Again, because we must limit our design techniques to those which are considered presently reasonable, we can not choose such high cycle temperatures that we eliminate the possibilities of employing the various aluminum alloys. For this reason, the maximum cycle temperatures must be kept lower than 300 F, and this dictates a maximum cycle pressure ratio of approximately 3.

The final results indicate that the non-tip burning pressure jet will require an installed power of about 2.27 times the desired rotor horsepower. Naturally, the fuel consumption on a rotor horsepower basis will also be 2.27 times that of the basic power plant installed. For gas turbines of .755 SFC, as assumed in this study, the overall SFC will therefore be about 1.72 lbs/hr/RHP.

THE TIP BURNING CYCLE

The obvious difference between the tip burning and non-tip burning cycles is that tip burning increases the jet velocity and power output. In general, to maintain high propulsive efficiences, the tip burning cycles favor higher tip speeds and somewhat lower pressure ratios. Within the limits of practical tip speeds and pressures, however, the propulsive efficiency is rather insensitive to variations of either.

The primary effect of tip burning is on the installed power plant requirements which are reduced in proportion to the amount of tip burning employed.

Figure 2 shows the characteristics of a tip burning pressure jet for cycle pressure ratios of 2 and 3, for a tip speed of 700 ft/sec. It should be noted that

the lower pressure cycle provides lower power plant weights, but the specific fuel consumption is higher than for the higher pressure.

The variation in fuel consumption with either pressure or tip temperature is really insignificant in comparison with the absolute value of the fuel consumption compared to either the geared turbine or reciprocating engine drive. For all practical purposes, in this comparative study, pressure jet specific fuel consumption of 1.7 lbs/hr/BHP is a satisfactory average.

Now, with regard to power plant weight, the effect of pressure and tip temperature is not negligible and must be accounted for. The greatest variation is due to tip temperature, while the effect of pressure is of lesser importance in comparison with the accuracy of the initial assumption of machinery weights.

For this study, it was assumed that the turboprop engine, plus driven compressor, weighed $\frac{1}{2}$ lb. per shaft horsepower of the turboprop engine. This value is slightly lower than present operational components would provide; however, it is exceptionally high compared to present possibilities. For example, the Rolls Royce Soar Turbojet of thrust/weight ratio of over 6 could be converted to a shaft work unit of HP/Wt ratio of better than 4. This trend to lighter weight turbo machinery is being aggressively pursued in this country as well, and we should be able to expect various machines of extreme low weight, particularly in the 3000 HP class. Obviously, developments in this direction will have a much greater effect than those due to variations in cycle pressure. For this reason, it appears that we can concentrate on a single pressure ratio for our studies and, if desirable, make a correction for power plant weights, depending upon our judgment of future trends. A pressure ratio of 2.5 is satisfactory for purposes of this analysis because it is not so high as to effect power plant weight estimates adversely and not low enough to present the possibility of frictional losses effecting the external aerodynamics or structural design.

Figure 3 shows a curve of the sum of power plant + fuel weights for a pressure jet helicopter as a function of the tip temperature and flight duration and a comparison with the geared turbine drive.

APPENDIX - PRESSURE JET POWER PLANTS

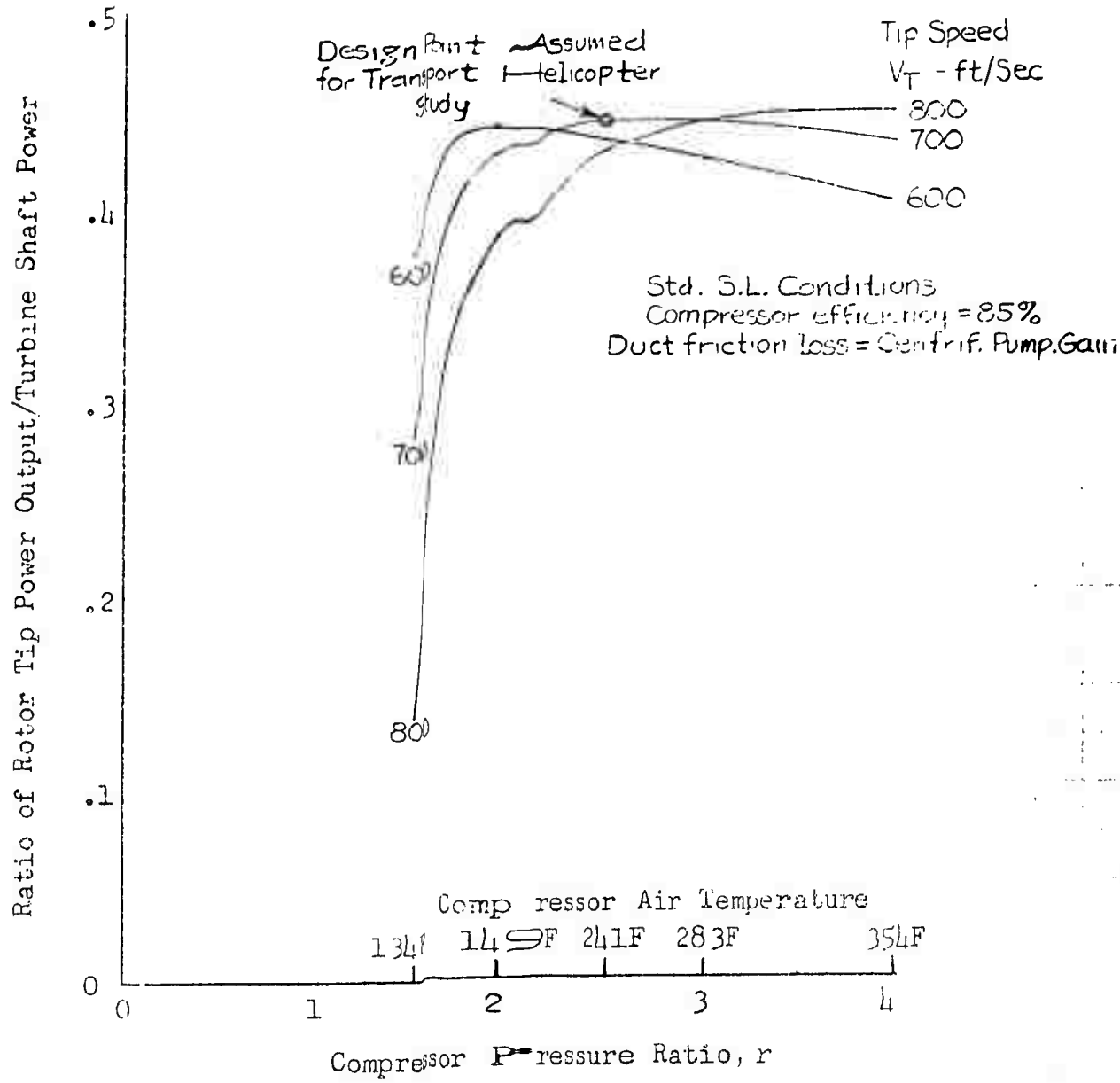

Figure 1: Non-Tip Burning Pressure Jet

TRANSPORT HELICOPTER DESIGN ANALYSIS METHODS

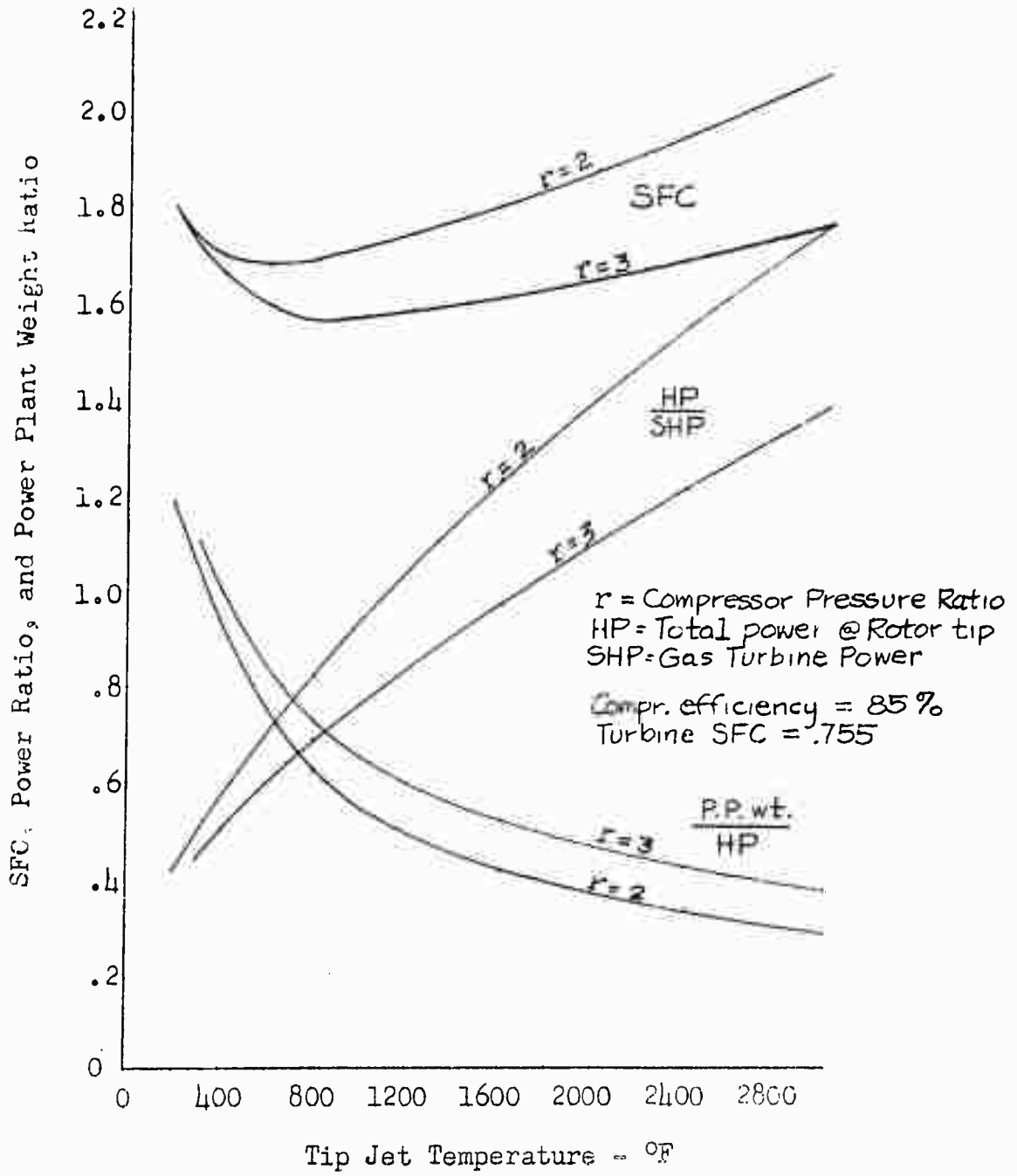

Figure 2: Tip Burning Pressure Jet Typical Characteristics @ Tip Speed V_T = 700 ft/sec

APPENDIX - PRESSURE JET POWER PLANTS

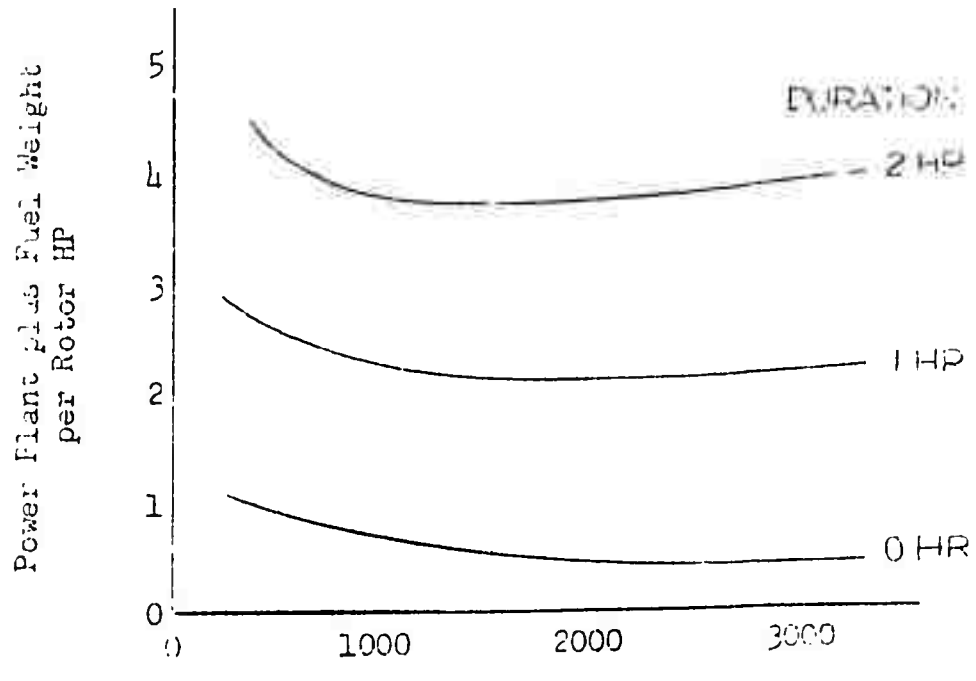

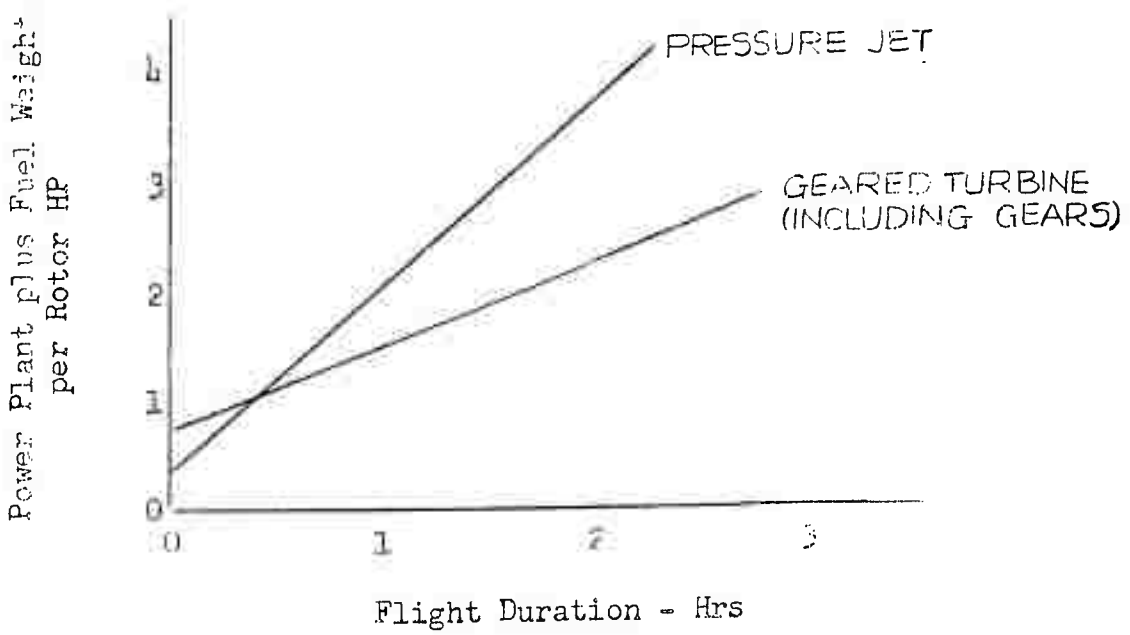

Figure 3: Pressure Jet Power Plant and Fuel Weights

APPENDIX - PRESSURE JET POWER PLANTS

BIBLIOGRAPHY

J. B. Nichols — Hovering Performance of Pressure Jet Propelled Helicopter Rotors
G. E. Report R-49-GL-90, 6/23/49
(XH-17 Project Report)

J. B. Nichols — Static and Total Pressure Changes Due to Friction Along a Constant Area Insulated Duct
G. E. Report R-49-GL-156, 10/24/49

J. B. Nichols — Compressible Flow of Air in Pipes
Kents Handbook, Power Section, 12th Ed.
p. 6-44

J. L. Flannery & C. D. Spencer — Ducted Pressure Jet Helicopter Study
Thermal Research and Engineering Company
Report of October 1953
USAF Contract AF 33(616)318

J. A. Johnson (et al) — Helicopter Propulsion System Study
Thermal Research and Engineering Company
Report of September 1952
USAF Contract AF 33(038)-22185

Also various papers by F. Doblhoff, R. Miller, Johnson & Eustice, and J. B. Nichols